Utilizing Chemoproteomics to Discover Novel Druggable Hotspots Targeted by Natural Products

By

Charles A. Berdan

A dissertation submitted in partial satisfaction of the

requirements for degree of

Doctor of Philosophy

in

Metabolic Biology

in the

Graduate Division

of the

University of California, Berkeley

Committee in Charge:

Associate Professor Daniel Nomura, Chair
Assistant Professor James Olzmann
Assistant Professor Roberto Zoncu

Spring 2019

Abstract

Utilizing Chemoproteomics to Discover Novel Druggable Hotspots Targeted by Natural Products

by

Charles A. Berdan

Doctor of Philosophy in Metabolic Biology

University of California, Berkeley

Associate Professor Daniel Nomura, Chair

It is estimated that over 1.7 million people will be diagnosed with cancer and 600,000 people will die from cancer in 2019. The need for new therapeutics against cancer is therefore imperative. Natural product based drug discovery has provided a multitude of effective answers to many diseases, however difficulties in synthesizing natural products, isolating them, and deciphering their mechanism of action can limit translating more natural products into the clinic. Coupling natural product based drug discovery with chemical genetics and with powerful chemoproteomic strategies can allow for new questions to be asked and potentially new therapeutics to be developed even from formerly well-characterized molecules.

Parthenolide, a natural product from the feverfew plant and member of the large family of sesquiterpene lactones, exerts multiple biological and therapeutic activities including anti-inflammatory and anti-cancer effects. Herein, we further study parthenolide mechanism of action using activity-based protein profiling (ABPP)-based chemoproteomic platforms to map additional covalent targets engaged by parthenolide in human breast cancer cells. We find that parthenolide, as well as other related exocyclic methylene lactone-containing sesquiterpenes, covalently modify cysteine 427 (C427) of focal adhesion kinase 1 (FAK1) leading to impairment of FAK1-dependent signaling pathways and breast cancer cell proliferation, survival, and motility. These studies reveal a novel functional target exploited by members of a large family of anticancer natural products.

DEDICATION

Mom, Dad, Michele, and Amanda, this is for you. It is only with your constant love and support that I have been able to accomplish anything at all, and I am forever grateful.

Thank you, and I love you.

TABLE OF CONTENTS

LIST OF FIGURES

ACKNOWLEDGEMENTS

Adapted with permission from Biorxiv, doi: 10.1101/550806, Charles A. Berdan, Raymond Ho, Haley S. Lehtola, Milton To, Xirui Hu, Tucker R. Huffman, Yana Petri, Chad R. Altobelli, Sasha G. Demeulenaere, James A. Olzmann, Thomas J. Maimone, Daniel K. Nomura, “Parthenolide Covalently Targets and Inhibits Focal Adhesion Kinase in Breast Cancer Cells.” Copyright © 2019 Elsevier

CHAPTER ONE: Chemoproteomic platforms as tools for natural product drug discovery

Introduction

It is estimated that over 1.7 million people will be diagnosed with cancer and over 600,000 people will die of the disease in 2019 alone[1]. Currently the arsenal of tools against cancer primarily includes resection, radiation therapy, immunotherapy, and chemotherapy[1–4]. The metastatic spread of cancer, it's primary cause of death, often prevents the utilization of more physical therapies such as resection and radiation and necessitates more targeted therapies to prevent cancer related death[2,5]. Unfortunately there are currently limited targeted solutions against many of the most aggressive cancers. The absence of targeted therapeutics is often associated with the worst prognoses among cancers[1,4]. It is therefore imperative that we develop new targeted therapeutics in the fight against cancer.

Natural products as a tool for drug discovery

In the past several decades numerous techniques and tools have been developed to aid in early drug development in an attempt to increase the likelihood of finding novel small molecule inhibitors[6]. Natural products, or chemical compounds derived from naturally occurring biological sources such as plants, animals, bacteria, and fungi, have been a rich source of therapeutic activity since time immemorial and represent some of the most successful drugs on the market even in the past several decades[7–9]. By some estimates natural product derived therapeutics account for 50-70% of FDA approved therapeutics in use today[10].

Hallmark examples include the discoveries of penicillin and streptomycin, both of which were separately awarded Nobel Prizes in Physiology and Medicine[11–13]. More recently, the discovery of avermectins was awarded the same prize and provides effective treatments for onchocerciasis, lymphatic filariasis, and malaria[14]. Less lauded but equally as important examples also exist, including the utilization of salicin and later acetylsalicylic acid to treat pain[15], colchicine to treat gout[16], paclitaxel to treat various types of cancer[17], and mevastatin and later atorvastatin to lower cholesterol and treat CVD[18,19]. These keystone examples solidify natural products as an effective tool for the creation of novel and effective therapeutics **(Fig. 1.1)**.

Natural product based drug discovery has several key advantages over other synthetic chemical based drug discovery strategies. Perhaps the greatest strength is the unparalleled chemical diversity provided by natural products. Many chemical scaffolds are intricate in design, debatably past the scope of even the best medicinal chemists. Adding to this, numerous compounds have complex components that are impossible or taxing to synthesize with current synthetic strategies, resulting in an entire classes of potential therapeutics unattainable without the utilization of these natural resources. Lastly, natural product evolution has happened over the course of millennia by organisms with specific ends in mind. This long-dated 'design' results in compounds

often tailor made for specific goals, such as in the instance of antimicrobial agents or toxins[8–10,20].

While natural products represent a great opportunity in drug development, numerous weaknesses can be noted when compared to other discovery techniques. The complicated milieu of chemical inside organisms can make isolation and identification of specific bioactive compounds difficult to achieve. Similarly, the isolation of bioactive compounds at large enough scale for study and later utilization can be challenging for those created in slow-growing or –metabolizing organisms. Further, the uniqueness in chemical diversity can lead to difficulty in the creation of more biologically specific or potent analogues, or when study requires chemical modification. Finally, the determination of the specific targets of many natural products can be made additionally complicated by all of these issues[8–10,20].

With these difficulties in mind it is imperative that additional techniques be available for the study of natural products in the fight against disease.

Technologies to aid in natural product target elucidation

One great difficulty in the creation of effective therapeutics from natural products is the determination of their direct protein targets. In the very earliest natural products studies, humans were exposed to a biological substance through ingestion, inhalation, or contact and a useful phenotype was observed. Today it is not enough for a therapeutic to just have notable effects, the suite of targets it has must also be known and fully characterized, among many other considerations. As such, numerous techniques have been developed to determine the specific targets of natural products.

Capture affinity chromatography can be use to determine the direct target of a small molecule drug by appending the small molecule to a resin and then either running the captured protein along a gel or by incorporating SILAC to couple the technique to mass spectrometry (MS). This technique has been utilized to great success in many seminal discoveries such as that of the trapoxin family of histone deacetylase inhibitors[21], as well as the characterization of the immunosuppressant natural product FK506[22,23], among numerous others. Complicating the use of capture affinity chromatography is the requirement that the natural product be amenable to derivatization, somewhat limiting its use.

More recently, cellular thermal shift assay (CESTA) has emerged as a technology to allow for the identification of compound target engagement without requiring modification of the natural product. By treating a cell lysate with a natural product of interest and then heating to denaturation, untargeted proteins denature and are removed from the solution whereas protein targets remain soluble for downstream elucidation[24]. The technology has been successfully utilized to determine novel targets of numerous natural product and natural product derived compounds including hordenine[25] and methotrexate[26] among others. The technology is still in its nascence

and while shown to be robust also demonstrates difficulty in downstream target identification, off-target analyses, and assay flexibility[27,28].

Numerous additional technologies have shown promise over the past several decades as well, including fluorescence or bioluminescence resonance energy transfer (FRET and BRET, respectively) assays such as is the elucidation of APT1 target engagement by palmostatin B[29], or the hypothesized uses of enzyme complementation reporter assays towards natural product target engagement identification[27,30]. Most are accompanied by a series of limitations including required ligand or protein modification, singular target identification, or limited *in vivo* application. It therefore continues to be imperative that we develop additional tools for the elucidation of novel drug targets by natural products.

Activity-based protein profiling as a tool for natural product target discovery

Activity-based protein profiling (ABPP) has recently emerged as a tool that circumvents many of the systemic difficulties posed by the aforementioned technologies while also acting more flexibly than many other techniques. When used competitively against covalent acting natural products, such as those with known epoxides, Michael acceptors, free aldehydes, and β-lactams and β-lactones **(Fig. 1.2)**, ABPP can be used as a universal assay strategy for target identification for any protein targeted by ABPP[31–36].

ABPP uses activity-based and reactivity based probes to map reactive, functional and druggable hotspots directly in complex proteomes. A reactivity-based probe consists of at least two components, an electrophilic warhead capable of reacting with nucleophilic amino acid side-chains and an analytical tag for the detection of probe-labeled proteins[34,36]. Numerous activity- and reactivity-based probes have been developed over the past two decades, including probes for serines, cysteines, methionines, arginines, and lysines[32,37–41] **(Fig. 1.3A)**. Adding to the flexibility of the technique is that reactivity based probes do are not necessarily limited to targeting enzyme active site amino acids, allowing for access to much more of the proteome than other techniques and providing a more robust characterization of the proteins impacted by a natural product. Additionally, the analytical tag can vary to provide various functionalities to the technique. By utilizing a fluorophore, in-gel fluorescence visualization, live cell fluorescence visualization, or fluorescence polarization assays can be performed. Similarly, biotin can be utilized for avidin-enrichment and subsequent MS-based quantification, or alkynes for biorthoginal conjugation of handles for subsequent analyses of protein activities[33,36]. Furthermore, should the natural product be amenable to derivitization it can also be turned into a reactivity-based probe to further assess bioselectivity[42]. Finally, these probes can be utilized *in vivo* for direct target identification as well as *in vitro* and *ex vivo* for biological characterization and target engagement in pre-clinical testing in various models including humans[33].

One notably powerful ABPP technique is termed isotopic tandem orthogonal proteolysis-enabled activity-based protein profiling (isoTOP-ABPP). Coupling activity

based probes to an azide functionalized TEV-protease recognition peptide linker containing a biotin group for avidin-enrichment of probel-labeled proteins and an isotopically light or heavy valine for quantitative ratiometric MS-based proteomic analysis, the reactivity of a probe against specific amino acid sites can be identified and quantitatively compared. Further, by competing covalently acting natural products against an activity- or reactivity-based probe, such as in competitive isoTOP-ABPP target discovery can be enabled[42–45]. Furthermore, because the probes act on entire amino acid classes, proteome-wide selectivity can be assessed and new targets of otherwise well characterized natural products can be discovered. Taken as a whole, ABPP and isoTOP-ABPP can serve as a valuable tool in the interrogation of proteins modified by covalent acting natural products **(Fig. 1.3B-1.3C)**.

Using chemical genetics to easily access druggable space targeted by natural products

As mentioned earlier, while natural products present as large sources of potential therapeutics, efforts are often stifled by the ability to produce natural products at large enough scale for testing and subsequent use. If the direct protein target of a natural product can be determined, it can be more efficacious to access this protein target with a fully synthetic small molecule. Coupling natural product target identification via isoTOP-ABPP to chemical genetics does just this.

Traditionally, chemical genetics uses vast small-chemical libraries to elicit particular predetermined phenytopic readouts *in vitro* using primary culture or immortalized cell lines, such as cell death or signaling, or in recombinant protein systems, looking for outputs such as protein activity[46–48]. These techniques reveal bottlenecks throughout their process; recombinant protein assays require knowledge of the specific protein before beginning the assay; *in vitro* and *ex vivo* cell assays can fail to note off-target effects. Independent of these issues is also the challenge in producing high affinity small molecule drugs, as most ‘good’ hits are somewhere in the low uM range, whereas a high affinity therapeutic would ideally have low nM efficiacy.

By coupling natural product target identification with chemical genetics many of the difficulties found with natural product drug discovery. First, it is possible to utilize impure chemical mixtures in the initial natural product screening and subsequently target the same protein targets with the small molecule inhibitor. Therefore, should a natural product be difficult to purify or synthesize, small molecule inhibitors targeting the same site might conversely be easier to synthesize at scales required for downstream tests. Additionally, it is possible to test several thousand compounds in an attempt to find the most potent or selective small molecule for a given protein target, whereas this can be difficult with natural products. Similarly, while downstream medicinal chemistry can be difficult to perform on complex natural products, small chemical ligands can be designed with derivitization and modification in mind, potentially accelerating medicinal chemistry efforts[10,35,46–48].

Similarly, pairing with an isoTOP-ABPP natural product based system as well can circumvent difficulties seen in working with chemical genetics alone. The initial determination of a protein target, potentially those not initially known, can allow for more targeted small molecule design. Further, the marriage of the techniques does not limit initial small molecule targeting to only kinetically active proteins but allows for targeting of potentially “undruggable” proteins. Taken as a whole, utilizing natural product based drug discovery alongside chemical genetics, specifically when enabled by ABPP techniques, can potentially accelerate natural product target identification and drug discovery and creation techniques.

Concluding remarks

The diseases that plague the world today are punctuated by complex systems of action, as well as a surprising lack of answers for them. Solutions to these illnesses will likely not be conceived by a singular drug discovery technique but by a marriage of many fields and the combination of a multitude of techniques. Natural product based drug discovery as well as chemical genetics both provide several opportunities in therapeutic development, however both are mired with insufficiencies when used alone. Bridging the gap between the two techniques is ABPP, and with these techniques utilized in tandem it is possible to answer questions that were before considered unanswerable.

Figures

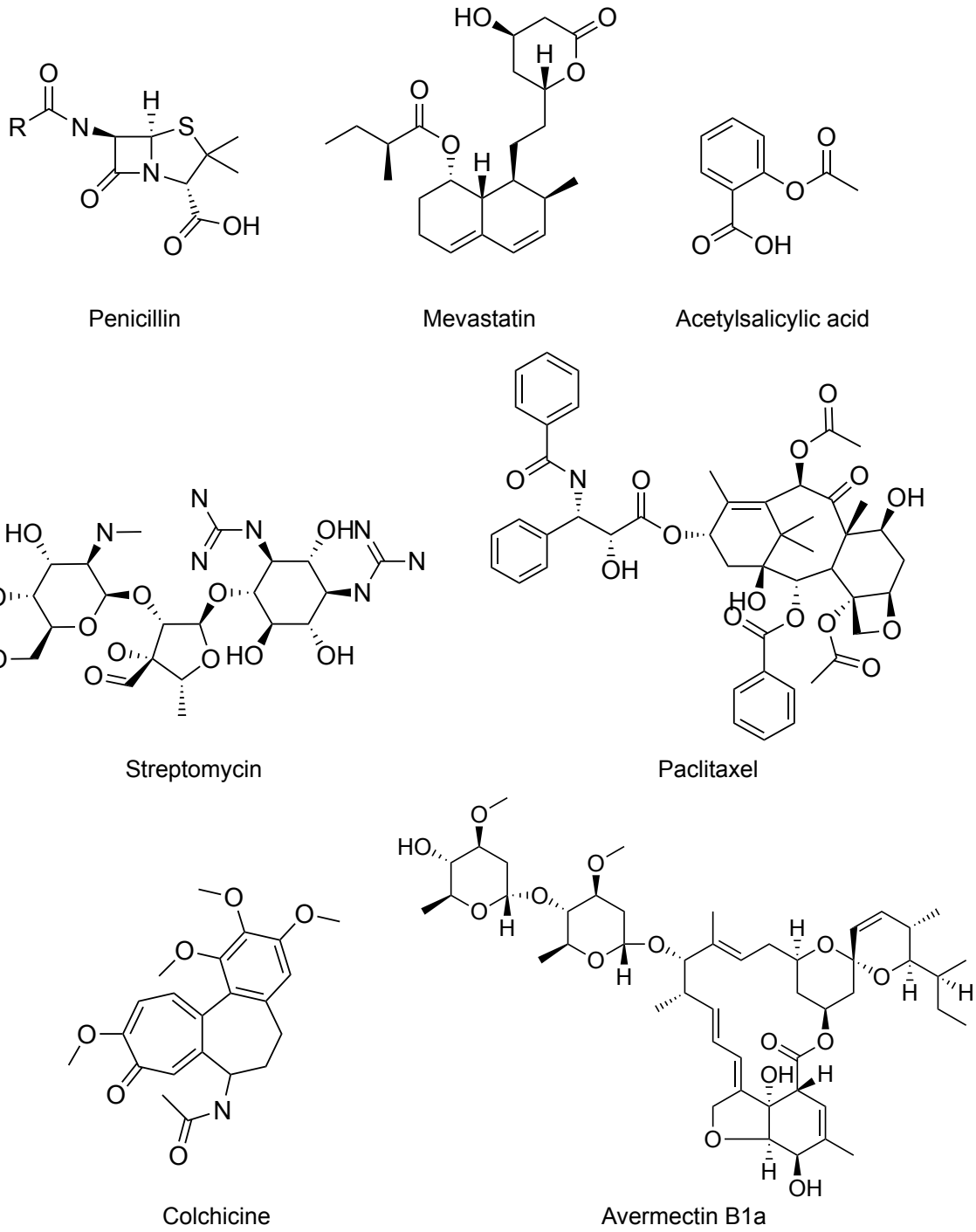

Figure 1.1. Selected keystone natural product therapeutics. Classical examples of natural products and natural product derived therapeutics that have been used to great effect over the past hundred years. The breadth of chemical diversity the make natural products a valuable tool in drug discovery.

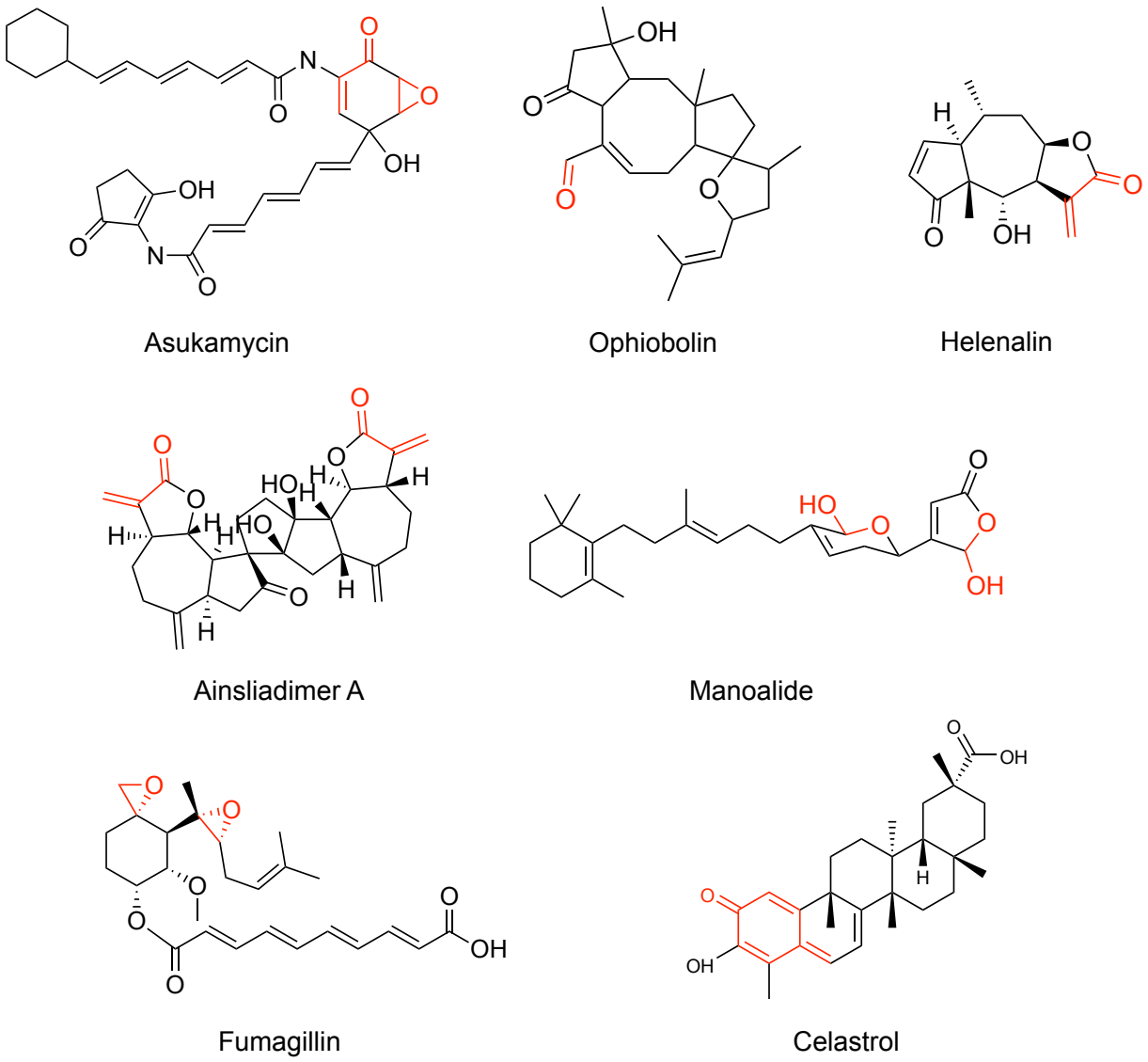

Figure 1.2. Natural products containing covalent acting sidegroups. There is a wide variety of natural products containing covalent acting sidegroups such as epoxides, Michael acceptors, and free aldehydes. This subclass of natural products is amenable to study using techniques that require covalent modification of protein targets, such as in activity based protein profiling.

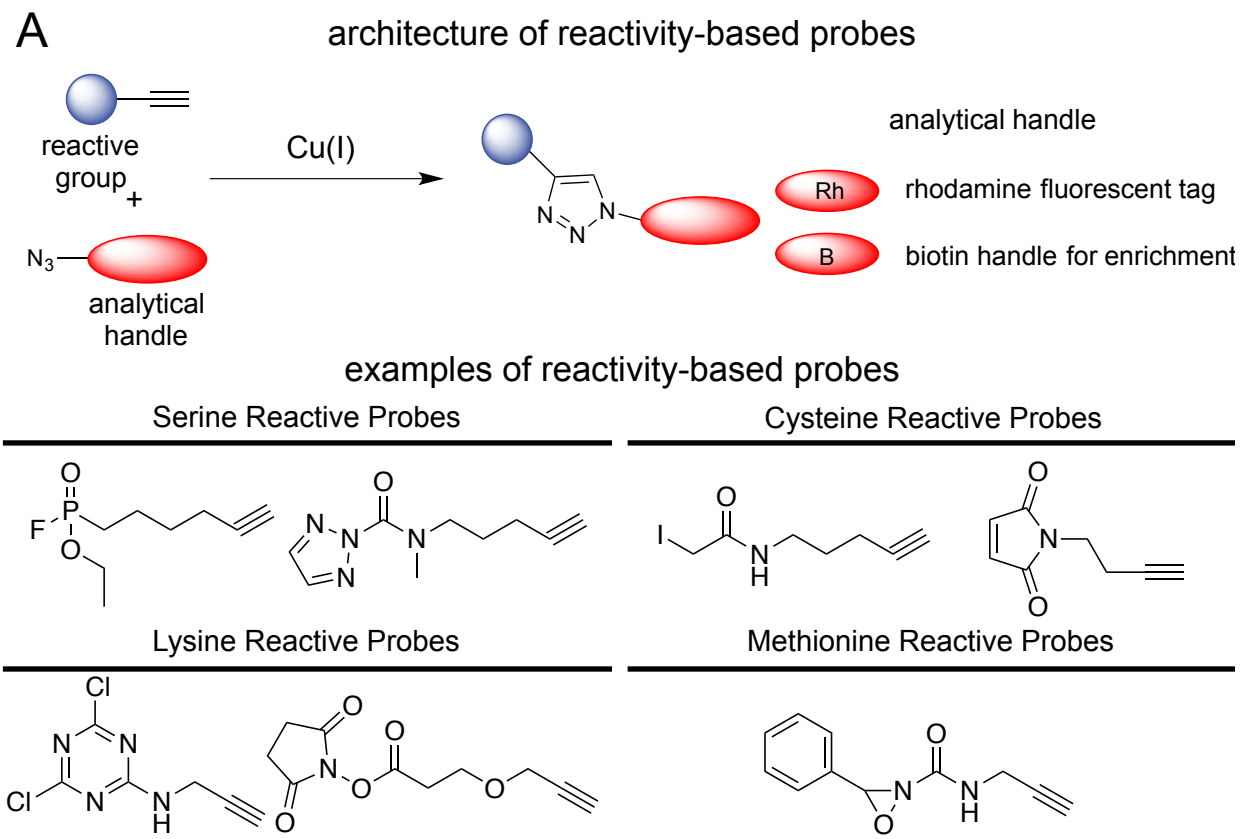
A
architecture of reactivity-based probes
reactive group
+
N3
analytical handle
Cu(I)
analytical handle
Rh
rhodamine fluorescent tag
B
biotin handle for enrichment
examples of reactivity-based probes
Serine Reactive Probes
Cysteine Reactive Probes
Lysine Reactive Probes
Methionine Reactive Probes

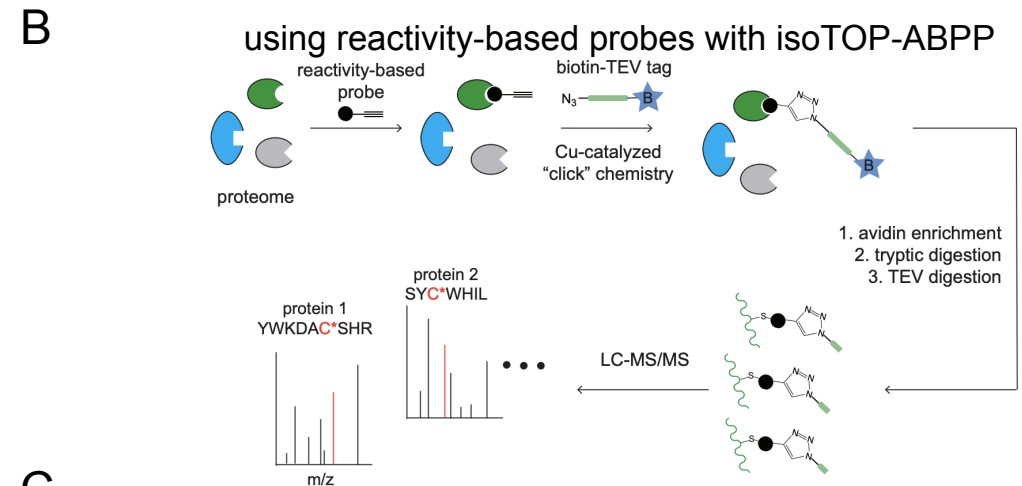
B
using reactivity-based probes with isoTOP-ABPP
reactivity-based probe
proteome
biotin-TEV tag
Cu-catalyzed "click" chemistry
1. avidin enrichment
2. tryptic digestion
3. TEV digestion
LC-MS/MS
protein 1
YWKDAC*SHR
protein 2
SYC*WHIL
m/z

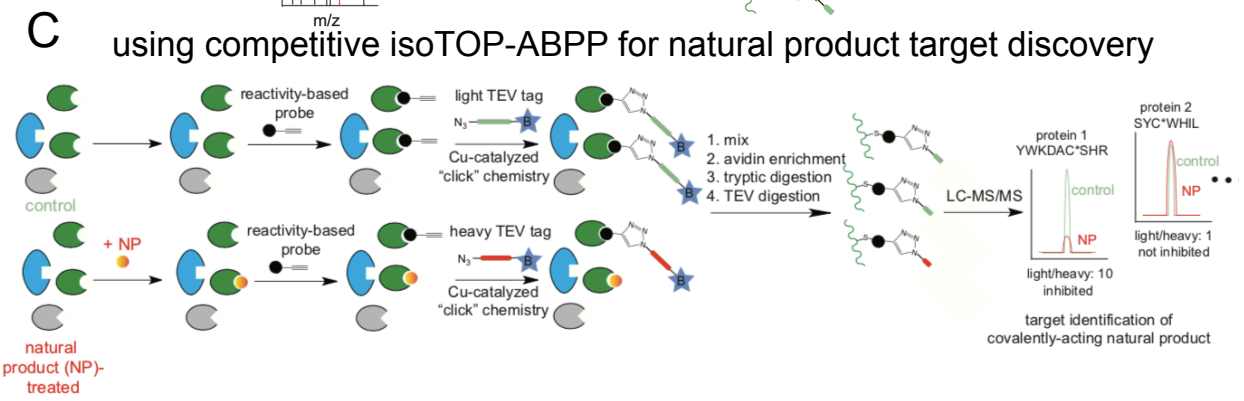
C
using competitive isoTOP-ABPP for natural product target discovery
control
reactivity-based probe
light TEV tag
Cu-catalyzed "click" chemistry
+ NP
natural product (NP)-treated
heavy TEV tag
1. mix
2. avidin enrichment
3. tryptic digestion
4. TEV digestion
LC-MS/MS
protein 1
YWKDAC*SHR
control
NP
light/heavy: 10 inhibited
protein 2
SYC*WHIL
light/heavy: 1 not inhibited
target identification of covalently-acting natural product

Figure 1.3. ABPP platforms and applications. (A) Design of activity- and reactivity-based bioorthogonal probe. **(B)** Reactivity based probes can be used with isoTOP-ABPP to map the proteome. Following proteome labeling with the reactivity based probe containing both a biotin tag and a TEV protease cleavage sequence the peptides are digested and then assessed by LC-MS/MS. **(C)** Direct protein targets can be assessed using competitive isoTOP-ABPP. Pretreatment of proteome with covalent natural product or vehicle followed by incubation with a reactivity based probe of an isotopically light or heavy analytical biotin handle bearing a TEV protease cleavage sequence, followed by mixing the proteomes in a 1:1 ratio, avadin enrichment of probe-labeled proteins, TEV digestion to release probe-modified tryptic peptides, and quantitative proteomic analysis of probe modified peptides. Mapping where the ligand displaced the probe allows for assessment of natural product targets as well as assessment of proteome-wide selectivity.

CHAPTER TWO: Parthenolide Covalently Targets and Inhibits Focal Adhesion Kinase in Breast Cancer Cells

Introduction

Parthenolide, a natural product found in the feverfew plant (*Tanacetum parthenium)*, possesses myriad therapeutic activities, including anti-inflammatory and anti-cancer effects. Through covalent bond formation between its reactive α-methylene-γ-butyrolactone moiety and various protein targets, multiple cellular signaling pathways are impacted [49–53]. Moreover, this natural product belongs to the broader family of sesquiterpene lactones (estimated at > 5000 members), many members of which are also cytotoxic and have been hypothesized or shown to act through covalent mechanisms [54,55]. Parthenolide impairs cancer pathogenicity or confers chemotherapy or radiation sensitivity across a wide range of cancer types, including leukemia, colorectal, glioblastoma, cervical, liver, prostate, lung, pancreatic, skin, and breast cancers [56–68]. Despite possessing multi-target activity and exhibiting cytotoxicity across a wide range of human cancers, parthenolide is remarkably well-tolerated in humans [69].

Using a biotinylated parthenolide analog, previous studies by the lab of Crews established that one of the primary targets that drives the anti-inflammatory and anti-cancer activity of parthenolide is IKK-β wherein cysteine 179 (C179) is modified thus impairing IKK-β and NFκB signaling [50]. Additional studies have revealed other direct targets of parthenolide that may help to explain the therapeutic properties of this natural product, including targeting of specific cysteines within heat shock protein Hsp72 and STAT3 downstream signaling targets such as Janus kinases JAK2 [51,53]. Moreover, this natural product has also been shown to affect additional cell signaling pathways including induction of oxidative stress and apoptosis, focal adhesion kinase 1 (FAK1) signaling, HIF-1α signaling, epithelial-to-mesenchymal transition, Wnt/β-catenin signaling, MAPK signaling, and mitochondrial function [50,57,64,67,70–72]. Based on the broader scope of influence on these biological pathways and systems, parthenolide likely still possesses additional targets that are not yet fully elucidated. In previous works investigating the direct targets of parthenolide, multiple studies have revealed unique ligandable and functional cysteines within their respective proteins that could be targeted to influence cellular signaling and pathogenicity. Recent studies have shown that activity-based protein profiling (ABPP)-based chemoproteomic platforms can be utilized to uncover unique and functional druggable hotspots and modalities that can be accessed by covalently-acting small-molecules and natural products that may not be obvious using standard drug discovery paradigms [73–78]. ABPP uses reactivity-based chemical probes to profile proteome-wide reactive, ligandable, and functional sites directly in complex proteomes. When used in a competitive manner, covalently-acting small-molecules can be competed against binding of reactivity-based probes to map the proteome-wide targets of these compounds [73–76,79,80]. Importantly, this technology allows for the interrogation of natural products in their unmodified form.

Parthenolide has anti-cancer activity

In this study, we used ABPP chemoproteomic platforms to map additional targets of parthenolide in breast cancer cells uncovering additional druggable hotspots which may contribute to the cell signaling and anti-cancer effects of parthenolide **(Fig. 2.1A)**.

Parthenolide impaired cell proliferation and serum-free cell survival, induced cell death, thwarted early cell motility, and significantly attenuated *in vivo* tumor xenograft growth in estrogen receptor, progesterone receptor, and HER2 receptor-negative breast cancer (triple-negative breast cancer, TNBC) cells—231MFP or HCC38 cells—in a time-dependent and dose-responsive manner **(Fig. 2.1B-2.1F, Fig. 2.2A-2.2C).** The impairment in cell viability induced by parthenolide, evidenced by propidium iodide and Annexin-V-positive cells, may be due to various forms of cell death, including apoptosis, necrosis, or ferroptosis. We show that parthenolide leads to the activation of caspase 3/7 and that this cell death is significantly attenuated by the pan-caspase inhibitor Q-VD-OPh indicating that parthenolide impairs cell viability in a caspase-dependent manner **(Fig. 2.2C)**, suggesting that a portion of the cell death is apoptotic. We note that we are observing anti-tumorigenic effects at a relatively low dose of 30 mg/kg, despite observing cell viability impairments at 50 μM high concentrations. This may be because of the covalent nature of parthenolide and accumulating target engagement over time. Since parthenolide irreversibly binds to their targets, the targets will stay bound to parthenolide until the protein turns over. TNBCs show the worst prognoses due to the lack of key druggable targets and there are few targeted therapies [81]. Our data suggested that parthenolide may be effective at attenuating TNBC pathogenicity.

Mapping and characterizing functional targets of parthenolide

We next used ABPP methods to identify additional targets of parthenolide in breast cancer cells. To confirm that parthenolide was not completely non-specific, we first performed a competitive gel-based ABPP experiment in which we competed parthenolide against labeling of 231MFP breast cancer cell proteomes with a rhodamine-functionalized cysteine-reactive iodoacetamide (IA-rhodamine) probe. While this method is imprecise, we observed that parthenolide did not broadly inhibit global proteome-wide cysteine reactivity **(Fig. 2.3A).** Using a more specific, previously-reported alkyne-functionalized parthenolide probe (parthenolide-alkyne) [53], we observed multiple labeled proteins in 231MFP proteomes, of which some, but not all, targets were competed by parthenolide **(Fig. 2.3A)**. Collectively, these results indicated that parthenolide does possess multiple protein targets in 231MFP proteomes, but that this natural product is not completely promiscuous in its reactivity.

While the parthenolide-alkyne probe could be used to identify additional targets of this natural product, we sought to map the specific amino acids within these targets that were engaged by unfunctionalized parthenolide. Thus, we next used isotopic tandem orthogonal proteolysis-enabled ABPP (isoTOP-ABPP) to identify specific ligandable sites targeted by parthenolide in 231MFP breast cancer proteomes. We competed parthenolide binding against the broadly cysteine-reactive alkyne-functionalized iodoacetamide probe (iodoacetamide-alkyne, IA-alkyne) directly in 231MFP TNBC proteomes using previously established methods **(Fig. 2.4A, Table 1)** [73–75,79,82]. This analysis revealed three highly engaged targets of parthenolide that showed isotopically light vehicle-treated to heavy parthenolide-treated probe-modified peptide ratios of greater than 10, indicating >90 % engagement of these sites—focal adhesion kinase 1 (FAK1) C427, paraoxonase 3 (PON3) C240, and DNA-protein kinase (DNA-PK or

PRKDC) C729. FAK1 C427 was the top target showing the highest ratio, and thus we placed subsequent focus on investigating the role of FAK1-dependent effects of parthenolide in breast cancer cells **(Fig. 2.4A; Table 1)**. While the role of PON3 in cancer cells is unclear, FAK1 and PRKDC are known to be important drivers of cancer cell signaling and DNA repair, respectively. Notably, FAK1 and PRKDC inhibitors have been shown to impair both cell survival and cell proliferation in cancer cells and are being pursued in the clinic[83–85]. Since C427 of FAK1 was the most highly engaged target in this study, we focused our attention on investigating the FAK1-dependent effects of parthenolide in TNBC cells.

We validated the interaction of parthenolide with C427 of FAK1 using several complementary approaches. We first validated the interaction of parthenolide with FAK1 in which we showed parthenolide prevention of pure human FAK1 kinase domain cysteine-reactivity with a rhodamine-functionalized iodoacetmide probe (IA-rhodamine) by gel-based ABPP **(Fig. 2.4A)**. Based on previous studies, we conjectured that parthenolide reacted covalently with C427 of FAK1 through a homo-Michael addition involving the α/β unsaturated lactone **(Fig. 2.4B)** [50]. Second, we demonstrated that parthenolide covalently reacts with C427 of FAK1 by identifying this parthenolide adduct on human FAK1 kinase domain by LC-MS/MS **(Fig. 2.4C).** We also demonstrated that IA-rhodamine labeling of pure human FAK1 was abrogated in the C427A mutant and that no additional inhibition of remaining IA-rhodamine labeling of FAK1 was observed with parthenolide treatment **(Fig. 2.4D).** Using a parthenolide-alkyne probe, we further showed that this probe labeled wild-type FAK1 protein, and that this labeling was prevented by parthenolide or in the C427A mutant FAK1 protein **(Fig. 2.4E)**.

Previous studies have shown that FAK1 is amplified or overexpressed across a large fraction of breast tumors wherein FAK1 activity and expression is correlated with poor prognosis. FAK1 has been shown to be important in breast cancer cell survival, proliferation, and migration [84,86]. To determine whether any of the observed parthenolide-mediated proliferative, survival, or migration impairments were dependent on FAK1, we assessed parthenolide effects on these phenotypes under FAK1 knockdown in 231MFP breast cancer cells **(Fig. 2.4F-2.4G).** FAK1 knockdown confers significant resistance to parthenolide-mediated impairments in cell proliferation, serum-free cell survival, and cell migration, particularly at early time-points, compared to control cells **(Fig. 2.4F-2.4G)**, demonstrating that FAK1 contributes to the anti-cancer effects of parthenolide. Because parthenolide rapidly impairs cell proliferation and survival, we do note that the migration phenotypes shown here are likely confounded by reduced cell viability from parthenolide treatment. Interestingly, FAK1 knockdown by small-interfering RNA (siRNA) did not impair basal cell proliferation, survival, or migration. We postulate that this lack of effect may either be due to the multi-target polypharmacological nature of parthenolide, or potential adaptation to FAK1 knockdown during the inherently slower process of siRNA-mediated knockdown compared to acute inhibition of FAK1. We later show evidence for the latter hypothesis.

We next sought to determine whether parthenolide functionally inhibits FAK1 activity and signaling. Based on previously reported crystal structures of FAK1, C427 resided in

a loop region proximal to the ATP site, indicating that covalent modification of this site may be inhibitory [87]. Consistent with this premise, we showed that FAK1 activity was inhibited by parthenolide *in vitro* with pure human FAK1 kinase domain in a substrate activity assay **(Fig. 2.4H)**. While this manuscript was under revision, an elegant study describing the first structure-guided design, synthesis, and characterization of a FAK1 inhibitor that also covalently targeted C427 of FAK1 and inhibited its function was reported [88]. Importantly, this report gives further credence to our hypothesis of the functional relevance of this cysteine and its effects on cancer cell proliferation.

FAK1 is activated through membrane recruitment by growth factors, extracellular matrix, and integrin signaling followed by subsequent autophosphorylation at Y397. This produces an SH2-binding domain, which in-turn recruits Src and promotes semi-autophosphorylation of Y576/577 of FAK1. The fully active FAK1/Src complex can now recruit, phosphorylate, and activate numerous targets including p130Cas/Bcar1 and paxillin (PXN) to drive cell motility and cytoskeletal modifications [84,89] **(Fig. 2.4I)**. We show that parthenolide, but not the analog dimethylaminoparthenolide (DMAPT) which lacks a reactive Michael acceptor, impaired multiple components of the FAK1 signaling pathway, including phosphorylation of FAK1 itself, as well as p130Cas and PXN phosphorylation *in situ* in 231MFP breast cancer cells **(Fig. 2.4J-2.4K).** While FAK1 knockdown itself did not affect p130Cas and PXN phosphorylation, FAK1 knockdown conferred total resistance to parthenolide-mediated inhibition of p130Cas and PXN phosphorylation observed in siControl 231MFP cells **(Fig. 2.4L)**. These results suggest that the slower or longer knockdown of FAK1 by siRNA leads to a rewiring of FAK1 signaling to maintain p130Cas and PXN activity, but that the acute parthenolide-mediated inhibition of FAK1 signaling is still FAK1-dependent and contributes to the viability and motility impairments observed **(Fig. 2.4F-2.4G).**

Activation of FAK1 has also been shown to recruit phosphatidyl inositol-3-kinase (PI3K) to activate AKT/PKC-mediated cell survival pathways **(Fig. 2.4F)** [84,89]. While we observed inhibition of AKT phosphorylation with parthenolide treatment, this inhibition was not attenuated in siFAK1 cells and was thus not mediated by parthenolide interactions with FAK1, but rather through interactions with other targets **(Fig. 2.3B)**. Consistent with known interaction of parthenolide with IKK-β to inhibit IKK-β and NFκB signaling [50], NFκB phosphorylation was inhibited by parthenolide and this inhibition was also not driven through FAK1 **(Fig. 2.3C)**. Nonetheless, our data demonstrates that C427 of FAK1 is both a covalent and functional target of parthenolide that contributes to acute inhibition of specific arms of the FAK1 signaling pathway and the overall anti-cancer effects of parthenolide.

Characterizing other sesquiterpene lactones effects on FAK1

Parthenolide, which belongs to the germacrene family of sesquiterpenes, is just one natural product among hundreds of known sesquiterpene lactones containing the reactive α-methylene-γ-butyrolactone motif (Jackson et al., 2017). Many of these plant metabolites possess notable anti-cancer properties and have been employed in traditional medicine regimes [90,91]. Given the accessibility of C427, we wondered if other

related sesquiterpene lactones can also target this residue. The related germacranolide costunolide and the guaianolide natural product dehydrocostus lactone, which both contain α-methylene-γ-butyrolactone pharmacophores, impaired 231MFP breast cancer cell survival **(Fig. 2.5A)**. On the other hand, the eudesmane-type sesquiterpene natural product α-Santonin, which does not contain this reactive functional group did not impair 231MFP cell survival **(Fig. 2.5A).** Consistent with these results, parthenolide, costunolide, and dehydrocostus lactone, but not α-santonin, exhibited FAK1 cysteine reactivity as shown by competitive IA-rhodamine labeling of FAK1 **(Fig. 2.5B)**. Moreover, the more highly oxidized guaianolide sesquiterpene mikanokryptin [92], which also possesses differing stereochemistry relative to dehydrocostus lactone, also showed FAK1 cysteine reactivity and impaired 231MFP breast cancer cell proliferation and survival **(Fig. 2.5C-2.5E)**. Taken together, these findings indicate some flexibility in targeting this druggable hotspot with sesquiterpene natural products harboring reactive α-methylene-γ-butyrolactone homo-Michael acceptors. We do note, however, that this reactive cysteine has not been pinpointed in previous target identification studies employing related natural products [93].

Using chemical genetics to develop a small molecule inhibitor of FAK1

In accordance with Chen's findings [88], we also discovered small, fully-synthetic covalent binders of FAK C427 via a cysteine-reactive covalent ligand screen using gel-based ABPP against the pure human FAK1 kinase domain **(Fig. 2.6-2.8; Table 2).** After screening 149 covalent ligands, we found 15 potential hits that impaired IA-rhodamine labeling of FAK1 **(Fig. 2.6)**. We then evaluated these 15 compounds for 231MFP survival and proliferation impairment to identify compounds that gave similar responses to parthenolide **(Fig. 2.7A)**. This led us to 3 promising leads, namely TRH 1-191, TRH 1-23, and TRH 1-171 **(Fig. 2.7A)**. We then tested these compounds for FAK1 signaling impairment. While all three impaired Y397 FAK1 phosphorylation in 231MFP cells, TRH 1-191 was superior **(Fig. 2.7B)**. We further confirmed that TRH 1-191 impaired FAK1 IA-rhodamine labeling at comparable concentrations to parthenolide without causing any artifactual protein precipitation which may arise from non-specific reactivity **(Fig. 2.7C-2.7D)**. While TRH 1-191 is a simple chloroacetamide fragment, we showed that a structurally similar negative control compound TRH 1-189 did not react with FAK1 and had no impact on FAK1 signaling **(Fig. 2.7D-2.7E)**. We also showed the corresponding TRH 1-191 covalent adduct on C427 of FAK1 by LC-MS/MS **(Fig. 2.8A-2.8B)**. TRH 1-191 also inhibited FAK1 activity *in vitro* with pure FAK1 kinase domain protein and impaired FAK1 signaling *in situ* in 231MFP breast cancer cells **(Fig. 2.8C-2.8D)**. TRH 1-191 may thus represent an additional scaffold for targeting C427 of FAK1 to inhibit FAK1 signaling in cancer cells.

Conclusions

Here, we have used ABPP-based chemoproteomic platforms to identify C427 of FAK1 as a novel ligandable and functional site targeted by the anti-cancer natural product parthenolide. This target adds further complexity to the polypharmacological landscape of parthenolide which also includes IKK-β, heat shock protein Hsp72, and thioredoxin

reductase as targets [50,53,94]. Moreover, these findings also implicate a broad array of widely examined natural products as potential FAK impairment agents. Previous studies have shown that parthenolide and other sesquiterpene lactone natural products inhibit the FAK1 signaling pathway, but the mechanism through which parthenolide inhibited this pathway was poorly understood [95,96]. Our study indicates that these natural products inhibit FAK1 signaling through targeting C427 of FAK1 to inhibit FAK1 activity and downstream signaling. The contribution of these effects to global cytotoxicity warrants further future study among other sesquiterpene lactone natural products. Furthermore, our study highlights the utility of using chemoproteomic platforms for discovering unique druggable modalities that are accessed by covalently-acting natural products.

Previous studies have shown that parthenolide and other sesquiterpene lactone natural products inhibit the FAK1 signaling pathway, but the mechanism through which parthenolide inhibited this pathway was poorly understood. In this study, we use chemoproteomic platforms to identify C427 within FAK1 as a novel and functional site targeted by multiple sesquiterpene lactone natural products, including parthenolide, to impair FAK1-dependent signaling pathways and breast cancer cell proliferation, survival, and motility **(Fig 2.9)**.

Experimental Model and Subject Details

Chemicals

Parthenolide and dimethylaminoparthenolide were obtained from Cayman Chemicals. Synthesis of the parthenolide-alkyne probe was performed as previously reported [53]. All other chemicals were obtained from Millipore-Sigma unless otherwise noted. Antibodies were obtained from Cell Signaling Technologies unless otherwise noted. Mikanokryptin was synthesized as previously described [92]. Synthesis and characterization of cysteine-reactive covalent ligands screened against FAK1 were either described previously or described in Supporting Methods [74,75,97].

Cell Culture

Professor Benjamin Cravatt's group provided the 231MFP cells. The generation of these cells have been described previously [98]. HCC38 and HEK293T cells were obtained from American Type Culture Collection (ATCC). 231MFP cells were cultured in L-15 (HyClone) media supplemented with 10% fetal bovine serum (FBS) (Gibco) and 2 mM glutamine at 37^{o} C and 0% CO_2. HCC38 cells were cultured in RPMI (Gibco) supplemented with 10 % FBS and 2 mM glutamine at 37^{o} C and 5% CO_2. HEK293T cells were cultured in DMEM (Gibco) supplemented with 10 % FBS and 2 mM glutamine at 37^{o} C and 5% CO_2.

In Vivo Animal Studies

Animal experiments were conducted in accordance with the guidelines of the Institutional Animal Care and Use Committee (IACUC) of the University of California, Berkeley. Female immune-deficient SCID mice (6-8 weeks old) purchased from Taconic laboratories were used for tumor xenograft studies.

Method Details

Cell proliferation and survival

Serum-containing cell proliferation and serum-free cell survival were assessed by Hoechst stain as previously described [75,99]. Briefly, we seeded cells at 1 x 10^4 and 2 x 10^4 cells/well, respectively, in 150 μL serum-containing or serum-free media in 96-well plates overnight. The next day, cells were treated with an additional 50 μL of DMSO vehicle or compound-containing media for 24 or 48 h before fixation and staining with 10 % formalin and Hoechst 33342 (Invitrogen) according to manufacturer's protocol. Wells were washed with PBS, and fluorescence was measured using a fluorescent plate reader with an excitation and emission of 350 nm and 461 nm, respectively.

Measuring cell migration

Cells (5 x 10^4) were placed in collagen-coated Transwell chambers (Corning) and incubated in DMSO vehicle or compound-containing serum-free media for 6 h. Migrated cells were fixed and stained with Diff-Quik solution (Dade Behring) and non-migrated cells were removed using a cotton swab. Migrated cells were imaged and counted at 200 x magnification. An average of cells in three fields for one migration chamber represents n=1.

Flow cytometry to measure apoptosis

Apoptotic analyses were performed following cell exposure (6 cm plates, 1 x 10^6 cells) to DMSO vehicle or compound-containing serum-free media using flow cytometry. Briefly, media and trypsinized cells were pelleted by centrifugation at 500 x g for 5 min, washed once in PBS, resuspended in binding buffer (10 mM HEPES/NaOH at pH 7.4, 140 nM NaCl, 2.5 mM $CaCl_2$) containing propidium iodide (BD) and FITC-conjugated Annexin V (BD) and incubated for 15 min. Cells were then diluted with additional binding buffer to a final volume of 0.5 mL and the fluorescence measured using a BD Biosciences LSR Fortessa cytometer. Annexin-V positive, propidium iodide negative cells were considered early apoptotic and Annexin-V positive, propidium iodide positive cells were considered late apoptotic, as previously described [100]. Data analysis was performed using FlowJo software and quantified for three biological replicates per condition.

Caspase 3/7 activity was performed using the CellEvent Caspase-3/7 Green Flow Cytometry Assay Kit (Thermo) according to manufacturer's specifications. Cells (1 x 10^6) were pretreated with DMSO vehicle or 20 μM caspase inhibitor Q-VD-OPh for 1 h and then with DMSO vehicle or compound-containing serum-free media for an

additional 4 h. Cells were then harvested and pelleted as described above and then resuspended in 0.5 mL PBS containing 500 nM CellEvent Reagent before incubating for 30 min at 37°C. For the final 5 minutes of incubation, SYTOX AADvanced was added to a final concentration of 1 μM. FlowJo Software was used for data analysis, and the percentage of cells exhibiting active caspase-3/7 was quantified for three biological replicates per condition. A t-test was employed for all statistical analyses.

Tumor Xenograft Studies

C.B17 SCID female mice (6-8 weeks old) were injected subcutaneously in the flank with 231MFP cells (1 x 10^6 cells) suspended in serum-free media. Mice were exposed via intraperitoneal injection with either vehicle (18:1:1 PBS/ethanol/PEG40) or 30 mg/kg parthenolide once per day starting 2 weeks, respectively, after injection of cancer cells. Tumor size was assessed weekly by caliper measurements.

RNA interference knockdown of FAK1

Cells were plated in 6-well plates overnight (2 x 10^5 cells/well). Cells were then treated with Dharmafect1 reagent (GE) and either non-targeting siRNA oligonucleotide (siControl, D-001810-10-05, GE) or siFAK1 oligonucleotides (L-003164-00, GE) were transfected for 48 h according to manufacturer instructions. Cells were then reseeded for survival and proliferation as described above. Knockdown was confirmed by Western blotting.

Vectors for FAK1 kinase control and C427A overexpression

The full length FAK1 expression vector was purchased from VectorBuilder (FAK1 sequence NM_005607.4). To express just the kinase domain (AA393-698) Gibson Assembly was performed using the pCMV6-Entry (C-term FLAG + Myc tag) using the primers CTGCCGCCGCGATCGCCatggaaacagatgattatgctgagattataga, TCGAGCGGCCGCGTACGCGTtcttctggactccatcctcatgcgctcttcttgct to amplify the FAK1 kinase domain ORF with desired overlaps, and ACGCGTACGCGGCCG, GGCGATCGCGGCGG to linearize the pCMV6-Entry backbone using a Gibson Assembly Cloning Kit (New England Biolabs) according to manufacturer protocol. To achieve the C427A mutant, site-directed mutagenesis was performed using Q5 Site-Directed Mutagenesis Kit (New England BioLabs) using the primers ACTTGGACGAGCTATTGGAGAAGGC, TCTATTCTTTCTCTTTGAATCTC according to manufacturer protocol.

FAK1 C427A Overexpression

HEK293T cells were seeded at 30% confluency in 15 cm dishes in 10%. On the day of transfection media was replaced with DMEM containing 2.5 % FBS and 500μL Opti-MEM (Thermo) containing 10μg pCMV6-Entry-FAK1 either control or C427A vector and 50 μg polyethylenimine was added to the plate. 48 h later cells were scraped into 1 mL PBS and pelleted at 2,000 g for 5 min at 4^o C and the supernatant removed before

freezing at -80^{o} C to achieve cell lysis. Pellets were then resuspended in 500 μL PBS and further lysed by probe tip sonication at 15 % amplitude for 2 x 10 s on ice. Lysates were cleared by centrifugation at 21,000 g for 20 min at 4^{o} C and the resulting supernatant was mixed with 30 μL anti-FLAG resin (Genescript) and rotated at 4^{o} C for 2 h before washing 3 x with 500 μL PBS and subsequent elution of FLAG-tagged proteins with 100 μL of 250 ng/μL 3 x FLAG peptide (APExBIO) in PBS. Resultant peptides were further concentrated and 3 x FLAG peptide removed using Amicon centrifugal filtration devices (Millipore).

Western Blotting

Cells (1 x 10^{6} cells) were plated in 6 cm dishes in complete media the night before experiment. Cells were washed with PBS and placed in DMSO vehicle or compound-containing serum-free media for 2 h before being washed and collected into a lysis buffer containing protease and phosphatase inhibitors. Proteins were separated on a 4-20% Tris-Glycine precast Midi-PROTEAN TGX SDS/PAGE gel (BioRad). Proteins were then transferred to a PVDF membrane using the iBlot system (Invitrogen). Membranes were blocked in 5 % nonfat milk in TBST and incubated in primary antibodies overnight according to manufacturer instructions. Membranes were then washed in TBST and probed with secondary antibody (Li-Cor) and visualized using a fluorescent scanner (Li-Cor). Quantitation was performed using ImageJ.

FAK1 Activity Assay

FAK1 kinase domain (0.1μg) was preincubated with DMSO vehicle or compound (100 μM) for 30 minutes at room temperature in 5 μL buffer containing 40 mM Tris, 20 mM $MgCl_2$, 2 mM $MnCl_2$, 4% DMSO, pH 7.4. ATP solution (5 μL of a 100 μM solution containing 0.1 μg 4:1 glycine:tyrosine peptide substrate (Promega)) was added and incubated at 37 ^{o}C for 20 min before the addition of ADP-Glo reagent (5μL) (Promega) for an additional 20 min incubation at room temperature. Kinase detection solution (10 μL) (Promega) was added and incubated for 15 minutes at room temperature and luminescence was measured on a plate reader.

IsoTOP-ABPP analysis of parthenolide targets

Cell lysate was collected and probe sonicated in PBS before diluting to 4 mg proteome per biological replicate. Samples were then preincubated with DMSO vehicle or parthenolide (50 μM) for 30 minutes at room temperature before labeling of proteomes with iodoacetamide (IA)-alkyne (10 μM) (Chess Organics) for 1 h at room temperature. Isotopically light (control) or heavy (treated) TEV-biotin handles (100 μM) were appended to probe-labeled proteins using CuAAC through sequential addition of tris(2-carboxyethyl) phosphine (1 mM, Sigma), tris[(1-benzyl-1H-1,2,3-triazol-4-yl)methyl]amine (34 mM, Sigma), copper (II), sulfate (1 mM, Sigma), and finally the linker functionalized with a TEV protease recognition sequence along with an isotopically light or heavy valine, and incubated for 1 h at room temperature. Probe-labeled proteins were subsequently mixed in a 1:1 ratio and precipitated by

centrifugation at 6500 x g and washed in ice cold methanol, resuspended and washed again and then denatured and resolubilized by heating in 1.2 % SDS/PBS to 80 ^{o}C for 5 min. Insoluble components were precipitated by centrifugation at 6500 x g and soluble proteome was diluted in 5 mL 0.2 % SDS/PBS before overnight incubation at 4 ^{o}C with an additional 170 μL resuspended avadin-agarose beads. Bead-linked proteins were then washed three times in PBS and water and then resuspended in 6 M urea/PBS before being reduced in DTT (1 mM, Sigma) and heated to 65 ^{o}C for 20 min, alkylated with iodoacetamide (18 mM, Sigma) and heated to 37 ^{o}C for 30 min, then washed and resuspended in 2 M urea and trypsinized overnight with 0.5 mg/mL sequencing grade trypsin (Promega) at 37 ^{o}C. Tryptic peptides were then eluted and the remaining beads were washed three times in PBS and water, once in TEV buffer solution (water, TEV buffer, 100 mM DTT), and resuspended in TEV buffer with Ac-TEV protease and incubated overnight at 29 ^{o}C. TEV-digested peptides were then isolated, acidified with formic acid (1.2 M, Spectrum), and prepared for LC-MS/MS analysis, as previously described [75,97].

Proteomic profiling to determine sites of modification of parthenolide and TRH 1-191

FAK1 kinase domain (AA393-698) (Promega) (25 μg) was pre-incubated with DMSO vehicle or compound (parthenolide or TRH 1-191) (100 μM) for 30 min at room temperature. Samples were then treated with isotopically light (control) or heavy (treated) iodoacetamide (Iodoacetamide-$^{13}C_2$, 2-d_2, #721328, Millipore-Sigma) for 1 h at room temperature before combination of control and treated samples and subsequent precipitation with 20% trichloroacetic acid for 2 h at -80^{o} C. Proteins were pelleted at 20,000 x *g* and washed with ice cold 10 mM HCl / 90% acetone before resuspension in 60 μL 4 M Urea and 0.5 x ProteaseMax (Promega), vortexed, and then subsequently diluted with an additional 40 μL 100 mM ammonium bicarbonate. Samples were incubated at 60^{o} C for 30 min following the addition of 10 μL 110 mM TCEP, before dilution with 120 μL 0.04 x ProteaseMax and 5 μg/μL sequencing grade trypsin (Promega) in PBS. Samples were digested overnight at 37^{o} C in a rocking incubator before acidification with 12 μL formic acid and storage at -80^{o} C until MS analysis.

MS analysis

Total peptides from TEV protease digestion for isoTOP-ABPP or tryptic peptides for shotgun proteomics were pressure loaded onto 250 μm tubing packed with Aqua C18 reverse phase resin (Phenomenex) and previously equilibrated using an Agilent 600 series HPLC using gradient from 100% buffer A to 100% buffer B over 10 min, followed by a 5 min wash with 100% buffer B and a 5 min wash with 100% buffer A. Samples were then attached to an equilibrated 13 cm laser pulled column packed with 10 cm Aqua C18 reverse-phase resin and 3 cm of strong-cation exchange resin using a MicroTee PEEK 360 mm fitting (Thermo Fisher Scientific #p-888), and then analyzed using a Q-Exactive Plus mass spectrometer (Thermo Fisher Scientific) using a Multidimenstional Protein Identification Technology (MudPIT), using 0 %, 25 %, 50 %, 80 %, and 100 % salt bumps of 500 mM aqueous ammonium acetate and a gradient of

5-55 % buffer B in buffer A (buffer A: 95:5 water:acetonitrile, 0.1 % formic acid; buffer B 80:20 acetonitrile:water, 0.1 % formic acid). Data was collected in data-dependent acquisition mode with dynamic exclusion enabled (60 s). One full MS (MS1) scan (400-1800 m/z) was followed by 15 MS2 scans (ITMS) of the nth most abundant ions. Heated capillary temperature was set to 200 C and the nanospray voltage was set to 2.75 kV, as previously described [75,97].

Data was extracted using Raw Extractor 1.9.9.2 (Scripps Research Institute) in the form of MS1 and MS2 files and was subsequently searched against the Uniprot human database using ProLuCID search methodology in IP2 v.3 (Integrated Proteomics Applications, Inc.) [101]. For isoTOP-ABPP, peptides were analyzed with a static modification for cysteine carboxyaminomethylation (+57.02146) and differential modifications for light or heavy TEV tags (+464.28596 and +470.29977, respectively) for cysteine, and methionine oxidation, with up to two total modifications per peptide. For proteomic analysis of while FAK1 tryptic digests, peptides were searched with differential modifications for light or heavy iodoacetamide (+57.02146 and +61.04073, respectively) on cysteines, for parthenolide or TRH 1-191 addition (+248.14125 or + 259.04001, respectively) on cysteines, and methionine oxidation, with up to two total modifications per peptide fragment. In both analyses, peptides were required to have at least one tryptic end and in isoTOP-ABPP all fragments must contain the TEV modification. To ensure a peptide false-positive of less than 5% ProLuCID data were filtered through DTASelect prior to downstream analyses [102]. Only peptides that were present in at least two out of four biological replicates were interpreted for final quantification and only those peptides with light to heavy ratios >10 that appeared in three out of four biological replicates were considered as targets of parthenolide.

Gel-Based ABPP

Recombinant FAK1 kinase domain was diluted to .002 μg/μL in PBS and 50 μL protein solution was treated with DMSO vehicle or compound for 30 min at room temperature. Samples were then incubated with IA-rhodmaine (1 μM) (Thermo) for 1 h at room temperature in the dark before separating proteins by SDS/PAGE. Probe-labeled proteins were analyzed by in-gel fluorescence using a Bio-Rad gel scanner and fluorescent bands were quantified using Image J.

Quantification and Statistical Analysis

Microsoft Excel and Graphpad Prism software were used for statistical analysis. Statistical and quantification details of experiments can be found in the figure legends. Significance was defined a $p<0.05$ between comparison groups.

Figures

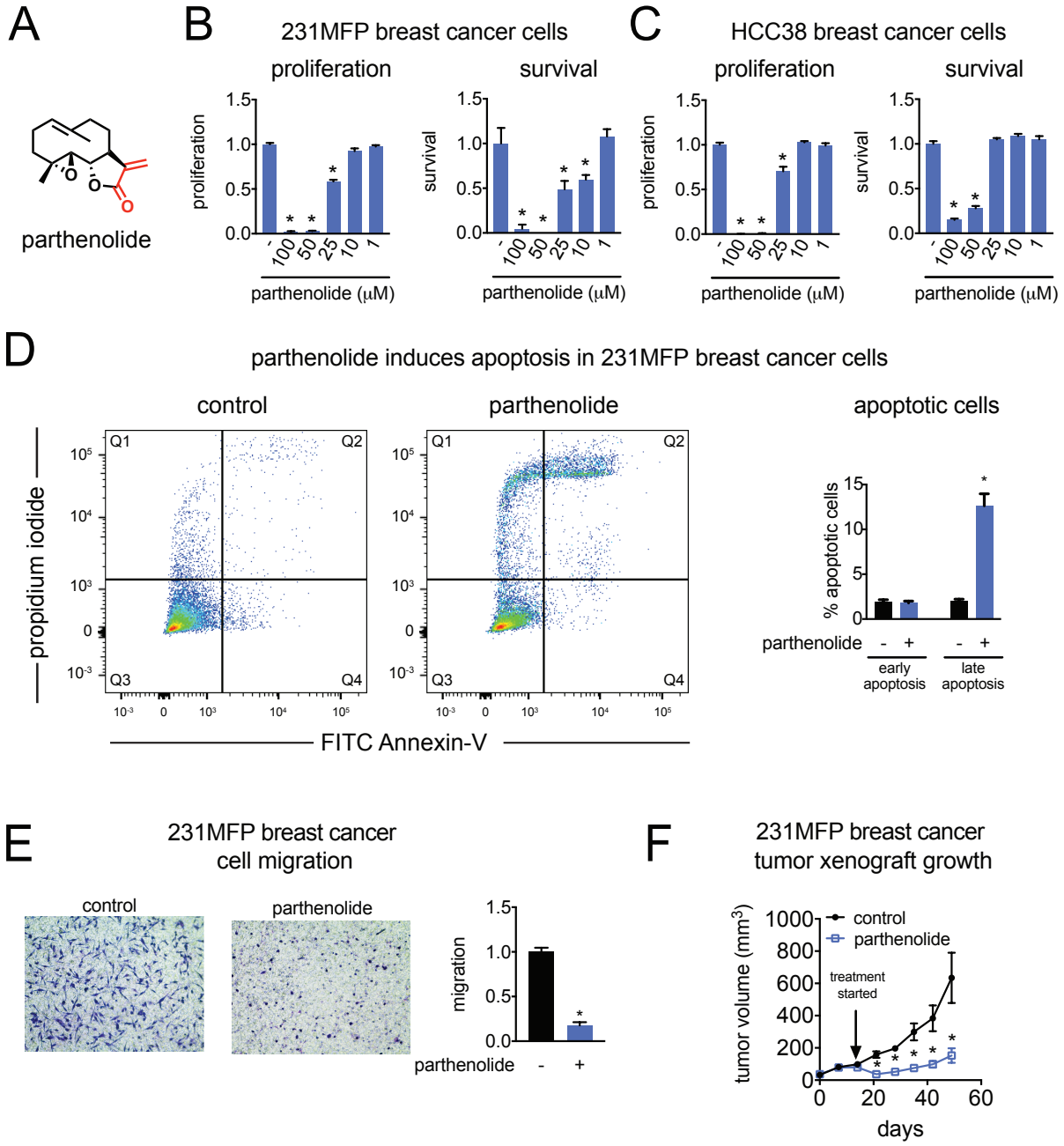

Figure 2.1. Parthenolide impairs TNBC pathogenicity. (**A**) Structure of parthenolide (red denotes cysteine-reactive enone). **(B-C)** 231MFP **(B)** and HCC38 **(C)** breast cancer cell 48 h survival and proliferation from cells treated with DMSO control or parthenolide assessed by Hoechst stain. **(D)** Percent early-stage and late-stage apoptotic cells assessed by flow cytometry after treating cells with DMSO control or parthenolide (50 μM) for 2 h. Shown on the left panels are representative FACS data. On the right bar graph are noted early apoptotic cells defined as FITC+/PI- and late apoptotic cells defined as FITC+/PI+ cells. **(E)** Migration of 231MFP cells treated with DMSO control or parthenolide (50 μM) for 6 h. Representative image of migrated cells

are shown. **(F)** 231MFP tumor xenograft growth in immune-deficient SCID mice treated with vehicle (18:1:1 saline:ethanol:PEG40) or parthenolide (30 mg/kg ip) daily once per day with treatment initiated after tumor establishment 14 days after tumor implantation. Images shown in **(E)** are representative of n=3. Data shown in **(B-F)** are average ± sem, n=3-6/group. Significance is expressed as *$p<0.05$ compared to vehicle-treated controls.

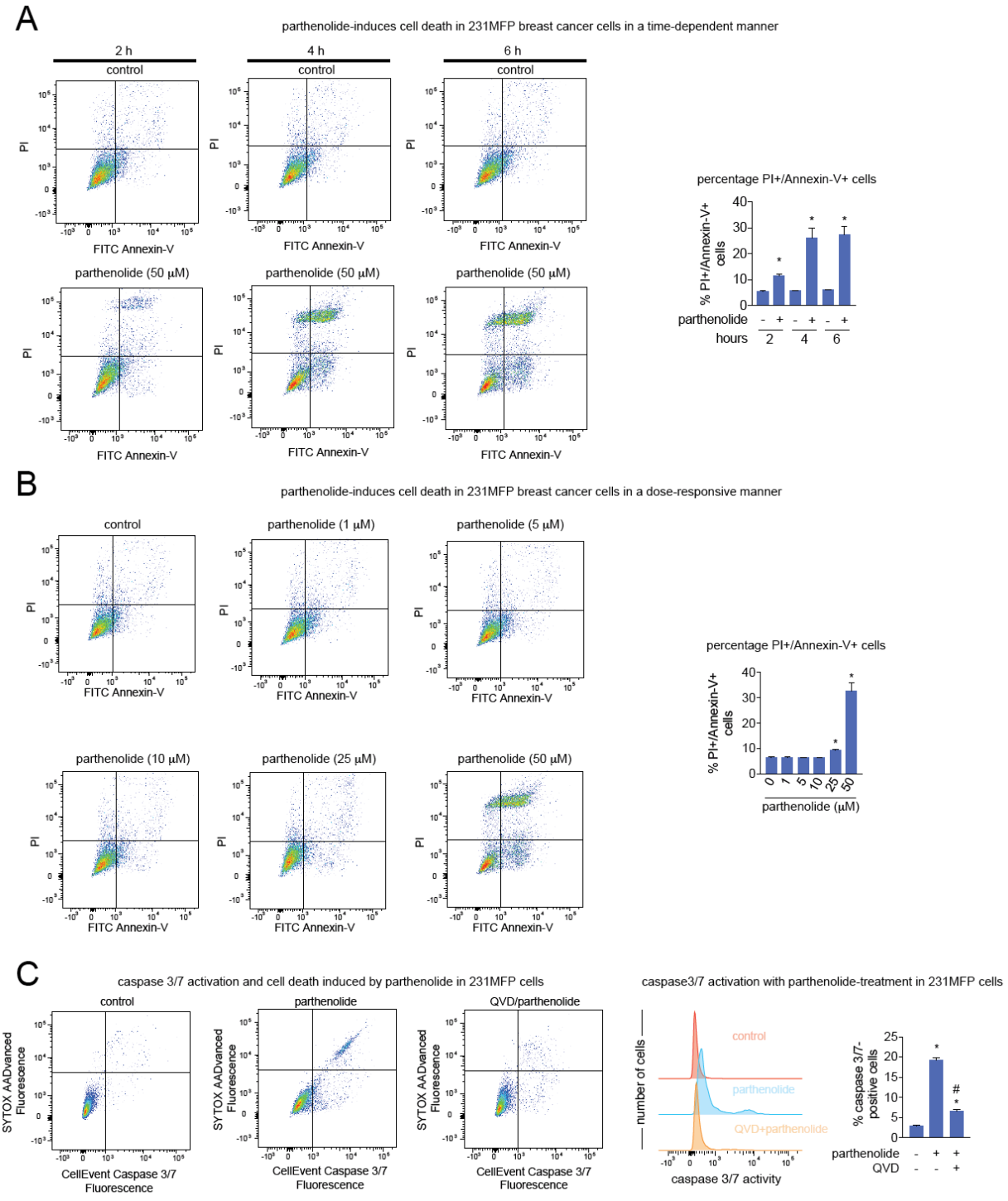

Figure 2.2. Parthenolide induces cell death in a time-dependent and dose-responsive manner. (**A)** 231MFP breast cancer cells were treated with DMSO vehicle or parthenolide (50 μM) for 2, 4, and 6 h and percentage of cell death was assessed by flow cytometry. Shown on the right bar graph are percentage PI+/Annexin-V+ cells. **(B)** 231MFP breast cancer cells were treated with DMSO vehicle or parthenolide (1-50 μM)

for 6 h and cell death was assessed by flow cytometry. Shown on the right bar graph are percentage PI+/Annexin-V+ cells. **(C)** 231MFP breast cancer cells were treated with DMSO vehicle or the caspase inhibitor Q-VD-OPh (QVD) (20 μM) for 1 h prior to treatment of cells with DMSO vehicle or parthenolide (50 μM) for 4 h and caspase 3/7 activation and cell death was assessed by flow cytometry. Percentage of cells exhibiting active caspase 3/7 were quantified and shown in the right bar graph. Images shown in **(A-C)** are representative of n=3. Data shown in **(A-C)** are average ± sem, n=3 biological replicates/group. Significance is expressed as *$p<0.05$ compared to vehicle-treated controls**.**

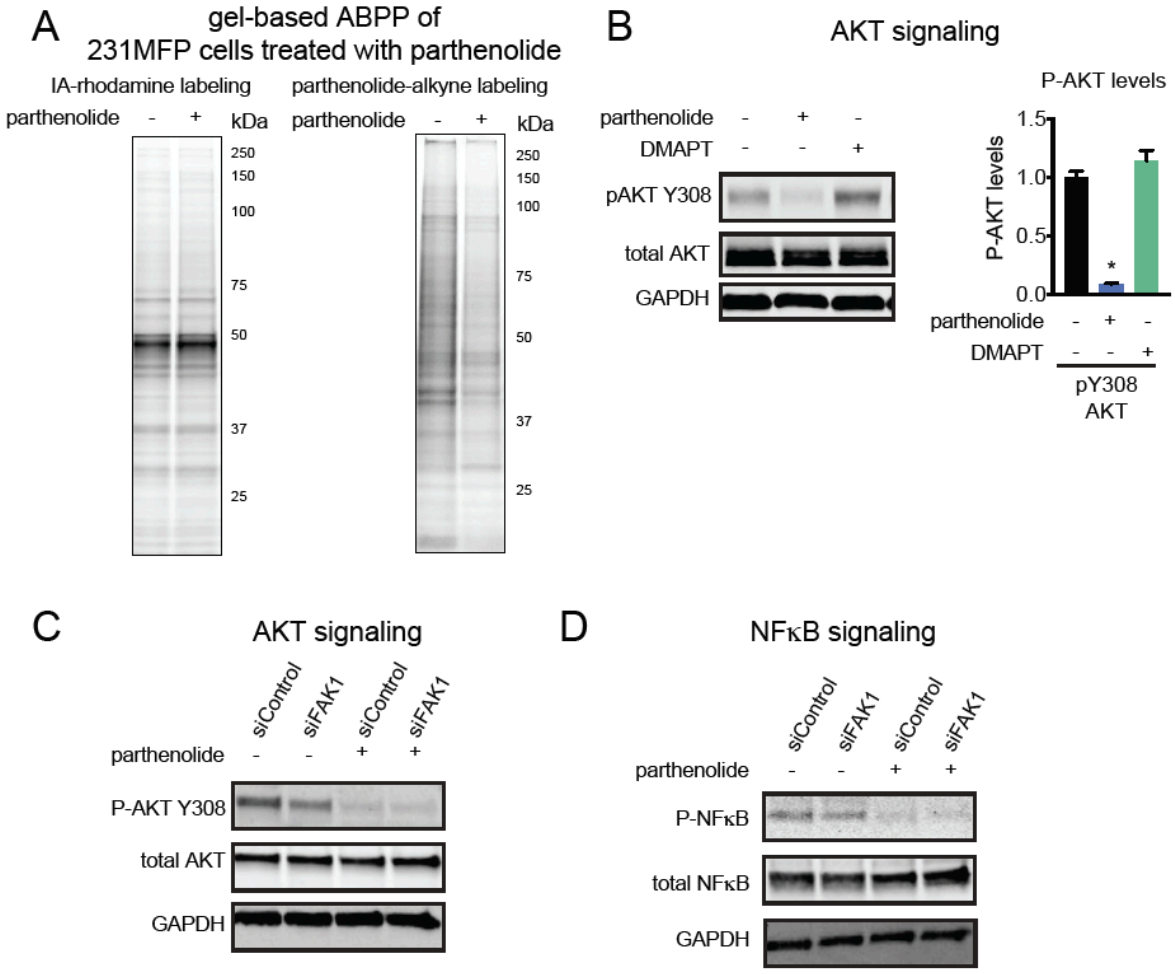

Figure 2.3. Effects of parthenolide. (**A)** Gel-based ABPP analysis of parthenolide in 231MFP proteomes *in situ*. In the left panel, 231MFP cells were pre-incubated with parthenolide (50 μM) for 30 min prior to labeling with IA-rhodamine (1 μM) for 1 h, after which cells were harvested and subjected to SDS/PAGE and in-gel fluorescence. In the right panel, 231MFP cells were pre-incubated with parthenolide (50 μM) for 30 min prior to parthenolide-alkyne labeling (50 μM) for 1 h, after which rhodamine-azide was appended by CuAAC, and proteome was separated by SDS/PAGE and visualized by in-gel fluorescence. **(B)** AKT signaling in 231MFP cells treated with vehicle DMSO, parthenolide (50 μM), or DMAPT (50 μM) for 2 h, assessed by Western blotting. **(C, D)** AKT **(C)** and NFκB **(D)** signaling in 231MFP siControl and siFAK1 cells treated with vehicle DMSO or parthenolide (50 μM) for 2 h. Gels shown in **(A-D)** are representative gels of n=3 biological replicates/group. Bar graph shown in **(B)** is average ± sem, n=3/group.

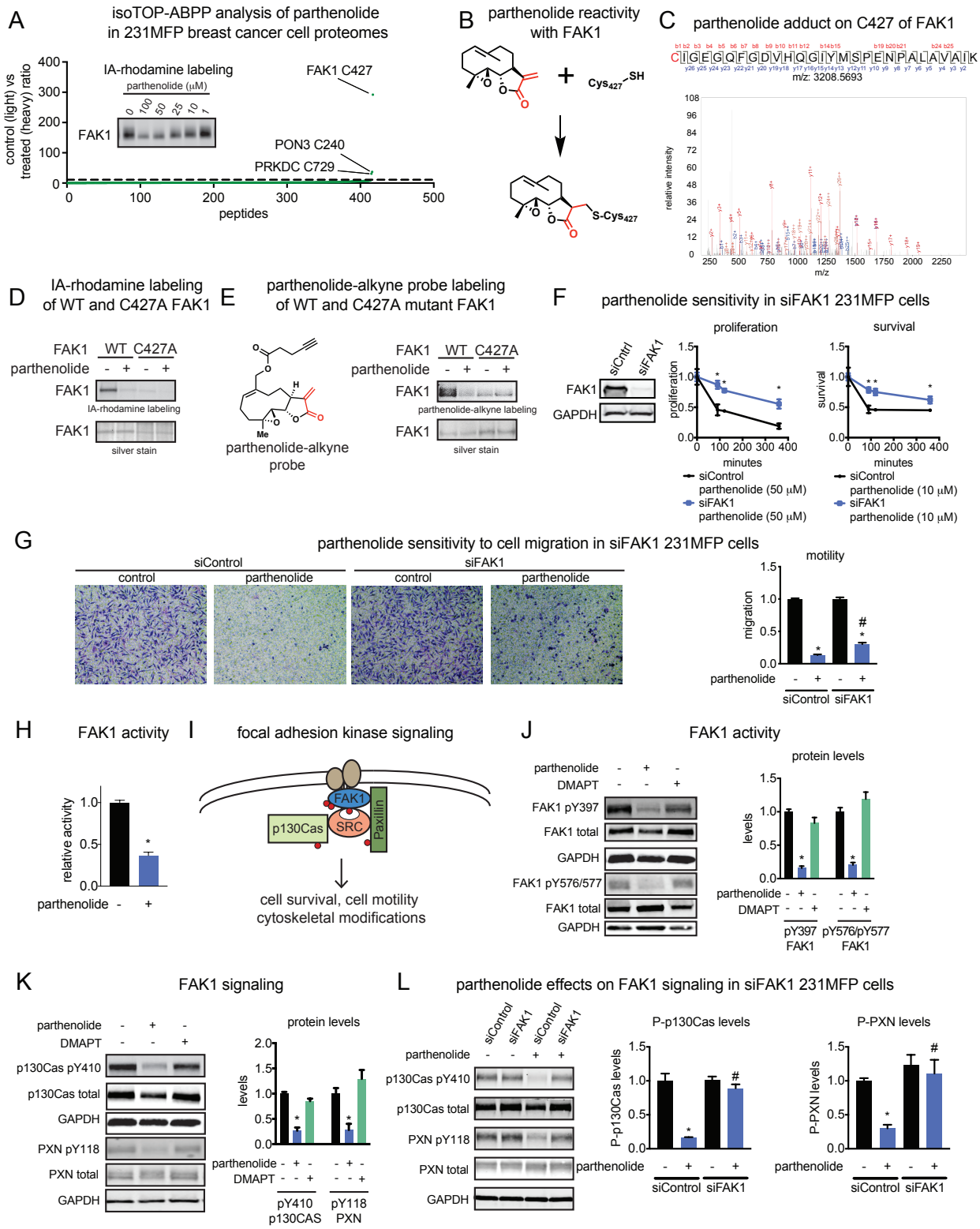

Figure 2.4. Parthenolide targets an allosteric cysteine in FAK1 to inhibit FAK1 activity and signaling. (A) isoTOP-ABPP analysis of parthenolide in 231MFP cell lysate. 231MFP proteomes were pre-treated with DMSO vehicle or parthenolide (50 μM) for 30 min prior to IA-alkyne (100 μM) labeling for 1 h. Shown are probe-modified

peptides detected in at least two of out four biological replicates and the control (isotopically light) versus parthenolide-treated (isotopically heavy) ratios for each peptide. Those probe-modified peptides showing ratios >10 are peptides that were observed in three out of four biological replicates. Shown in the inset is gel-based ABPP analysis of parthenolide competition against IA-rhodamine labeling of pure human FAK1 kinase domain. **(B)** Proposed reactivity of parthenolide with C427 of FAK1. **(C)** Mass spectrometry data of covalent parthenolide adduct on C427 of human FAK1 protein. Pure human FAK1 kinase domain was labeled with parthenolide (100 μM) for 30 minutes and subsequently digested with trypsin for LC-MS/MS proteomic analysis. **(D)** Gel-based ABPP analysis of recombinant human wild-type and C427A mutant FAK1 kinase domain protein pre-incubated with parthenolide (50 μM) for 30 min prior to IA-rhodamine labeling (1 μM) for 1 h. Proteins were separated by SDS/PAGE and visualized by in-gel fluorescence. Also shown is silver-staining of the gel as a loading control. **(E)** Parthenolide-alkyne probe labeling of recombinant human wild-type and C427A mutant FAK1 kinase domain protein pre-incubated with parthenolide (50 μM) for 30 min prior to parthenolide-alkyne labeling (50 μM) for 1h. Rhodamine-azide was appended to probe-labeled protein by CuAAC and proteins were separated by SDS/PAGE and visualized by in-gel fluorescence. Also shown is silver-staining of the gel as a loading control. **(F)** FAK1 knockdown in 231MFP cells using siControl or siFAK1 oligonucleotides confirmed by Western blotting. Serum-containing cell proliferation and serum-free cell survival in siControl or siFAK1 231MFP cells treated with parthenolide (10 μM) for the reported time period. **(G)** Cell migration in siControl or siFAK1 231MFP cells treated with parthenolide (10 μM) for 4 h. **(H)** FAK1 activity with pure human FAK1 protein pre-treated with vehicle DMSO or parthenolide (100 μM) for 30 min before addition of peptide substrate and ATP. Activity was assessed by substrate peptide phosphorylation reading out ADP release using an ADP-Glo kinase assay. **(I)** FAK1 signaling pathways. **(J-K)** FAK1 signaling assessed by Western blotting in 231MFP cells treated with vehicle DMSO or parthenolide (50 μM) for 2 h. **(L)** FAK1 signaling assessed by Western blotting in siControl and siFAK1 cells treated with vehicle DMSO or parthenolide (50 μM) for 2 h. Gels shown in **(A, D-F, J-L)** are representative images from n=3 biological replicates/group. Data shown in **(F-H, J-L)** are average ± sem, n=3-6/group. Significance is expressed as *$p<0.05$ compared to vehicle-treated controls, # comparing parthenolide-treated siFAK1 cells compared to parthenolide-treated siControl cells. **Figure 2.2** is related to **Table 1** and **Figure 2.5**.

A

231MFP breast cancer cell survival of parthenolide versus other sesquiterpene lactones

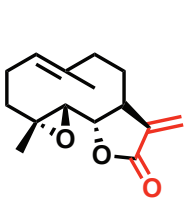

parthenolide

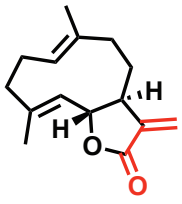

costunolide

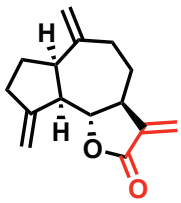

dehydrocostus lactone

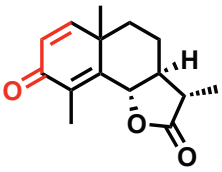

α-santonin

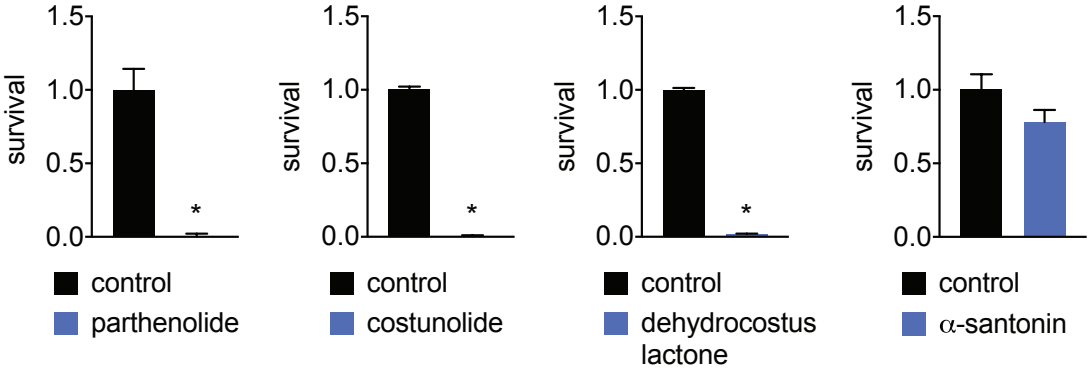

B

IA-rhodamine labeling of pure FAK1 protein

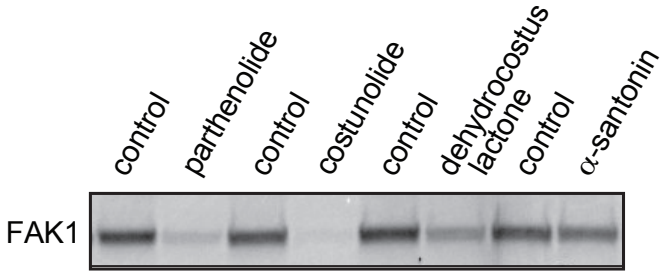

C

mikanokryptin

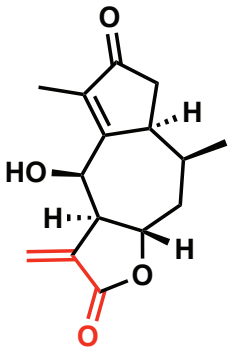

D

IA-rhodamine labeling of pure FAK1 protein

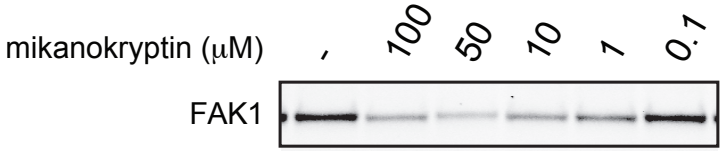

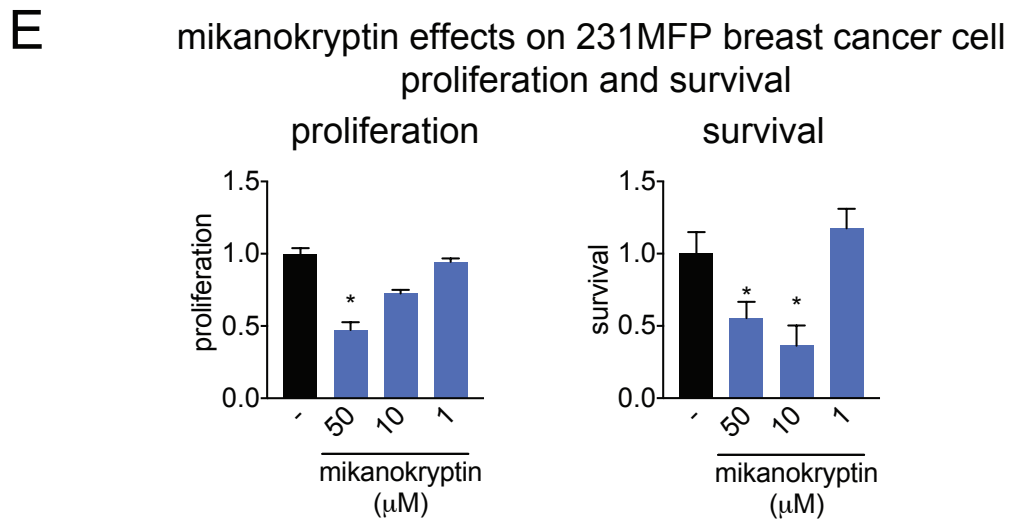

Figure 2.5. Other sesquiterpene lactones also interact with FAK1 and impair TNBC cell viability. **(A)** 231MFP cell survival (48 h) after treatment with DMSO vehicle or parthenolide and other sesquiterpene lactones (50 μM) assessed by Hoechst stain. **(B)** Gel-based ABPP analysis of parthenolide and other sesquiterpene lactones. Pure human FAK1 kinase domain was pre-treated with DMSO vehicle or natural products (50 μM) for 30 min prior to IA-rhodamine labeling (1 μM) for 1 h and then analyzed by in-gel fluorescence. **(C)** Structure of mikanokryptin. Cysteine-reactive enone highlighted in red. **(D)** Gel-based ABPP analysis of mikanokryptin analyzed as described in **(B)**. **(E)** 231MFP breast cancer cell proliferation and survival (48 h) after treatment of cells with DMSO vehicle or mikanokryptin. Gels shown in **(B, D)** are representative of n=3. Data shown in **(A, E)** are average ± sem, n=6/group. Significance is expressed as *p<0.05 compared to vehicle-treated controls.

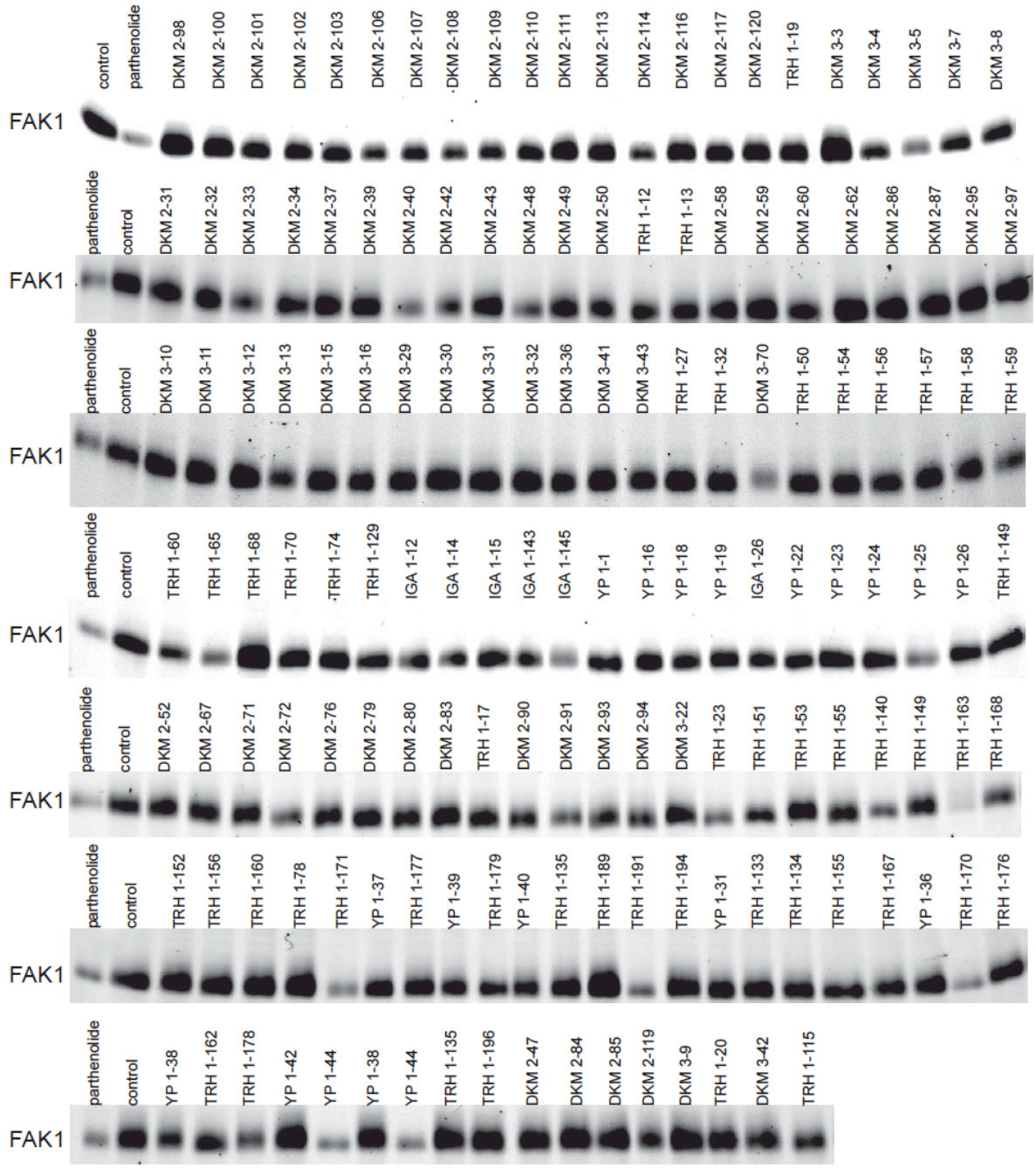

Figure 2.6. Covalent ligand screen against FAK1. Gel-based ABPP screening of cysteine-reactive fragment library (50 μM, 30 min pre-incubation) against IA-rhodamine labeling (1 μM, 1 labeling). Probe-labeled proteins were analyzed by in-gel fluorescence.

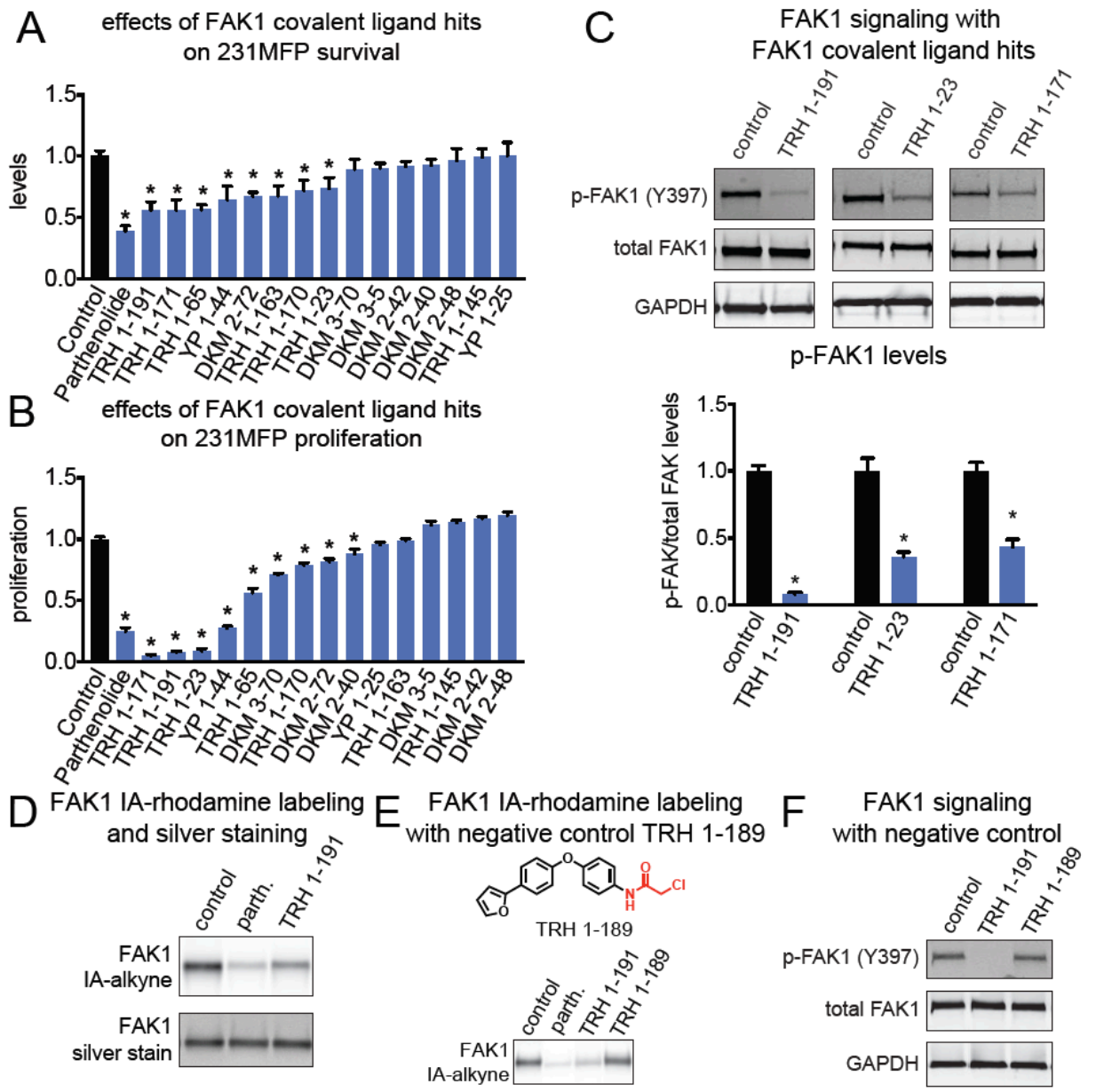

Figure 2.7. Effects of FAK1 covalent ligands on breast cancer cells. (**A, B**) 231MFP breast cancer cell survival and proliferation (48 h) from cells treated with DMSO vehicle, parthenolide, or FAK1 covalent ligand hits (50 μM), assessed by Hoechst stain. **(C)** FAK1 signaling in breast cancer cells treated with DMSO vehicle or FAK1 covalent ligand hits (50 μM). Gel images are representative images from n=3. **(D)** Gel-based ABPP and silver staining analysis of parthenolide and TRH 1-191 *in vitro* treatment with human FAK1 pure protein. FAK1 protein was pre-incubated with parthenolide or TRH 1-191 (50 μM, 30 min) prior to IA-rhodamine labeling (11 μM, 1 h) and in-gel fluorescence analysis. Gels were also silver stained to confirm equal FAK1 protein loading. **(E)** Gel-based ABPP analysis of TRH 1-191 analog TRH 1-189 that does not inhibit FAK1 IA-alkyne labeling. **(F)** FAK1 signaling assessed by Western blotting. 231MFP cells were treated with DMSO vehicle or TRH 1-191 or TRH 1-189 (50 μM) for 2 h. **(G)** 231MFP

breast cancer cell survival and proliferation (48 h) from cells treated with DMSO vehicle, TRH 1-191, or TRH 1-189 (50 μM), assessed by Hoechst stain. Data shown are average ± sem, n=3-6/group. Significance is expressed as *p<0.05 compared to vehicle-treated controls.

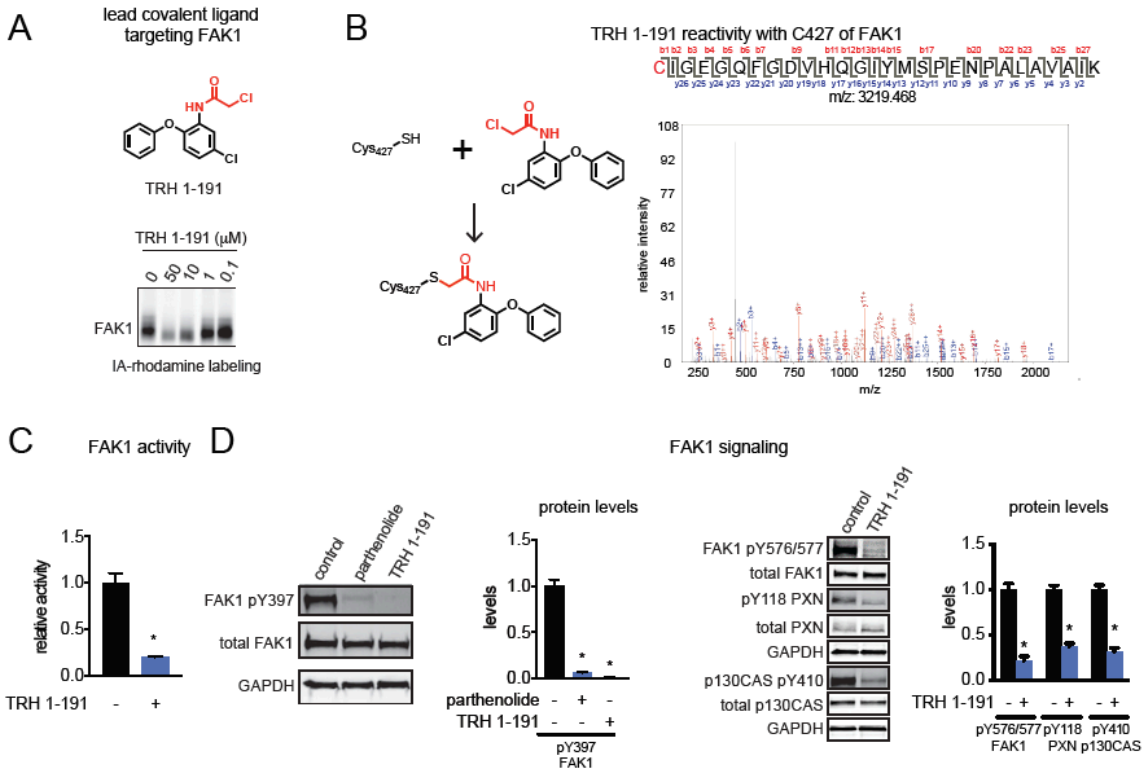

Figure 2.8. Covalent ligand TRH 1-191 reacts with C427 of FAK1 and inhibits FAK1 signaling and breast cancer pathogenicity. (A) Structure of TRH 1-191 showing the cysteine-reactive chloroacetamide warhead in red. Shown below is a gel-based ABPP analysis of TRH 1-191 competition against IA-rhodamine labeling of pure human FAK1 protein. **(B)** Presumed reaction of TRH 1-191 with C427 FAK1 and mass spectrometry data showing the TRH 1-191 adduct on C427 of FAK1. Pure human FAK1 kinase domain was treated with TRH 1-191 (100 μM) and the protein was subsequently digested with trypsin for LC-MS/MS analysis. **(C)** FAK1 activity of pure human FAK1 kinase domain assessed by peptide substrate phosphorylation and read-out by ADP-Glo kinase assay. FAK1 protein was treated with DMSO vehicle or TRH 1-191 (100 μM) for 30 min prior to addition of substrates. **(D)** FAK1 signaling assessed by Western blotting in 231MFP cells treated with vehicle DMSO or TRH 1-191 (50 μM) for 2 h. Gels shown in **(A, D)** are representative of n=3. Data shown in **(C-D)** are average ± sem, n=3 biological replicates/group. Significance is expressed as *p<0.05 compared to vehicle-treated controls.

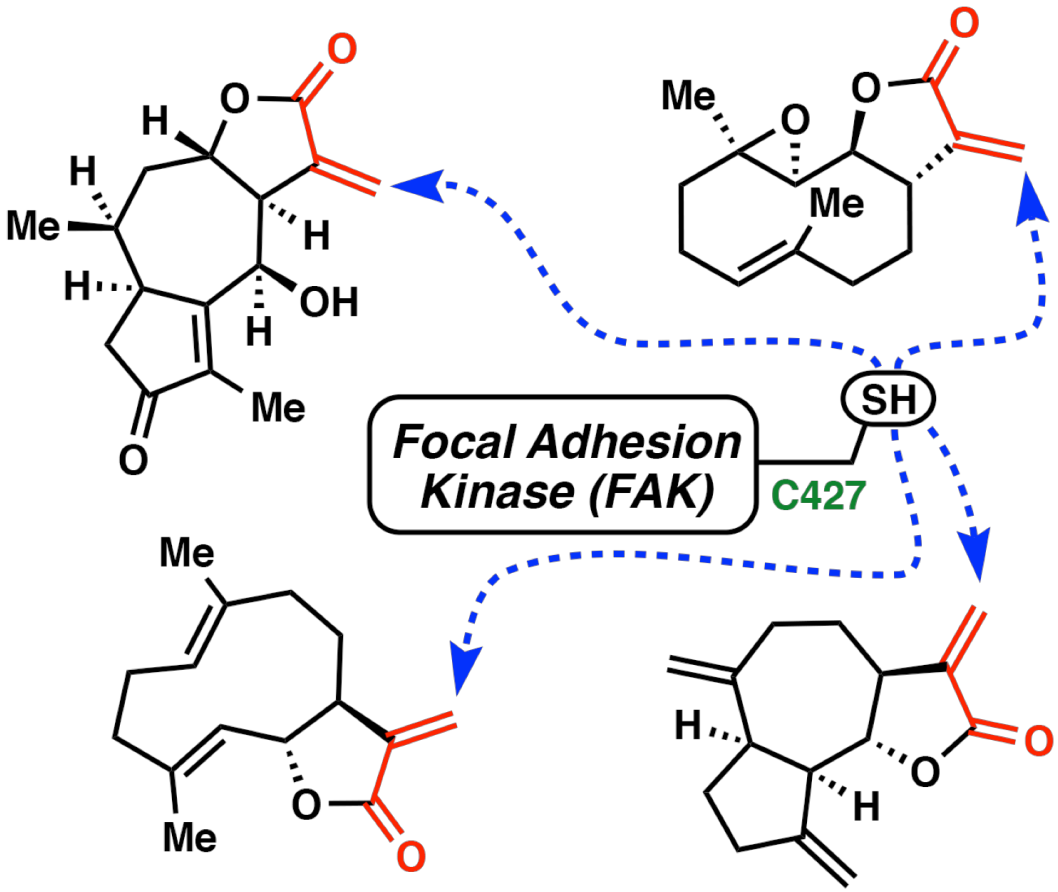

Figure 2.9. Graphical abstraction of sesquiterpene lactone action. Using chemoproteomic platforms we identified C427 within FAK1 as a novel and functional site targeted by multiple sesquiterpene lactone natural products including parthenolide.

CHAPTER THREE: Conclusions

For thousands of years humans have used natural products as tools for treating and curing disease. Technology today has expanded the tool-belt of the modern drug developer to include a suite of new tools that no longer limit him to discovering and utilizing what is readily available in nature. While it is imperative that we implement new technologies to combat the complex diseases of our era, it is also important that we look back and utilize these new tools to potentially expand the versatility of longstanding tools. Technologies such as chemoproteomics and chemical genetics are well poised to expand on the versatility of natural product based drug discovery, capable of finding new targets in the proteome in hopes of exploiting them in the fight against today's most pernicious illnesses.

In this work I show that triple negative breast cancer is susceptible to the natural product parthenolide as well as a host of other sesquiterpene lactone natural products. Then, by utilizing isoTOP-ABPP chemoproteomic platforms I uncover that some of the mechanism of action behind parthenolide's anti-cancer activity is driven by the covalent modification of C427 on FAK1, modification of which results in loss of FAK1 functionality. Notably, C427 is a druggable hotspot not known to be targeted by this or any other natural product before these studies. Further, I demonstrate that inhibition of this site alone is sufficient to inhibit triple negative cancer growth and survival, potentially unlocking another use for this family of natural products.

Further, upon discovery of the druggable hotspot's exploitability, I perform a small fragment molecule library screen against recombinant FAK1 in an attempt to find a more synthetically tractable molecule against the hotspot. Additionally, I demonstrate that TRH 1-191 is capable of binding to FAK1 at C427 and phenocopies parthenolide's anticancer activities.

These studies taken as a whole show that the future of therapeutics is not built on just one method of drug discovery but on many. Tools such as chemoproteomics and chemical genetics are powerful in their own right but are even stronger when utilized in tandem with older technologies such as natural product based drug discovery. As the field of chemical biology advances, the focus will continue to be on finding new small molecule inhibitors against targets driving illnesses such as cardiovascular disease, cancer, and Alzheimer's disease. With the tools of both past and future generations and the creativity in combining them it may be possible to someday treat and cure these diseases.

REFERENCES

1. American Cancer Society. Cancer Facts & Figures 2019. 76 (2019).

2. Li, Z. & Kang, Y. Emerging therapeutic targets in metastatic progression: A focus on breast cancer. *Pharmacol. Ther.* **161**, 79–96 (2016).

3. Urruticoechea, A. *et al.* Recent Advances in Cancer Therapy: An Overview. *Curr. Pharm. Des.* **16**, 3–10 (2010).

4. Zugazagoitia, J. *et al.* Current Challenges in Cancer Treatment. *Clin. Ther.* **38**, 1551–1566 (2016).

5. Polyak, K. & Weinberg, R. A. Transitions between epithelial and mesenchymal states: acquisition of malignant and stem cell traits. *Nat. Rev. Cancer* **9**, 265–273 (2009).

6. Hughes, J., Rees, S., Kalindjian, S. & Philpott, K. Principles of early drug discovery: Principles of early drug discovery. *Br. J. Pharmacol.* **162**, 1239–1249 (2011).

7. Butler, M. S. Chapter 11. A Snapshot of Natural Product-Derived Compounds in Late Stage Clinical Development at the End of 2008. in *RSC Biomolecular Sciences* (eds. Buss, A. D. & Butler, M. S.) 321–354 (Royal Society of Chemistry, 2009). doi:10.1039/9781847559890-00321

8. Newman, D. J. & Cragg, G. M. Natural Products as Sources of New Drugs from 1981 to 2014. *J. Nat. Prod.* **79**, 629–661 (2016).

9. Shen, B. A New Golden Age of Natural Products Drug Discovery. *Cell* **163**, 1297–1300 (2015).

10. Pye, C. R., Bertin, M. J., Lokey, R. S., Gerwick, W. H. & Linington, R. G. Retrospective analysis of natural products provides insights for future discovery trends. *Proc. Natl. Acad. Sci.* **114**, 5601–5606 (2017).

11. Fleming, A. On the antibacterial action of cultures of a penicillium, with special reference to their use in the isolation of B. influenzae. *Br. J. Exp. Pathol.* **10**, 226–236 (1929).

12. Waksman, S. A. & Tishler, M. The Chemical Nature of Actinomycin, an Antimicrobial substance produced by actinomyces antibioticus. *JBiol Chem* **143**, 529–528 (1942).

13. Zaffiri, L., Gardner, J. & Toledo-Pereyra, L. H. History of Antibiotics. From Salvarsan to Cephalosporins. *J. Invest. Surg.* **25**, 67–77 (2012).

14. Ōmura, S. & Shiomi, K. Discovery, chemistry, and chemical biology of microbial products. *Pure Appl. Chem.* **79**, 581–591 (2007).

15. *Inflammation in the pathogenesis of chronic diseases: the COX-2 controversy*. (Springer, 2007).

16. Pascart, T. & Lioté, F. Gout: state of the art after a decade of developments. *Rheumatology* (2018). doi:10.1093/rheumatology/key002

17. Weaver, B. A. How Taxol/paclitaxel kills cancer cells. *Mol. Biol. Cell* **25**, 2677–2681 (2014).

18. Endo, A. A historical perspective on the discovery of statins. *Proc. Jpn. Acad. Ser. B* **86**, 484–493 (2010).

19. Tobert, J. A. Lovastatin and beyond: the history of the HMG-CoA reductase inhibitors. *Nat. Rev. Drug Discov.* **2**, 517–526 (2003).

20. Drahl, C., Cravatt, B. F. & Sorensen, E. J. Protein-Reactive Natural Products. *Angew. Chem. Int. Ed.* **44**, 5788–5809 (2005).

21. Taunton, J., Collins, J. L. & Schreiber, S. L. Synthesis of Natural and Modified Trapoxins, Useful Reagents for Exploring Histone Deacetylase Function. *J. Am. Chem. Soc.* **118**, 10412–10422 (1996).

22. Harding, M. W., Galat, A., Uehlingt, D. E. & Schreibert, S. L. A receptor for the immunosuppresant FK506 is a cis-trans peptidyl-prolyl isomerase. *Nature* **341**, 3 (1989).

23. Schreiber, S. L. & Crabtree, G. R. The mechanismof action of cyclosporinA and FK506. *Immunol. Today* **13**, 136–142 (1992).

24. Jafari, R. *et al.* The cellular thermal shift assay for evaluating drug target interactions in cells. *Nat. Protoc.* **9**, 2100–2122 (2014).

25. Park, H., Ha, J., Koo, J. Y., Park, J. & Park, S. B. Label-free target identification using in-gel fluorescence difference via thermal stability shift. *Chem. Sci.* **8**, 1127–1133 (2017).

26. Huber, K. V. M. *et al.* Proteome-wide drug and metabolite interaction mapping by thermal-stability profiling. *Nat. Methods* **12**, 1055–1057 (2015).

27. Schürmann, M., Janning, P., Ziegler, S. & Waldmann, H. Small-Molecule Target Engagement in Cells. *Cell Chem. Biol.* **23**, 435–441 (2016).

28. Seashore-Ludlow, B. & Lundbäck, T. Early Perspective: Microplate Applications of the Cellular Thermal Shift Assay (CETSA). *J. Biomol. Screen.* **21**, 1019–1033 (2016).

29. Dekker, F. J. *et al.* Small-molecule inhibition of APT1 affects Ras localization and signaling. *Nat. Chem. Biol.* **6**, 449–456 (2010).

30. Parker, C. N., Ottl, J., Gabriel, D. & Zhang, J.-H. Chapter 8. Advances in Biological Screening for Lead Discovery. in *RSC Biomolecular Sciences* (eds. Buss, A. D. & Butler, M. S.) 243–271 (Royal Society of Chemistry, 2009). doi:10.1039/9781847559890-00243

31. Fonovic, M. & Bogyo, M. Activity Based Probes for Proteases: Applications to Biomarker Discovery,Molecular Imaging and Drug Screening. *Curr. Pharm. Des.* **13**, 253–261 (2007).

32. Liu, Y., Patricelli, M. P. & Cravatt, B. F. Activity-based protein profiling: The serine hydrolases. *Proc. Natl. Acad. Sci.* **96**, 14694–14699 (1999).

33. Moellering, R. E. & Cravatt, B. F. How Chemoproteomics Can Enable Drug Discovery and Development. *Chem. Biol.* **19**, 11–22 (2012).

34. Nomura, D. K., Dix, M. M. & Cravatt, B. F. Activity-based protein profiling for biochemical pathway discovery in cancer. *Nat. Rev. Cancer* **10**, 630–638 (2010).

35. Nomura, D. K. & Maimone, T. J. Target Identification of Bioactive Covalently Acting Natural Products. in *Activity-Based Protein Profiling* (eds. Cravatt, B. F., Hsu, K.-L. & Weerapana, E.) **420**, 351–374 (Springer International Publishing, 2018).

36. Roberts, A. M., Ward, C. C. & Nomura, D. K. Activity-based protein profiling for mapping and pharmacologically interrogating proteome-wide ligandable hotspots. *Curr. Opin. Biotechnol.* **43**, 25–33 (2017).

37. Lin, S. *et al.* Redox-based reagents for chemoselective methionine bioconjugation. *Science* **355**, 597–602 (2017).

38. Montgomery, D. C. & Meier, J. L. Mapping Lysine Acetyltransferase–Ligand Interactions by Activity-Based Capture. in *Methods in Enzymology* **574**, 105–123 (Elsevier, 2016).

39. Shannon, D. A. *et al.* Investigating the Proteome Reactivity and Selectivity of Aryl Halides. *J. Am. Chem. Soc.* **136**, 3330–3333 (2014).

40. Shannon, D. A. & Weerapana, E. Covalent protein modification: the current landscape of residue-specific electrophiles. *Curr. Opin. Chem. Biol.* **24**, 18–26 (2015).

41. Ward, C. C., Kleinman, J. I. & Nomura, D. K. NHS-Esters As Versatile Reactivity-Based Probes for Mapping Proteome-Wide Ligandable Hotspots. *ACS Chem. Biol.* **12**, 1478–1483 (2017).

42. Counihan, J. L., Ford, B. & Nomura, D. K. Mapping proteome-wide interactions of reactive chemicals using chemoproteomic platforms. *Curr. Opin. Chem. Biol.* **30**, 68–76 (2016).

43. Backus, K. M. *et al.* Proteome-wide covalent ligand discovery in native biological systems. *Nature* **534**, 570–574 (2016).

44. Louie, S. M. *et al.* GSTP1 Is a Driver of Triple-Negative Breast Cancer Cell Metabolism and Pathogenicity. *Cell Chem. Biol.* **23**, 567–578 (2016).

45. Wang, C., Weerapana, E., Blewett, M. M. & Cravatt, B. F. A chemoproteomic platform to quantitatively map targets of lipid-derived electrophiles. *Nat. Methods* **11**, 79–85 (2014).

46. Burdine, L. Target Identification in Chemical GeneticsThe (Often) Missing Link. *Chem. Biol.* **11**, 593–597 (2004).

47. Florian, S., Hümmer, S., Catarinella, M. & Mayer, T. U. Chemical genetics: Reshaping biology through chemistry. *HFSP J.* **1**, 104–114 (2007).

48. Knight, Z. A. & Shokat, K. M. Chemical Genetics: Where Genetics and Pharmacology Meet. *Cell* **128**, 425–430 (2007).

49. Ghantous, A., Sinjab, A., Herceg, Z. & Darwiche, N. Parthenolide: from plant shoots to cancer roots. *Drug Discov. Today* **18**, 894–905 (2013).

50. Kwok, B. H., Koh, B., Ndubuisi, M. I., Elofsson, M. & Crews, C. M. The anti-inflammatory natural product parthenolide from the medicinal herb Feverfew directly binds to and inhibits IkappaB kinase. *Chem. Biol.* **8**, 759–766 (2001).

51. Liu, M. *et al.* Parthenolide Inhibits STAT3 Signaling by Covalently Targeting Janus Kinases. *Mol. Basel Switz.* **23**, (2018).

52. Mathema, V. B., Koh, Y.-S., Thakuri, B. C. & Sillanpää, M. Parthenolide, a sesquiterpene lactone, expresses multiple anti-cancer and anti-inflammatory activities. *Inflammation* **35**, 560–565 (2012).

53. Shin, M. *et al.* Hsp72 Is an Intracellular Target of the α,β-Unsaturated Sesquiterpene Lactone, Parthenolide. *ACS Omega* **2**, 7267–7274 (2017).

54. Coricello, A. *et al.* A Walk in Nature. Sesquiterpene Lactones as Multi-Target Agents Involved in Inflammatory Pathways. *Curr. Med. Chem.* (2018). doi:10.2174/0929867325666180719111123

55. Quintana, J. & Estévez, F. Recent Advances on Cytotoxic Sesquiterpene Lactones. *Curr. Pharm. Des.* (2019). doi:10.2174/1381612825666190119114323

56. Diamanti, P., Cox, C. V., Moppett, J. P. & Blair, A. Parthenolide eliminates leukemia-initiating cell populations and improves survival in xenografts of childhood acute lymphoblastic leukemia. *Blood* **121**, 1384–1393 (2013).

57. Kim, S. L., Park, Y. R., Lee, S. T. & Kim, S.-W. Parthenolide suppresses hypoxia-inducible factor-1α signaling and hypoxia induced epithelial-mesenchymal transition in colorectal cancer. *Int. J. Oncol.* **51**, 1809–1820 (2017).

58. Morel, K. L., Ormsby, R. J., Bezak, E., Sweeney, C. J. & Sykes, P. J. Parthenolide Selectively Sensitizes Prostate Tumor Tissue to Radiotherapy while Protecting Healthy Tissues In Vivo. *Radiat. Res.* **187**, 501–512 (2017).

59. Kim, S.-L. *et al.* Parthenolide suppresses tumor growth in a xenograft model of colorectal cancer cells by inducing mitochondrial dysfunction and apoptosis. *Int. J. Oncol.* **41**, 1547–1553 (2012).

60. Anderson, K. N. & Bejcek, B. E. Parthenolide induces apoptosis in glioblastomas without affecting NF-kappaB. *J. Pharmacol. Sci.* **106**, 318–320 (2008).

61. Jeyamohan, S., Moorthy, R. K., Kannan, M. K. & Arockiam, A. J. V. Parthenolide induces apoptosis and autophagy through the suppression of PI3K/Akt signaling pathway in cervical cancer. *Biotechnol. Lett.* **38**, 1251–1260 (2016).

62. Ralstin, M. C. *et al.* Parthenolide cooperates with NS398 to inhibit growth of human hepatocellular carcinoma cells through effects on apoptosis and G0-G1 cell cycle arrest. *Mol. Cancer Res. MCR* **4**, 387–399 (2006).

63. Sun, Y. *et al.* The radiosensitization effect of parthenolide in prostate cancer cells is mediated by nuclear factor-kappaB inhibition and enhanced by the presence of PTEN. *Mol. Cancer Ther.* **6**, 2477–2486 (2007).

64. Lin, M. *et al.* Parthenolide suppresses non-small cell lung cancer GLC-82 cells growth via B-Raf/MAPK/Erk pathway. *Oncotarget* **8**, 23436–23447 (2017).

65. Liu, W. *et al.* Parthenolide suppresses pancreatic cell growth by autophagy-mediated apoptosis. *OncoTargets Ther.* **10**, 453–461 (2017).

66. Lesiak, K. *et al.* Parthenolide, a sesquiterpene lactone from the medical herb feverfew, shows anticancer activity against human melanoma cells in vitro. *Melanoma Res.* **20**, 21–34 (2010).

67. Carlisi, D. *et al.* Parthenolide and DMAPT exert cytotoxic effects on breast cancer stem-like cells by inducing oxidative stress, mitochondrial dysfunction and necrosis. *Cell Death Dis.* **7**, e2194 (2016).

68. Sweeney, C. J. *et al.* The sesquiterpene lactone parthenolide in combination with docetaxel reduces metastasis and improves survival in a xenograft model of breast cancer. *Mol. Cancer Ther.* **4**, 1004–1012 (2005).

69. Curry, E. A. *et al.* Phase I dose escalation trial of feverfew with standardized doses of parthenolide in patients with cancer. *Invest. New Drugs* **22**, 299–305 (2004).

70. Carlisi, D. *et al.* Parthenolide sensitizes hepatocellular carcinoma cells to TRAIL by inducing the expression of death receptors through inhibition of STAT3 activation. *J. Cell. Physiol.* **226**, 1632–1641 (2011).

71. Jafari, N., Nazeri, S. & Enferadi, S. T. Parthenolide reduces metastasis by inhibition of vimentin expression and induces apoptosis by suppression elongation factor α - 1 expression. *Phytomedicine Int. J. Phytother. Phytopharm.* **41**, 67–73 (2018).

72. Zhang, X. *et al.* Parthenolide Promotes Differentiation of Osteoblasts Through the Wnt/β-Catenin Signaling Pathway in Inflammatory Environments. *J. Interferon Cytokine Res. Off. J. Int. Soc. Interferon Cytokine Res.* **37**, 406–414 (2017).

73. Backus, K. M. *et al.* Proteome-wide covalent ligand discovery in native biological systems. *Nature* **534**, 570–574 (2016).

74. Bateman, L. A. *et al.* Chemoproteomics-enabled covalent ligand screen reveals a cysteine hotspot in reticulon 4 that impairs ER morphology and cancer pathogenicity. *Chem. Commun. Camb. Engl.* **53**, 7234–7237 (2017).

75. Grossman, E. A. *et al.* Covalent Ligand Discovery against Druggable Hotspots Targeted by Anti-cancer Natural Products. *Cell Chem. Biol.* **24**, 1368-1376.e4 (2017).

76. Hacker, S. M. *et al.* Global profiling of lysine reactivity and ligandability in the human proteome. *Nat. Chem.* **9**, 1181–1190 (2017).

77. Spradlin, J. N. *et al.* Harnessing the Anti-Cancer Natural Product Nimbolide for Targeted Protein Degradation. *bioRxiv* 436998 (2018). doi:10.1101/436998

78. Ward, C. C. *et al.* Covalent Ligand Screening Uncovers a RNF4 E3 Ligase Recruiter for Targeted Protein Degradation Applications. *bioRxiv* 439125 (2018). doi:10.1101/439125

79. Roberts, A. M., Ward, C. C. & Nomura, D. K. Activity-based protein profiling for mapping and pharmacologically interrogating proteome-wide ligandable hotspots. *Curr. Opin. Biotechnol.* **43**, 25–33 (2017).

80. Wang, C., Weerapana, E., Blewett, M. M. & Cravatt, B. F. A chemoproteomic platform to quantitatively map targets of lipid-derived electrophiles. *Nat. Methods* **11**, 79–85 (2014).

81. Dawson, S. J., Provenzano, E. & Caldas, C. Triple negative breast cancers: clinical and prognostic implications. *Eur. J. Cancer Oxf. Engl. 1990* **45 Suppl 1**, 27–40 (2009).

82. Weerapana, E. *et al.* Quantitative reactivity profiling predicts functional cysteines in proteomes. *Nature* **468**, 790–795 (2010).

83. Helleday, T., Petermann, E., Lundin, C., Hodgson, B. & Sharma, R. A. DNA repair pathways as targets for cancer therapy. *Nat. Rev. Cancer* **8**, 193–204 (2008).

84. Sulzmaier, F. J., Jean, C. & Schlaepfer, D. D. FAK in cancer: mechanistic findings and clinical applications. *Nat. Rev. Cancer* **14**, 598–610 (2014).

85. Lv, H. *et al.* Licochalcone A Upregulates Nrf2 Antioxidant Pathway and Thereby Alleviates Acetaminophen-Induced Hepatotoxicity. *Front. Pharmacol.* **9**, (2018).

86. Luo, M. & Guan, J.-L. Focal Adhesion Kinase: a Prominent Determinant in Breast Cancer Initiation, Progression and Metastasis. *Cancer Lett.* **289**, 127–139 (2010).

87. Iwatani, M. *et al.* Discovery and characterization of novel allosteric FAK inhibitors. *Eur. J. Med. Chem.* **61**, 49–60 (2013).

88. Yen-Pon, E. *et al.* Structure-Based Design, Synthesis, and Characterization of the First Irreversible Inhibitor of Focal Adhesion Kinase. *ACS Chem. Biol.* **13**, 2067–2073 (2018).

89. Frame, M. C., Patel, H., Serrels, B., Lietha, D. & Eck, M. J. The FERM domain: organizing the structure and function of FAK. *Nat. Rev. Mol. Cell Biol.* **11**, 802–814 (2010).

90. Silva Castro, E. da *et al.* Antileukemic Properties of Sesquiterpene Lactones : A systematic review. *Anticancer Agents Med. Chem.* (2017). doi:10.2174/1871520617666170918130126

91. Ren, Y., Yu, J. & Kinghorn, A. D. Development of Anticancer Agents from Plant-Derived Sesquiterpene Lactones. *Curr. Med. Chem.* **23**, 2397–2420 (2016).

92. Hu, X., Xu, S. & Maimone, T. J. A Double Allylation Strategy for Gram-Scale Guaianolide Production: Total Synthesis of (+)-Mikanokryptin. *Angew. Chem. Int. Ed Engl.* **56**, 1624–1628 (2017).

93. Tian, C. *et al.* Multiplexed Thiol Reactivity Profiling for Target Discovery of Electrophilic Natural Products. *Cell Chem. Biol.* **24**, 1416-1427.e5 (2017).

94. Duan, D., Zhang, J., Yao, J., Liu, Y. & Fang, J. Targeting Thioredoxin Reductase by Parthenolide Contributes to Inducing Apoptosis of HeLa Cells. *J. Biol. Chem.* **291**, 10021–10031 (2016).

95. Kwak, S. W., Park, E. S. & Lee, C. S. Parthenolide induces apoptosis by activating the mitochondrial and death receptor pathways and inhibits FAK-mediated cell invasion. *Mol. Cell. Biochem.* **385**, 133–144 (2014).

96. Liu, Y.-R. *et al.* Alantolactone, a sesquiterpene lactone, inhibits breast cancer growth by antiangiogenic activity via blocking VEGFR2 signaling. *Phytother. Res. PTR* **32**, 643–650 (2018).

97. Roberts, A. M. *et al.* Chemoproteomic Screening of Covalent Ligands Reveals UBA5 As a Novel Pancreatic Cancer Target. *ACS Chem. Biol.* **12**, 899–904 (2017).

98. Jessani, N. *et al.* Carcinoma and stromal enzyme activity profiles associated with breast tumor growth in vivo. *Proc. Natl. Acad. Sci. U. S. A.* **101**, 13756–13761 (2004).

99. Louie, S. M. *et al.* GSTP1 Is a Driver of Triple-Negative Breast Cancer Cell Metabolism and Pathogenicity. *Cell Chem. Biol.* **23**, 567–578 (2016).

100. Anderson, K. E., To, M., Olzmann, J. A. & Nomura, D. K. Chemoproteomics-Enabled Covalent Ligand Screening Reveals a Thioredoxin-Caspase 3 Interaction Disruptor That Impairs Breast Cancer Pathogenicity. *ACS Chem. Biol.* **12**, 2522–2528 (2017).

101. Xu, T. *et al.* ProLuCID: An improved SEQUEST-like algorithm with enhanced sensitivity and specificity. *J. Proteomics* **129**, 16–24 (2015).

102. Tabb, D. L., McDonald, W. H. & Yates, J. R. DTASelect and Contrast: tools for assembling and comparing protein identifications from shotgun proteomics. *J. Proteome Res.* **1**, 21–26 (2002).

APPENDICIES

Table Legends

Table 1. IsoTOP-ABPP analysis of parthenolide targets. List of probe-modified peptides, protein designations, and their light to heavy ratios for those peptides identified in two out of four biological replicates. 231MFP breast cancer cell proteomes were treated with DMSO vehicle or parthenolide (50 μM) for 30 min followed by labeling with IA-alkyne (100 μM) for 1 h. Probe-labeled proteins were then subjected to CuAAC-mediated appendage of a biotin-azide tag bearing a TEV protease recognition site and an isotopically light (for control) or heavy (for parthenolide-treated) valine. Control and treated proteomes were combined in a 1:1 ratio and probe-modified proteins were avidin-enriched and tryptically digested. Probe-modified tryptic peptides were subsequently avidin-enriched and eluted using TEV protease. Probe-modified peptides were analyzed by LC-MS/MS and light and heavy peptides were quantified. Shown are average ratios for each peptide from n=4. **Table 1** is related to **Figure 2.2.**

Table 2. **Structures of cysteine-reactive covalent ligands screened against FAK1.** **Table 2** is related to **Figures 2.6-2.8**.

Table 1: IsoTOP-ABPP analysis of parthenolide targets

Peptide	PTM index	L/H	uniprot ID	protein ID	Prep #s
IELGRC*IGEGQFGDVHQGG PGLLNLK	C427	291.9423683	Q05397	Q05397 Focal adhesion kinase 1 (Fragment) OS=Homo sapiens GN=PTK2 PE=1 SV=1 #	3
YFASRMFC*LR	C240	37.17061744	C9JZ99	C9JZ99 Serum paraoxonase/lactonase 3 OS=Homo sapiens GN=PON3 PE=1 SV=1 #	3
DELLASC*LTFLLSLPHNIIELD VR	C729	31.00164218	P78527	P78527 DNA-dependent protein kinase catalytic subunit OS=Homo sapiens GN=PRKDC PE=1 SV=3 #	3
C*EHCDCLQGFQLTHSLGGG TGSGMGTLLISK	C87;C124	9.54777	K7ESM5 Q9BUF5	K7ESM5 Tubulin beta-6 chain (Fragment) OS=Homo sapiens GN=TUBB6 PE=1 SV=1 # Q9BUF5 Tubulin beta-6 chain OS=Homo sapiens GN=TUBB6 PE=1 SV=1 #	2
GYNHPC*GFVCSPMEENPAY SK	C151	8.27146	P59095	P59095 StAR-related lipid transfer protein 6 OS=Homo sapiens GN=STARD6 PE=1 SV=1 #	2
YLEC*SALTQR	C113;C157;C157; C113;C157;C150	8.213695357	J3QLK0 P15153 P60763 B1AH77 P63000 B1AH80	J3QLK0 Ras-related C3 botulinum toxin substrate 3 (Fragment) OS=Homo sapiens GN=RAC3 PE=1 SV=1 # P15153 Ras-related C3 botulinum toxin substrate 2 OS=Homo sapiens GN=RAC2 PE=1 SV=1 # P60763 Ras-related C3 botulinum toxin substrate 3 OS=Homo sapiens GN=RAC3 PE=1 SV=1 # B1AH77 Ras-related C3 botulinum toxin substrate 2 OS=Homo sapiens GN=RAC2 PE=1 SV=1 # P63000 Ras-related C3 botulinum toxin substrate 1 OS=Homo sapiens GN=RAC1 PE=1 SV=1 # B1AH80 Ras-related C3 botulinum toxin substrate 2 OS=Homo sapiens GN=RAC2 PE=1 SV=1 #	2
DLETLKSLC*R	C308;C340	7.41856	M0QY25 Q86YD1	M0QY25 Prostate tumor-overexpressed gene 1 protein OS=Homo sapiens GN=PTOV1 PE=1 SV=1 # Q86YD1 Prostate tumor-overexpressed gene 1 protein OS=Homo sapiens GN=PTOV1 PE=1 SV=1 #	2
C*LHNFLTDGVPAEGAFTEDF QGLR	C316;C268	7.329020388	G3V1A6 P57764	G3V1A6 Gasdermin domain containing 1# isoform CRA_d OS=Homo sapiens GN=GSDMD PE=1 SV=1 # P57764 Gasdermin-D OS=Homo sapiens GN=GSDMD PE=1 SV=1 #	4

QNPHFC*TQDAGRPSDLEQG CSWANVK	C192;C192;C192	7.32757	Q7Z442 A0A087X120 Q7Z442	Q7Z442-3 Isoform 3 of Polycystic kidney disease protein 1-like 2 OS=Homo sapiens GN=PKD1L2 # A0A087X120 Polycystic kidney disease protein 1-like 2 OS=Homo sapiens GN=PKD1L2 PE=4 SV=1 # Q7Z442 Polycystic kidney disease protein 1-like 2 OS=Homo sapiens GN=PKD1L2 PE=1 SV=4 #	2
RAC*SETLAESR	C431;C367;C29;C 11;C315;C4;C315	7.23309553	A8K0R7 H0YM94 H0YM06 H0YKI3 A8K0R7 H0YNU6 A8K0R7	A8K0R7-5 Isoform 3 of Zinc finger protein 839 OS=Homo sapiens GN=ZNF839 # H0YM94 Zinc finger protein 839 (Fragment) OS=Homo sapiens GN=ZNF839 PE=1 SV=1 # H0YM06 Zinc finger protein 839 (Fragment) OS=Homo sapiens GN=ZNF839 PE=1 SV=1 # H0YKI3 Zinc finger protein 839 (Fragment) OS=Homo sapiens GN=ZNF839 PE=1 SV=1 # A8K0R7 Zinc finger protein 839 OS=Homo sapiens GN=ZNF839 PE=2 SV=1 # H0YNU6 Zinc finger protein 839 (Fragment) OS=Homo sapiens GN=ZNF839 PE=1 SV=1 # A8K0R7-2 Isoform 2 of Zinc finger protein 839 OS=Homo sapiens GN=ZNF839 #	3
AC*FCIDNEALYDICFR	C199	6.9188187	Q9H4B7	Q9H4B7 Tubulin beta-1 chain OS=Homo sapiens GN=TUBB1 PE=1 SV=1 #	2
C*ALSSPSLAFTPPIK	C120;C238;C255	6.902903898	Q8NFH5 Q8NFH5 Q8NFH5	Q8NFH5-3 Isoform 3 of Nucleoporin NUP53 OS=Homo sapiens GN=NUP35 # Q8NFH5-2 Isoform 2 of Nucleoporin NUP53 OS=Homo sapiens GN=NUP35 # Q8NFH5 Nucleoporin NUP53 OS=Homo sapiens GN=NUP35 PE=1 SV=1 #	4
QIPAITC*IQSQWR	C781	6.897522626	P46940	P46940 Ras GTPase-activating-like protein IQGAP1 OS=Homo sapiens GN=IQGAP1 PE=1 SV=1 #	3
TTC*SSGSALGPGAGAAQPS ASPLEGLLDLSYPR	C12;C12;C12	6.77158	Q96FZ5 F8WDZ3 Q96FZ5	Q96FZ5 CKLF-like MARVEL transmembrane domain-containing protein 7 OS=Homo sapiens GN=CMTM7 PE=2 SV=1 # F8WDZ3 CKLF-like MARVEL transmembrane domain-containing protein 7 OS=Homo sapiens GN=CMTM7 PE=1 SV=1 # Q96FZ5-2 Isoform 2 of CKLF-like MARVEL transmembrane domain-containing protein 7 OS=Homo sapiens GN=CMTM7 #	3

LFQPC*FLGMESCGIHETTFNSIMK	C965;C965;C965;C928	6.590293682	A5A3E0 Q6S8J3 P0CG38 P0CG39	A5A3E0 POTE ankyrin domain family member F OS=Homo sapiens GN=POTEF PE=1 SV=2 # Q6S8J3 POTE ankyrin domain family member E OS=Homo sapiens GN=POTEE PE=1 SV=3 # P0CG38 POTE ankyrin domain family member I OS=Homo sapiens GN=POTEI PE=3 SV=1 # P0CG39 POTE ankyrin domain family member J OS=Homo sapiens GN=POTEJ PE=3 SV=1 #	4
STC*SLTPALAAHFSENLIK	C553;C450;C508;C401	6.476535882	Q9BTA9 Q9BTA9 Q9BTA9 A0A0A0MRT2	Q9BTA9 WW domain-containing adapter protein with coiled-coil OS=Homo sapiens GN=WAC PE=1 SV=3 # Q9BTA9-5 Isoform 4 of WW domain-containing adapter protein with coiled-coil OS=Homo sapiens GN=WAC # Q9BTA9-2 Isoform 2 of WW domain-containing adapter protein with coiled-coil OS=Homo sapiens GN=WAC # A0A0A0MRT2 WW domain-containing adapter protein with coiled-coil OS=Homo sapiens GN=WAC PE=1 SV=1 #	2
NIIQPPSCVLHYYNVPLC*VTEETFTK	C430;C459;C459;C464;C464;C430	6.232916111	Q8WVV9 Q8WVV9 C9IYN3 D6W592 Q8WVV9 B7WPG3	Q8WVV9-5 Isoform 5 of Heterogeneous nuclear ribonucleoprotein L-like OS=Homo sapiens GN=HNRNPLL # Q8WVV9-4 Isoform 4 of Heterogeneous nuclear ribonucleoprotein L-like OS=Homo sapiens GN=HNRNPLL # C9IYN3 Heterogeneous nuclear ribonucleoprotein L-like OS=Homo sapiens GN=HNRNPLL PE=1 SV=2 # D6W592 Heterogeneous nuclear ribonucleoprotein L-like OS=Homo sapiens GN=HNRPLL PE=1 SV=1 # Q8WVV9 Heterogeneous nuclear ribonucleoprotein L-like OS=Homo sapiens GN=HNRNPLL PE=1 SV=1 # B7WPG3 Heterogeneous nuclear ribonucleoprotein L-like OS=Homo sapiens GN=HNRNPLL PE=1 SV=1 #	2
VGVGTC*GIADKPMTQYQDTSK	C214	6.177925	O75940	O75940 Survival of motor neuron-related-splicing factor 30 OS=Homo sapiens GN=SMNDC1 PE=1 SV=1 #	2
LC*YVALDFEQEMAMAASSSSLEK	C917	6.171389832	P0CG38	P0CG38 POTE ankyrin domain family member I OS=Homo sapiens GN=POTEI PE=3 SV=1 #	3
GVGQVGMAC*AISILGKSLADELALVDVLEDK	C36	6.064995122	P07195	P07195 L-lactate dehydrogenase B chain OS=Homo sapiens GN=LDHB PE=1 SV=2 #	2
LLQPDFQPVC*ASQLYPR	C258;C201;C265	6.02285	Q9UJW0 Q9UJW0 Q9UJW0	Q9UJW0 Dynactin subunit 4 OS=Homo sapiens GN=DCTN4 PE=1 SV=1 # Q9UJW0-2 Isoform 2 of Dynactin subunit 4 OS=Homo sapiens GN=DCTN4 # Q9UJW0-3 Isoform 3 of Dynactin subunit 4 OS=Homo sapiens GN=DCTN4 #	4

DTFDHPTLIENESIC*DEFAPNLK	C241;C241	5.87456	Q14865 Q14865	Q14865 AT-rich interactive domain-containing protein 5B OS=Homo sapiens GN=ARID5B PE=1 SV=3 # Q14865-3 Isoform 3 of AT-rich interactive domain-containing protein 5B OS=Homo sapiens GN=ARID5B #	3
TSC*GSPNYAAPEVISGR	C174;C185;C200;C174	5.613287687	A0A087WXX9 Q13131 Q13131 P54646	A0A087WXX9 5'-AMP-activated protein kinase catalytic subunit alpha-2 OS=Homo sapiens GN=PRKAA2 PE=1 SV=1 # Q13131 5'-AMP-activated protein kinase catalytic subunit alpha-1 OS=Homo sapiens GN=PRKAA1 PE=1 SV=4 # Q13131-2 Isoform 2 of 5'-AMP-activated protein kinase catalytic subunit alpha-1 OS=Homo sapiens GN=PRKAA1 # P54646 5'-AMP-activated protein kinase catalytic subunit alpha-2 OS=Homo sapiens GN=PRKAA2 PE=1 SV=2 #	3
HDVNC*EVVAVSVDSHFSHLAWINTPR	C127;C109	5.544235987	P30048 P30048	P30048 Thioredoxin-dependent peroxide reductase# mitochondrial OS=Homo sapiens GN=PRDX3 PE=1 SV=3 # P30048-2 Isoform 2 of Thioredoxin-dependent peroxide reductase# mitochondrial OS=Homo sapiens GN=PRDX3 #	2
LPLMEC*VQMTQDVQK	C360	5.49762	Q01813	Q01813 ATP-dependent 6-phosphofructokinase# platelet type OS=Homo sapiens GN=PFKP PE=1 SV=2 #	2
NAGNC*LSPAVIVGLLK	C369;C335	5.29321	O43175 Q5SZU1	O43175 D-3-phosphoglycerate dehydrogenase OS=Homo sapiens GN=PHGDH PE=1 SV=4 # Q5SZU1 D-3-phosphoglycerate dehydrogenase OS=Homo sapiens GN=PHGDH PE=1 SV=1 #	4
HFLSDTGMAC*R	C119	5.210937057	Q5TFE4	Q5TFE4 5'-nucleotidase domain-containing protein 1 OS=Homo sapiens GN=NT5DC1 PE=1 SV=1 #	2
ENFDEVVNDADIILVEFYAPWC*GHCK	;C206	5.16195	P01768 P13667	P01768 Ig heavy chain V-III region CAM OS=Homo sapiens PE=1 SV=1 # P13667 Protein disulfide-isomerase A4 OS=Homo sapiens GN=PDIA4 PE=1 SV=2 #	2
LC*SGPGIVGNVLVDPSAR	C245;C245	5.146475922	Q9Y5P6 Q9Y5P6	Q9Y5P6-2 Isoform 2 of Mannose-1-phosphate guanyltransferase beta OS=Homo sapiens GN=GMPPB # Q9Y5P6 Mannose-1-phosphate guanyltransferase beta OS=Homo sapiens GN=GMPPB PE=1 SV=2 #	2
QVQSLTC*EVDALKGTNESLER	C328	5.127409311	P08670	P08670 Vimentin OS=Homo sapiens GN=VIM PE=1 SV=4 #	4
LLAPDC*EIIQEVGK	C215	4.96606004	Q9NQT5	Q9NQT5 Exosome complex component RRP40 OS=Homo sapiens GN=EXOSC3 PE=1 SV=3 #	2

AC*LIFFDEIDAIGGAR	C270	4.668735925	P35998	P35998 26S protease regulatory subunit 7 OS=Homo sapiens GN=PSMC2 PE=1 SV=3 #	2
DVVVINLQNHEENLC*PEYPV FCPNNCAK	C188;C199	4.361680576	O00463 O00463	O00463 TNF receptor-associated factor 5 OS=Homo sapiens GN=TRAF5 PE=1 SV=2 # O00463-2 Isoform 2 of TNF receptor-associated factor 5 OS=Homo sapiens GN=TRAF5 #	2
GFAGVC*GFGGPYGETVATG PYR	C920;C892	4.120345036	Q9NZB2 Q9NZB2	Q9NZB2-6 Isoform F of Constitutive coactivator of PPAR-gamma-like protein 1 OS=Homo sapiens GN=FAM120A # Q9NZB2 Constitutive coactivator of PPAR-gamma-like protein 1 OS=Homo sapiens GN=FAM120A PE=1 SV=2 #	3
FTSC*VAFFNILNELNDYAGQ R	C69;C69;C69;C69 ;C69;C69	3.860189491	Q5T0N5 S4R347 Q5T0N5 Q5T0N5 Q5T0N5 Q5T0N5	Q5T0N5-3 Isoform 3 of Formin-binding protein 1-like OS=Homo sapiens GN=FNBP1L # S4R347 Formin-binding protein 1-like OS=Homo sapiens GN=FNBP1L PE=1 SV=1 # Q5T0N5-4 Isoform 4 of Formin-binding protein 1-like OS=Homo sapiens GN=FNBP1L # Q5T0N5 Formin-binding protein 1-like OS=Homo sapiens GN=FNBP1L PE=1 SV=3 # Q5T0N5-2 Isoform 2 of Formin-binding protein 1-like OS=Homo sapiens GN=FNBP1L # Q5T0N5-5 Isoform 5 of Formin-binding protein 1-like OS=Homo sapiens GN=FNBP1L #	3
DNTIEHLLPLFLAQLKDEC*P	C377	3.818399781	P30153	P30153 Serine/threonine-protein phosphatase 2A 65 kDa regulatory subunit A alpha isoform OS=Homo sapiens GN=PPP2R1A PE=1 SV=4 #	4
LEGDLTGPSVDVEVPDVELE C*PDAK	C2162	3.707755	Q09666	Q09666 Neuroblast differentiation-associated protein AHNAK OS=Homo sapiens GN=AHNAK PE=1 SV=2 #	2
FDDLQFFENC*GGGSFGSVY R	C22;C22;C22;C22	3.582557214	Q9NYL2 Q9NYL2 D4Q8H0 Q9NYL2	Q9NYL2-3 Isoform 3 of Mitogen-activated protein kinase kinase kinase MLT OS=Homo sapiens GN=ZAK # Q9NYL2-2 Isoform 2 of Mitogen-activated protein kinase kinase kinase MLT OS=Homo sapiens GN=ZAK # D4Q8H0 Mitogen-activated protein kinase kinase kinase MLT OS=Homo sapiens GN=pk PE=1 SV=1 # Q9NYL2 Mitogen-activated protein kinase kinase kinase MLT OS=Homo sapiens GN=ZAK PE=1 SV=3 #	2
ETTQNALQTPC*YTPYYVAPE VLGPEK	C203;C203	3.567146853	C9J8E1 Q16644	C9J8E1 MAP kinase-activated protein kinase 3 (Fragment) OS=Homo sapiens GN=MAPKAPK3 PE=1 SV=1 # Q16644 MAP kinase-activated protein kinase 3 OS=Homo sapiens GN=MAPKAPK3 PE=1 SV=1 #	2

VEPC*SLTPGYTK	C219;C218;C218;C218	3.467578646	Q96EB1 Q96EB1 Q96EB1 G5E9D4	Q96EB1-3 Isoform 3 of Elongator complex protein 4 OS=Homo sapiens GN=ELP4 # Q96EB1 Elongator complex protein 4 OS=Homo sapiens GN=ELP4 PE=1 SV=2 # Q96EB1-2 Isoform 2 of Elongator complex protein 4 OS=Homo sapiens GN=ELP4 # G5E9D4 Elongation protein 4 homolog (S. cerevisiae)# isoform CRA_b OS=Homo sapiens GN=ELP4 PE=1 SV=1 #	2
SNGLGPVMSGNTAYPVISC*PPLTPDWGVQDVWSSLR	C350	3.450473337	P22234	P22234 Multifunctional protein ADE2 OS=Homo sapiens GN=PAICS PE=1 SV=3 #	4
SMVSPVPSPTGTISVPNSC*PASPR	C254	3.41043437	P85037	P85037 Forkhead box protein K1 OS=Homo sapiens GN=FOXK1 PE=1 SV=1 #	2
LLSNMMC*QYR	C156;C160;C160	3.25087668	P28062 X5D2R7 P28062	P28062-2 Isoform 2 of Proteasome subunit beta type-8 OS=Homo sapiens GN=PSMB8 # X5D2R7 Proteasome subunit beta type OS=Homo sapiens GN=PSM8 PE=1 SV=1 # P28062 Proteasome subunit beta type-8 OS=Homo sapiens GN=PSMB8 PE=1 SV=3 #	2
VC*NFLASQVPFPSR	C214	3.207491701	Q99714	Q99714 3-hydroxyacyl-CoA dehydrogenase type-2 OS=Homo sapiens GN=HSD17B10 PE=1 SV=3 #	3
C*ASQAGMTAYGTR	C132	3.182250971	E9PDU6 Q15417 Q15417	E9PDU6 Calponin (Fragment) OS=Homo sapiens GN=CNN3 PE=1 SV=1 # Q15417 Calponin-3 OS=Homo sapiens GN=CNN3 PE=1 SV=1 # Q15417-2 Isoform 2 of Calponin-3 OS=Homo sapiens GN=CNN3 #	4
PC*DPSLTFDAITTLR	C255;C279	3.131830817	H7C1M3 P22894	H7C1M3 Neutrophil collagenase (Fragment) OS=Homo sapiens GN=MMP8 PE=1 SV=1 # P22894 Neutrophil collagenase OS=Homo sapiens GN=MMP8 PE=1 SV=1 #	2
AITIAGVPQSVTEC*VK	C158	3.019485	Q15365	Q15365 Poly(rC)-binding protein 1 OS=Homo sapiens GN=PCBP1 PE=1 SV=2 #	2
C*ASQSGMTAYGTR	C175;C136;C164;C196;C112	2.990175	Q99439 Q99439 B4DDF4 B4DUT8 A0A087X1X5	Q99439 Calponin-2 OS=Homo sapiens GN=CNN2 PE=1 SV=4 # Q99439-2 Isoform 2 of Calponin-2 OS=Homo sapiens GN=CNN2 # B4DDF4 Calponin OS=Homo sapiens GN=CNN2 PE=1 SV=1 # B4DUT8 Calponin OS=Homo sapiens GN=CNN2 PE=1 SV=1 # A0A087X1X5 Calponin (Fragment) OS=Homo sapiens GN=CNN2 PE=1 SV=1 #	2
AAVEEGIVLGGGC*ALLR	C442	2.968950595	P10809	P10809 60 kDa heat shock protein# mitochondrial OS=Homo sapiens GN=HSPD1 PE=1 SV=2 #	4
GLC*AIAQAESLR	C97	2.955549154	P23396	P23396 40S ribosomal protein S3 OS=Homo sapiens GN=RPS3 PE=1 SV=2 #	4

GFEVVYMTEPIDEYC*VQQLK	C521	2.941313905	P08238	P08238 Heat shock protein HSP 90-beta OS=Homo sapiens GN=HSP90AB1 PE=1 SV=4 #	3
AALAAC*PSSPFPPAMPR	C463;C502	2.940127068	Q8N2G8 Q8N2G8	Q8N2G8-3 Isoform 3 of GH3 domain-containing protein OS=Homo sapiens GN=GHDC # Q8N2G8 GH3 domain-containing protein OS=Homo sapiens GN=GHDC PE=1 SV=2 #	2
LCLNIC*VGESGDR	C25;C24	2.935962021	P62913 P62913	P62913 60S ribosomal protein L11 OS=Homo sapiens GN=RPL11 PE=1 SV=2 # P62913-2 Isoform 2 of 60S ribosomal protein L11 OS=Homo sapiens GN=RPL11 #	4
VDHPLSEQVHQPLLEEQCSI DEPLFEDQCSFDQPQPEEQC *IKTVK	C150	2.912205993	F8VNY5	F8VNY5 Thyroid transcription factor 1-associated protein 26 (Fragment) OS=Homo sapiens GN=CCDC59 PE=1 SV=1 #	3
NLSFFLTPPC*AR	C492;C492;C494	2.843789116	P42224 P42224 J3KPM9	P42224-2 Isoform Beta of Signal transducer and activator of transcription 1-alpha/beta OS=Homo sapiens GN=STAT1 # P42224 Signal transducer and activator of transcription 1-alpha/beta OS=Homo sapiens GN=STAT1 PE=1 SV=2 # J3KPM9 Signal transducer and activator of transcription OS=Homo sapiens GN=STAT1 PE=1 SV=1 #	3
LLQC*DPSSASQF	C185	2.84373872	P37235	P37235 Hippocalcin-like protein 1 OS=Homo sapiens GN=HPCAL1 PE=1 SV=3 #	3
NPLC*PLGQTVQSELFR	C115	2.789497412	Q9Y5R8	Q9Y5R8 Trafficking protein particle complex subunit 1 OS=Homo sapiens GN=TRAPPC1 PE=1 SV=1 #	3
C*ELSSSVQTDINLPYLTMDS SGPK	C317	2.788598375	P38646	P38646 Stress-70 protein# mitochondrial OS=Homo sapiens GN=HSPA9 PE=1 SV=2 #	4
IHESAGLPFFEIFVDAPLNIC*E SR	C155;C155	2.764647002	O95340 O95340	O95340 Bifunctional 3'-phosphoadenosine 5'-phosphosulfate synthase 2 OS=Homo sapiens GN=PAPSS2 PE=1 SV=2 # O95340-2 Isoform B of Bifunctional 3'-phosphoadenosine 5'-phosphosulfate synthase 2 OS=Homo sapiens GN=PAPSS2 #	3
VLTC*TDLEQGPNFFLDFENA QPTESEK	C10	2.754344512	Q9NUQ9	Q9NUQ9 Protein FAM49B OS=Homo sapiens GN=FAM49B PE=1 SV=1 #	3
STLTDSLVC*K	C41	2.752233135	P13639	P13639 Elongation factor 2 OS=Homo sapiens GN=EEF2 PE=1 SV=4 #	4
SC*PSFSASSEGTR	C9;C9;C9	2.741336373	D6RCP9 P27707 D6RFG8	D6RCP9 Deoxycytidine kinase OS=Homo sapiens GN=DCK PE=1 SV=1 # P27707 Deoxycytidine kinase OS=Homo sapiens GN=DCK PE=1 SV=1 # D6RFG8 Deoxycytidine kinase OS=Homo sapiens GN=DCK PE=1 SV=1 #	3

SVLC*STPTINIPASPFMQK	C22	2.72398967	Q96KB5 Q96KB5	Q96KB5 Lymphokine-activated killer T-cell-originated protein kinase OS=Homo sapiens GN=PBK PE=1 SV=3 # Q96KB5-2 Isoform 2 of Lymphokine-activated killer T-cell-originated protein kinase OS=Homo sapiens GN=PBK #	4
SVPC*ESNEANEANEANK	C16	2.70023	Q9NS25	Q9NS25 Sperm protein associated with the nucleus on the X chromosome B1 OS=Homo sapiens GN=SPANXB1 PE=2 SV=2 #	2
SC*SGVEFSTSGSSNTDTGK	C47;C47	2.686766378	A0A0A0MR02 P45880	A0A0A0MR02 Voltage-dependent anion-selective channel protein 2 (Fragment) OS=Homo sapiens GN=VDAC2 PE=1 SV=1 # P45880 Voltage-dependent anion-selective channel protein 2 OS=Homo sapiens GN=VDAC2 PE=1 SV=2 #	4
ECENC*DCLQGFQLTHSLGG GTGSGMGTLLISK	C127;C474	2.68667	Q13509 A0A0B4J269	Q13509 Tubulin beta-3 chain OS=Homo sapiens GN=TUBB3 PE=1 SV=2 # A0A0B4J269 Uncharacterized protein OS=Homo sapiens PE=1 SV=1 #	3
TDC*SPIQFESAWALTNIASG TSEQTK	C133	2.684715	P52292	P52292 Importin subunit alpha-1 OS=Homo sapiens GN=KPNA2 PE=1 SV=1 #	2
SGGLQTPEC*LSR	C439	2.64353515	P85037	P85037 Forkhead box protein K1 OS=Homo sapiens GN=FOXK1 PE=1 SV=1 #	2
VGVGPGSVC*TTR	C186	2.640755962	P36959	P36959 GMP reductase 1 OS=Homo sapiens GN=GMPR PE=1 SV=1 #	2
LTPGC*EAEAETEAICFFVQQ FTDMEHNR	C2359	2.602662869	P49327	P49327 Fatty acid synthase OS=Homo sapiens GN=FASN PE=1 SV=3 #	2
VAC*AEEWQESR	C87;C87	2.579408269	O75663 O75663	O75663 TIP41-like protein OS=Homo sapiens GN=TIPRL PE=1 SV=2 # O75663-2 Isoform 2 of TIP41-like protein OS=Homo sapiens GN=TIPRL #	2
FMC*AQLPNQVLESISIIDTPGI LSGAK	C138	2.549549215	Q9NZN4	Q9NZN4 EH domain-containing protein 2 OS=Homo sapiens GN=EHD2 PE=1 SV=2 #	2
DLNYC*FSGMSDHR	C267;C267;C267	2.529748848	P31943 G8JLB6 E9PCY7	P31943 Heterogeneous nuclear ribonucleoprotein H OS=Homo sapiens GN=HNRNPH1 PE=1 SV=4 # G8JLB6 Heterogeneous nuclear ribonucleoprotein H OS=Homo sapiens GN=HNRNPH1 PE=1 SV=1 # E9PCY7 Heterogeneous nuclear ribonucleoprotein H OS=Homo sapiens GN=HNRNPH1 PE=1 SV=1 #	4
LDVGNFSWGSECC*TR	C72	2.523384765	P62241	P62241 40S ribosomal protein S8 OS=Homo sapiens GN=RPS8 PE=1 SV=2 #	2

LDEC*EEAFQGTK	C103;C31;C92;C36;C92	2.46986	P61289 B3KQ25 P61289 K7ESG5 P61289	P61289-3 Isoform 3 of Proteasome activator complex subunit 3 OS=Homo sapiens GN=PSME3 # B3KQ25 Proteasome activator complex subunit 3 OS=Homo sapiens GN=PSME3 PE=1 SV=1 # P61289 Proteasome activator complex subunit 3 OS=Homo sapiens GN=PSME3 PE=1 SV=1 # K7ESG5 Proteasome activator complex subunit 3 OS=Homo sapiens GN=PSME3 PE=1 SV=1 # P61289-2 Isoform 2 of Proteasome activator complex subunit 3 OS=Homo sapiens GN=PSME3 #	2
EGDVAAC*YANPSLAQEELGWTAALGLDR	C307	2.44290667	Q14376	Q14376 UDP-glucose 4-epimerase OS=Homo sapiens GN=GALE PE=1 SV=2 #	2
HC*SQVDSVR	C112;C112;C112	2.429444736	Q14247 Q14247 Q14247	Q14247-3 Isoform 3 of Src substrate cortactin OS=Homo sapiens GN=CTTN # Q14247 Src substrate cortactin OS=Homo sapiens GN=CTTN PE=1 SV=2 # Q14247-2 Isoform 2 of Src substrate cortactin OS=Homo sapiens GN=CTTN #	2
TFC*GTPEYLAPEVLEDNDYGR	C310;C311;C248;C307;C307;C249	2.426486341	P31749 P31751 P31749 Q9Y243 Q9Y243 M0R0P9	P31749 RAC-alpha serine/threonine-protein kinase OS=Homo sapiens GN=AKT1 PE=1 SV=2 # P31751 RAC-beta serine/threonine-protein kinase OS=Homo sapiens GN=AKT2 PE=1 SV=2 # P31749-2 Isoform 2 of RAC-alpha serine/threonine-protein kinase OS=Homo sapiens GN=AKT1 # Q9Y243-2 Isoform 2 of RAC-gamma serine/threonine-protein kinase OS=Homo sapiens GN=AKT3 # Q9Y243 RAC-gamma serine/threonine-protein kinase OS=Homo sapiens GN=AKT3 PE=1 SV=1 # M0R0P9 RAC-beta serine/threonine-protein kinase OS=Homo sapiens GN=AKT2 PE=1 SV=1 #	4
LPLC*SLPGEPGNGPDQQLQR	C75	2.404870969	Q96GX2	Q96GX2 Putative ataxin-7-like protein 3B OS=Homo sapiens GN=ATXN7L3B PE=3 SV=2 #	4
MAGIFDVNTC*YGSPQSPQLIR	C467;C468;C428;C353	2.354375838	Q9BTX1 Q9BTX1 Q9BTX1 Q9BTX1	Q9BTX1-2 Isoform 2 of Nucleoporin NDC1 OS=Homo sapiens GN=NDC1 # Q9BTX1 Nucleoporin NDC1 OS=Homo sapiens GN=NDC1 PE=1 SV=2 # Q9BTX1-5 Isoform 5 of Nucleoporin NDC1 OS=Homo sapiens GN=NDC1 # Q9BTX1-6 Isoform 6 of Nucleoporin NDC1 OS=Homo sapiens GN=NDC1 #	2
DLSYC*LSGMYDHR	C267	2.353264799	P52597	P52597 Heterogeneous nuclear ribonucleoprotein F OS=Homo sapiens GN=HNRNPF PE=1 SV=3 #	2

GQVC*LPVISAENWKPATK	C86;C54;C144	2.352812524	P68036 P68036 P68036	P68036 Ubiquitin-conjugating enzyme E2 L3 OS=Homo sapiens GN=UBE2L3 PE=1 SV=1 # P68036-2 Isoform 2 of Ubiquitin-conjugating enzyme E2 L3 OS=Homo sapiens GN=UBE2L3 # P68036-3 Isoform 3 of Ubiquitin-conjugating enzyme E2 L3 OS=Homo sapiens GN=UBE2L3 #	3
YAEYFLRPMLQYVC*DNSP	C917;C933;C915	2.292289404	H0Y8C6 O00410 O00410	H0Y8C6 Importin-5 (Fragment) OS=Homo sapiens GN=IPO5 PE=1 SV=1 # O00410-3 Isoform 3 of Importin-5 OS=Homo sapiens GN=IPO5 # O00410 Importin-5 OS=Homo sapiens GN=IPO5 PE=1 SV=4 #	2
VVSGMVNC*NDDQGVLLGR	C230	2.289072502	P21980	P21980 Protein-glutamine gamma-glutamyltransferase 2 OS=Homo sapiens GN=TGM2 PE=1 SV=2 #	4
C*PFTGNVSIR	C60	2.245778125	P62280	P62280 40S ribosomal protein S11 OS=Homo sapiens GN=RPS11 PE=1 SV=3 #	4
VAC*ITEQVLTLVNK	C477	2.244882067	P04843	P04843 Dolichyl-diphosphooligosaccharide--protein glycosyltransferase subunit 1 OS=Homo sapiens GN=RPN1 PE=1 SV=1 #	3
C*ASQVGMTAPGTR	C215;C176;C204; C236;C152	2.227495	Q99439 Q99439 B4DDF4 B4DUT8 A0A087X1X5	Q99439 Calponin-2 OS=Homo sapiens GN=CNN2 PE=1 SV=4 # Q99439-2 Isoform 2 of Calponin-2 OS=Homo sapiens GN=CNN2 # B4DDF4 Calponin OS=Homo sapiens GN=CNN2 PE=1 SV=1 # B4DUT8 Calponin OS=Homo sapiens GN=CNN2 PE=1 SV=1 # A0A087X1X5 Calponin (Fragment) OS=Homo sapiens GN=CNN2 PE=1 SV=1 #	2
NMITGTSQADC*AVLIVAAGV GEFEAGISK	C111;M102 C111	2.198334536	P68104 Q05639 A0A087WV01 P68104	P68104 Elongation factor 1-alpha 1 OS=Homo sapiens GN=EEF1A1 PE=1 SV=1 # Q05639 Elongation factor 1-alpha 2 OS=Homo sapiens GN=EEF1A2 PE=1 SV=1 # A0A087WV01 Elongation factor 1-alpha OS=Homo sapiens GN=EEF1A1 PE=1 SV=1 # P68104-2 Isoform 2 of Elongation factor 1-alpha 1 OS=Homo sapiens GN=EEF1A1 #	4
VC*NYGLTFTQK	C66;C65	2.169408698	Q9Y277 Q9Y277	Q9Y277-2 Isoform 2 of Voltage-dependent anion-selective channel protein 3 OS=Homo sapiens GN=VDAC3 # Q9Y277 Voltage-dependent anion-selective channel protein 3 OS=Homo sapiens GN=VDAC3 PE=1 SV=1 #	4
LALFNPDVC*WDR	C44	2.158368485	O00483	O00483 Cytochrome c oxidase subunit NDUFA4 OS=Homo sapiens GN=NDUFA4 PE=1 SV=1 #	4

IIPTLEEGLQLPSPTATSQLPL ESDAVEC*LNYQHYK	C132;C132	2.143490159	P61978 P61978	P61978 Heterogeneous nuclear ribonucleoprotein K OS=Homo sapiens GN=HNRNPK PE=1 SV=1 # P61978-2 Isoform 2 of Heterogeneous nuclear ribonucleoprotein K OS=Homo sapiens GN=HNRNPK #	4
SSGC*FPNMAAK	C460	2.12800937	Q96I24	Q96I24 Far upstream element-binding protein 3 OS=Homo sapiens GN=FUBP3 PE=1 SV=2 #	2
NMITGTAPLDGC*ILVVAAND GPMPQTR	C147	2.1276	P49411	P49411 Elongation factor Tu# mitochondrial OS=Homo sapiens GN=TUFM PE=1 SV=2 #	2
C*MQLTDFILK	C54	2.05916	E7EPB3 P50914	E7EPB3 60S ribosomal protein L14 OS=Homo sapiens GN=RPL14 PE=1 SV=1 # P50914 60S ribosomal protein L14 OS=Homo sapiens GN=RPL14 PE=1 SV=4 #	2
FQSSAVMALQEASEAYLVGL FEDTNLC*AIHAK	C111	2.055224216	Q71DI3	Q71DI3 Histone H3.2 OS=Homo sapiens GN=HIST2H3A PE=1 SV=3 #	2
GSQMGTVQPIPC*LLSMPTR	C531 C559;M523	2.050939409	Q9NZB2 Q9NZB2	Q9NZB2-6 Isoform F of Constitutive coactivator of PPAR-gamma-like protein 1 OS=Homo sapiens GN=FAM120A # Q9NZB2 Constitutive coactivator of PPAR-gamma-like protein 1 OS=Homo sapiens GN=FAM120A PE=1 SV=2 #	3
C*SVLAAANSVFGR	C439;C482	2.036039425	B1AHB1 P33992	B1AHB1 DNA helicase OS=Homo sapiens GN=MCM5 PE=1 SV=1 # P33992 DNA replication licensing factor MCM5 OS=Homo sapiens GN=MCM5 PE=1 SV=5 #	2
AVASQLDC*NFLK	C207;C193	2.003739647	A0A087X2I1 P62333	A0A087X2I1 26S protease regulatory subunit 10B OS=Homo sapiens GN=PSMC6 PE=1 SV=1 # P62333 26S protease regulatory subunit 10B OS=Homo sapiens GN=PSMC6 PE=1 SV=1 #	3
VGIGPGSVC*TTR	C186;C204;C204	1.98345351	Q9P2T1 H0YNJ6 Q9P2T1	Q9P2T1 GMP reductase 2 OS=Homo sapiens GN=GMPR2 PE=1 SV=1 # H0YNJ6 GMP reductase OS=Homo sapiens GN=GMPR2 PE=1 SV=1 # Q9P2T1-2 Isoform 2 of GMP reductase 2 OS=Homo sapiens GN=GMPR2 #	3
NNAFPC*QVNIK	C712	1.927079418	Q9NQW6	Q9NQW6 Actin-binding protein anillin OS=Homo sapiens GN=ANLN PE=1 SV=2 #	2
HGFC*GIPITDTGR	C140	1.924111182	P12268	P12268 Inosine-5'-monophosphate dehydrogenase 2 OS=Homo sapiens GN=IMPDH2 PE=1 SV=2 #	4

ISAFGYLEC*SAK	C159;C159;C159	1.907469387	Q5JR08 P08134 E9PQH6	Q5JR08 Rho-related GTP-binding protein RhoC (Fragment) OS=Homo sapiens GN=RHOC PE=1 SV=7 # P08134 Rho-related GTP-binding protein RhoC OS=Homo sapiens GN=RHOC PE=1 SV=1 # E9PQH6 Rho-related GTP-binding protein RhoC (Fragment) OS=Homo sapiens GN=RHOC PE=1 SV=1 #	3
VFIMDSC*DELIPEYLNFIR	C366	1.890264027	P08238	P08238 Heat shock protein HSP 90-beta OS=Homo sapiens GN=HSP90AB1 PE=1 SV=4 #	4
LEGDLTGPSVGVEVPDVELEC*PDAK	C1900	1.889242134	Q09666	Q09666 Neuroblast differentiation-associated protein AHNAK OS=Homo sapiens GN=AHNAK PE=1 SV=2 #	3
GC*STVLSPEGSAQFAAQIFGLSNHLVWSK	C374	1.882081231	P22234	P22234 Multifunctional protein ADE2 OS=Homo sapiens GN=PAICS PE=1 SV=3 #	2
C*EFQDAYVLLSEK	C237	1.860424141	P10809	P10809 60 kDa heat shock protein# mitochondrial OS=Homo sapiens GN=HSPD1 PE=1 SV=2 #	4
WTQTLSELDLAVPFC*VNFR	C188	1.859439143	Q9Y266	Q9Y266 Nuclear migration protein nudC OS=Homo sapiens GN=NUDC PE=1 SV=1 #	3
VTFSC*AAGFGQR	C1113;C1227;C1118;C1245;C1210;C1252;C1230	1.858913739	Q14203 Q14203 Q14203 Q14203 Q14203 Q14203 E7EX90	Q14203-5 Isoform 5 of Dynactin subunit 1 OS=Homo sapiens GN=DCTN1 # Q14203-4 Isoform 4 of Dynactin subunit 1 OS=Homo sapiens GN=DCTN1 # Q14203-2 Isoform p135 of Dynactin subunit 1 OS=Homo sapiens GN=DCTN1 # Q14203-6 Isoform 6 of Dynactin subunit 1 OS=Homo sapiens GN=DCTN1 # Q14203-3 Isoform 3 of Dynactin subunit 1 OS=Homo sapiens GN=DCTN1 # Q14203 Dynactin subunit 1 OS=Homo sapiens GN=DCTN1 PE=1 SV=3 # E7EX90 Dynactin subunit 1 OS=Homo sapiens GN=DCTN1 PE=1 SV=1 #	4
VADSSPFALELLISDDCFVLDNGLC*GK	C290	1.853891195	P40121	P40121 Macrophage-capping protein OS=Homo sapiens GN=CAPG PE=1 SV=2 #	2

VLLSIC*SLLCDPNPDDPLVPEIAR	C109;C107;C107;C101;C78;C78;C107;C78;C108;C107	1.838712674	P61077 P61077 P61077 H9KV45 P62837 D6RAH7 A0A0A0MQU3 D6RFM0 A0A087WY85 P62837	P61077-3 Isoform 3 of Ubiquitin-conjugating enzyme E2 D3 OS=Homo sapiens GN=UBE2D3 # P61077 Ubiquitin-conjugating enzyme E2 D3 OS=Homo sapiens GN=UBE2D3 PE=1 SV=1 # P61077-2 Isoform 2 of Ubiquitin-conjugating enzyme E2 D3 OS=Homo sapiens GN=UBE2D3 # H9KV45 Ubiquitin-conjugating enzyme E2 D3 OS=Homo sapiens GN=UBE2D3 PE=1 SV=1 # P62837-2 Isoform 2 of Ubiquitin-conjugating enzyme E2 D2 OS=Homo sapiens GN=UBE2D2 # D6RAH7 Ubiquitin-conjugating enzyme E2 D3 OS=Homo sapiens GN=UBE2D3 PE=1 SV=1 # A0A0A0MQU3 Ubiquitin-conjugating enzyme E2 D2 OS=Homo sapiens GN=UBE2D2 PE=1 SV=1 # D6RFM0 Ubiquitin-conjugating enzyme E2 D2 (Fragment) OS=Homo sapiens GN=UBE2D2 PE=3 SV=1 # A0A087WY85 Ubiquitin-conjugating enzyme E2 D3 OS=Homo sapiens GN=UBE2D3 PE=1 SV=1 # P62837 Ubiquitin-conjugating enzyme E2 D2 OS=Homo sapiens GN=UBE2D2 PE=1 SV=1 #	2
ISLGLPVGAVINC*ADNTGAK	C28	1.827377953	P62829	P62829 60S ribosomal protein L23 OS=Homo sapiens GN=RPL23 PE=1 SV=1 #	4
LC*YVALDFENEMATAASSSSLEK	C219	1.825356774	P68133 P68032	P68133 Actin# alpha skeletal muscle OS=Homo sapiens GN=ACTA1 PE=1 SV=1 # P68032 Actin# alpha cardiac muscle 1 OS=Homo sapiens GN=ACTC1 PE=1 SV=1 #	4
HLNEIDLFHC*IDPNDSK	C62;C58;C58	1.804245	A0A087WYT3 Q15185 Q15185	A0A087WYT3 Prostaglandin E synthase 3 OS=Homo sapiens GN=PTGES3 PE=1 SV=1 # Q15185 Prostaglandin E synthase 3 OS=Homo sapiens GN=PTGES3 PE=1 SV=1 # Q15185-4 Isoform 4 of Prostaglandin E synthase 3 OS=Homo sapiens GN=PTGES3 #	2
SCYDLSC*HAR	C471	1.791524189	P41250	P41250 Glycine--tRNA ligase OS=Homo sapiens GN=GARS PE=1 SV=3 #	2
QGFGNLPIC*MAK	C863;C841;C919;C907	1.772902959	P11586 A0A087WVM4 F5H2F4 B7ZM99	P11586 C-1-tetrahydrofolate synthase# cytoplasmic OS=Homo sapiens GN=MTHFD1 PE=1 SV=3 # A0A087WVM4 Monofunctional C1-tetrahydrofolate synthase# mitochondrial OS=Homo sapiens GN=MTHFD1L PE=1 SV=1 # F5H2F4 C-1-tetrahydrofolate synthase# cytoplasmic OS=Homo sapiens GN=MTHFD1 PE=1 SV=1 # B7ZM99 MTHFD1L protein OS=Homo sapiens GN=MTHFD1L PE=1 SV=1 #	2

SGQGAFGNMC*R	C96	1.772503287	P36578	P36578 60S ribosomal protein L4 OS=Homo sapiens GN=RPL4 PE=1 SV=5 #	3
AVC*MLSNTTAIAEAWAR	C376;C376;C400; C376;C376	1.771680676	Q13748 P68363 C9J2C0 Q71U36 P68366	Q13748 Tubulin alpha-3C/D chain OS=Homo sapiens GN=TUBA3C PE=1 SV=3 # P68363 Tubulin alpha-1B chain OS=Homo sapiens GN=TUBA1B PE=1 SV=1 # C9J2C0 Tubulin alpha-8 chain (Fragment) OS=Homo sapiens GN=TUBA8 PE=1 SV=1 # Q71U36 Tubulin alpha-1A chain OS=Homo sapiens GN=TUBA1A PE=1 SV=1 # P68366 Tubulin alpha-4A chain OS=Homo sapiens GN=TUBA4A PE=1 SV=1 #	4
SGDAAIVDMVPGKPMC*VES FSDYPPLGR	C411;M383 C390	1.770581868	P68104 P68104	P68104 Elongation factor 1-alpha 1 OS=Homo sapiens GN=EEF1A1 PE=1 SV=1 # P68104-2 Isoform 2 of Elongation factor 1-alpha 1 OS=Homo sapiens GN=EEF1A1 #	4
TVDSQGPTPVC*TPTFLER	C237	1.766514426	Q9BYG3	Q9BYG3 MKI67 FHA domain-interacting nucleolar phosphoprotein OS=Homo sapiens GN=NIFK PE=1 SV=1 #	2
KAQC*PIVER	C66;C87;C66	1.760057146	P46782 M0R0R2 M0R0F0	P46782 40S ribosomal protein S5 OS=Homo sapiens GN=RPS5 PE=1 SV=4 # M0R0R2 40S ribosomal protein S5 OS=Homo sapiens GN=RPS5 PE=1 SV=1 # M0R0F0 40S ribosomal protein S5 (Fragment) OS=Homo sapiens GN=RPS5 PE=1 SV=1 #	3
FMC*AQLPNPVLDSISIIDTPGI LSGEK	C152;M137 C138	1.753235512	A0A024R571 Q9H4M9	A0A024R571 EH domain-containing protein 1 OS=Homo sapiens GN=EHD1 PE=1 SV=1 # Q9H4M9 EH domain-containing protein 1 OS=Homo sapiens GN=EHD1 PE=1 SV=2 #	3
LEFSIYPAPQVSTAVVEPYNSI LTTHTTLEHSDC*AFMVDNEA IYDICR	C200	1.751247515	P68363 Q71U36 P68366	P68363 Tubulin alpha-1B chain OS=Homo sapiens GN=TUBA1B PE=1 SV=1 # Q71U36 Tubulin alpha-1A chain OS=Homo sapiens GN=TUBA1A PE=1 SV=1 # Tubulin alpha-1C chain OS=Homo sapiens GN=TUBA1C PE=1 SV=1 # P68366 Tubulin alpha-4A chain OS=Homo sapiens GN=TUBA4A PE=1 SV=1 #	3
YGIIC*MEDLIHEIYTVGK	C186;C146	1.748078411	P18124 A8MUD9	P18124 60S ribosomal protein L7 OS=Homo sapiens GN=RPL7 PE=1 SV=1 # A8MUD9 60S ribosomal protein L7 OS=Homo sapiens GN=RPL7 PE=1 SV=1 #	4
GC*EVVVSGK	C134	1.725284422	P23396	P23396 40S ribosomal protein S3 OS=Homo sapiens GN=RPS3 PE=1 SV=2 #	2

LC*YVALDFEQEMATAASSSSLEK	C217;C217;C917	1.717199164	P63261 P60709 Q6S8J3	P63261 Actin# cytoplasmic 2 OS=Homo sapiens GN=ACTG1 PE=1 SV=1 # P60709 Actin# cytoplasmic 1 OS=Homo sapiens GN=ACTB PE=1 SV=1 # Q6S8J3 POTE ankyrin domain family member E OS=Homo sapiens GN=POTEE PE=1 SV=3 #	4
LEFSIYPAPQVSTAVVEPYNSILTTHTTLEHSDCAFMVDNEAIYDIC*R	C213;C213;C213	1.716579076	P68363 Q71U36 P68366	P68363 Tubulin alpha-1B chain OS=Homo sapiens GN=TUBA1B PE=1 SV=1 # Q71U36 Tubulin alpha-1A chain OS=Homo sapiens GN=TUBA1A PE=1 SV=1 # Tubulin alpha-1C chain OS=Homo sapiens GN=TUBA1C PE=1 SV=1 # P68366 Tubulin alpha-4A chain OS=Homo sapiens GN=TUBA4A PE=1 SV=1 #	2
TVPFLPLLGGC*IDDTILSR	C180;C190	1.715394179	Q7Z7H8 Q7Z7H8	Q7Z7H8 39S ribosomal protein L10# mitochondrial OS=Homo sapiens GN=MRPL10 PE=1 SV=3 # Q7Z7H8-2 Isoform 2 of 39S ribosomal protein L10# mitochondrial OS=Homo sapiens GN=MRPL10 #	4
VLDALFPCVQGGTTAIPGAFGC*GK	C221;C254	1.685884923	P38606 P38606	P38606-2 Isoform 2 of V-type proton ATPase catalytic subunit A OS=Homo sapiens GN=ATP6V1A # P38606 V-type proton ATPase catalytic subunit A OS=Homo sapiens GN=ATP6V1A PE=1 SV=2 #	3
GC*IVDANLSVLNLVIVK	C100	1.670656861	P62753	P62753 40S ribosomal protein S6 OS=Homo sapiens GN=RPS6 PE=1 SV=1 #	4
DHQPC*IIFMDEIDAIGGR	C242;C228	1.663369985	A0A087X2I1 P62333	A0A087X2I1 26S protease regulatory subunit 10B OS=Homo sapiens GN=PSMC6 PE=1 SV=1 # P62333 26S protease regulatory subunit 10B OS=Homo sapiens GN=PSMC6 PE=1 SV=1 #	2
LC*PNSTGAEIR	C240;C377	1.660217374	P35998 P35998	P35998-2 Isoform 2 of 26S protease regulatory subunit 7 OS=Homo sapiens GN=PSMC2 # P35998 26S protease regulatory subunit 7 OS=Homo sapiens GN=PSMC2 PE=1 SV=3 #	3
LFNTAVC*ESK	C721	1.649153326	Q9BXJ9	Q9BXJ9 N-alpha-acetyltransferase 15# NatA auxiliary subunit OS=Homo sapiens GN=NAA15 PE=1 SV=1 #	2
IQFNDLQSLLC*ATLQNVLR	C585	1.642791791	Q14974	Q14974 Importin subunit beta-1 OS=Homo sapiens GN=KPNB1 PE=1 SV=2 #	2
GVLMYGPPGC*GK	C179;C210	1.641176094	P43686 P43686	P43686-2 Isoform 2 of 26S protease regulatory subunit 6B OS=Homo sapiens GN=PSMC4 # P43686 26S protease regulatory subunit 6B OS=Homo sapiens GN=PSMC4 PE=1 SV=2 #	3
AINC*ATSGVVGLVNCLR	C1448	1.634534865	P49327	P49327 Fatty acid synthase OS=Homo sapiens GN=FASN PE=1 SV=3 #	4

ASATGMIIMDGVEVPEENVLPGASSLGGPFGC*LNNAR	C289;C289	1.631485	Q92947 Q92947	Q92947-2 Isoform Short of Glutaryl-CoA dehydrogenase# mitochondrial OS=Homo sapiens GN=GCDH # Q92947 Glutaryl-CoA dehydrogenase# mitochondrial OS=Homo sapiens GN=GCDH PE=1 SV=1 #	2
VMTIPYQPMPASSPVIC*AGGQDR	C194	1.626984736	Q15365	Q15365 Poly(rC)-binding protein 1 OS=Homo sapiens GN=PCBP1 PE=1 SV=2 #	4
AILFSQPLQITDTQQGC*IAPVELR	C716	1.626325548	Q8NBF2	Q8NBF2 NHL repeat-containing protein 2 OS=Homo sapiens GN=NHLRC2 PE=1 SV=1 #	4
TLSFYFPPC*GK	C388;C388	1.616377079	Q9UG63 Q9UG63	Q9UG63-2 Isoform 2 of ATP-binding cassette sub-family F member 2 OS=Homo sapiens GN=ABCF2 # Q9UG63 ATP-binding cassette sub-family F member 2 OS=Homo sapiens GN=ABCF2 PE=1 SV=2 #	2
YFAGNLASGGAAGATSLC*FVYPLDFAR	C129;C129	1.614518687	P12235 P05141	P12235 ADP/ATP translocase 1 OS=Homo sapiens GN=SLC25A4 PE=1 SV=4 # P05141 ADP/ATP translocase 2 OS=Homo sapiens GN=SLC25A5 PE=1 SV=7 #	2
LEVDAIVNAANSSLLGGGGVDGC*IHR	C186	1.60272095	Q9BQ69	Q9BQ69 O-acetyl-ADP-ribose deacetylase MACROD1 OS=Homo sapiens GN=MACROD1 PE=1 SV=2 #	4
AYEYVEC*PIR	C66	1.590184285	P53701	P53701 Cytochrome c-type heme lyase OS=Homo sapiens GN=HCCS PE=1 SV=1 #	2
ELEVLLMC*NK	C109;M90 C91 C91;M108	1.576832169	P62910 F8W727 D3YTB1	P62910 60S ribosomal protein L32 OS=Homo sapiens GN=RPL32 PE=1 SV=2 # F8W727 60S ribosomal protein L32 OS=Homo sapiens GN=RPL32 PE=1 SV=1 # D3YTB1 60S ribosomal protein L32 (Fragment) OS=Homo sapiens GN=RPL32 PE=1 SV=1 #	4
EIITLQLGQC*GNQIGFEFWK	C13	1.575063679	P23258	P23258 Tubulin gamma-1 chain OS=Homo sapiens GN=TUBG1 PE=1 SV=2 #	3
DLIMDNC*EELIPEYLNFIR	C178	1.573771375	Q58FG1	Q58FG1 Putative heat shock protein HSP 90-alpha A4 OS=Homo sapiens GN=HSP90AA4P PE=5 SV=1 #	2
DVQIGDIVTVGEC*RPLSK	C131	1.571372432	P62280	P62280 40S ribosomal protein S11 OS=Homo sapiens GN=RPS11 PE=1 SV=3 #	4
NWYVQPSC*ATSGDGLYEGLTWLTSNYK	C155	1.570610581	P62330	P62330 ADP-ribosylation factor 6 OS=Homo sapiens GN=ARF6 PE=1 SV=2 #	4
YLAEVAC*GDDR	C134	1.569516667	P27348	P27348 14-3-3 protein theta OS=Homo sapiens GN=YWHAQ PE=1 SV=1 #	2

LQGINC*GPDFTPSFANLGR	C662;C622;C575; C662;C575;C466; C622;C498;C669; C498;C466	1.563544672	Q04637 Q04637 E9PGM1 Q04637 Q04637 Q04637 E7EUU4 Q04637 Q04637 E7EX73 Q04637	Q04637 Eukaryotic translation initiation factor 4 gamma 1 OS=Homo sapiens GN=EIF4G1 PE=1 SV=4 # Q04637-3 Isoform B of Eukaryotic translation initiation factor 4 gamma 1 OS=Homo sapiens GN=EIF4G1 # E9PGM1 Eukaryotic translation initiation factor 4 gamma 1 OS=Homo sapiens GN=EIF4G1 PE=1 SV=1 # Q04637-8 Isoform 8 of Eukaryotic translation initiation factor 4 gamma 1 OS=Homo sapiens GN=EIF4G1 # Q04637-4 Isoform C of Eukaryotic translation initiation factor 4 gamma 1 OS=Homo sapiens GN=EIF4G1 # Q04637-6 Isoform E of Eukaryotic translation initiation factor 4 gamma 1 OS=Homo sapiens GN=EIF4G1 # E7EUU4 Eukaryotic translation initiation factor 4 gamma 1 OS=Homo sapiens GN=EIF4G1 PE=1 SV=1 # Q04637-5 Isoform D of Eukaryotic translation initiation factor 4 gamma 1 OS=Homo sapiens GN=EIF4G1 # Q04637-9 Isoform 9 of Eukaryotic translation initiation factor 4 gamma 1 OS=Homo sapiens GN=EIF4G1 # E7EX73 Eukaryotic translation initiation factor 4 gamma 1 OS=Homo sapiens GN=EIF4G1 PE=1 SV=1 # Q04637-7 Isoform 7 of Eukaryotic translation initiation factor 4 gamma 1 OS=Homo sapiens GN=EIF4G1 #	4
ALVDGPC*TQVR	C42;C42	1.558333465	E7EPB3 P50914	E7EPB3 60S ribosomal protein L14 OS=Homo sapiens GN=RPL14 PE=1 SV=1 # P50914 60S ribosomal protein L14 OS=Homo sapiens GN=RPL14 PE=1 SV=4 #	4
C*IPYAVLLEALALR	C110;C110;C110; C110	1.5545323	F5H248 Q9UBW8 F5GYF7 F5H7C6	F5H248 COP9 signalosome complex subunit 7a OS=Homo sapiens GN=COPS7A PE=1 SV=1 # Q9UBW8 COP9 signalosome complex subunit 7a OS=Homo sapiens GN=COPS7A PE=1 SV=1 # F5GYF7 COP9 signalosome complex subunit 7a (Fragment) OS=Homo sapiens GN=COPS7A PE=1 SV=7 # F5H7C6 COP9 signalosome complex subunit 7a (Fragment) OS=Homo sapiens GN=COPS7A PE=1 SV=1 #	2
KLFAPQQILQC*SPAN	C230;C263	1.54957	P04183 K7ERV3	P04183 Thymidine kinase# cytosolic OS=Homo sapiens GN=TK1 PE=1 SV=2 # K7ERV3 Thymidine kinase OS=Homo sapiens GN=TK1 PE=1 SV=1 #	2

LVIVGDGAC*GK	C16;C16;C16;C16;C16;C16	1.549145854	Q5JR08 C9JX21 C9JNR4 P61586 P08134 E9PQH6	Q5JR08 Rho-related GTP-binding protein RhoC (Fragment) OS=Homo sapiens GN=RHOC PE=1 SV=7 # C9JX21 Transforming protein RhoA OS=Homo sapiens GN=RHOA PE=1 SV=1 # C9JNR4 Transforming protein RhoA (Fragment) OS=Homo sapiens GN=RHOA PE=1 SV=1 # P61586 Transforming protein RhoA OS=Homo sapiens GN=RHOA PE=1 SV=1 # P08134 Rho-related GTP-binding protein RhoC OS=Homo sapiens GN=RHOC PE=1 SV=1 # E9PQH6 Rho-related GTP-binding protein RhoC (Fragment) OS=Homo sapiens GN=RHOC PE=1 SV=1 #	3
SLHDALC*VLAQTVK	C395	1.546252197	P78371	P78371 T-complex protein 1 subunit beta OS=Homo sapiens GN=CCT2 PE=1 SV=4 #	3
ECISIHVGQAGVQIGNAC*WELYCLEHGIQPDGQMPSDK	C20	1.541320452	P68363 Q71U36	P68363 Tubulin alpha-1B chain OS=Homo sapiens GN=TUBA1B PE=1 SV=1 # Q71U36 Tubulin alpha-1A chain OS=Homo sapiens GN=TUBA1A PE=1 SV=1 # Tubulin alpha-1C chain OS=Homo sapiens GN=TUBA1C PE=1 SV=1 #	3
VIIVQAC*R	C173;C258;C245;C328;C257;C258;C315;C202;C211	1.533391804	P51878 P49662 P51878 P51878 P51878 P49662 P51878 P49662 A0A087WZP8	P51878-3 Isoform 3 of Caspase-5 OS=Homo sapiens GN=CASP5 # P49662-4 Isoform 4 of Caspase-4 OS=Homo sapiens GN=CASP4 # P51878-6 Isoform 6 of Caspase-5 OS=Homo sapiens GN=CASP5 # P51878-5 Isoform 5 of Caspase-5 OS=Homo sapiens GN=CASP5 # P51878-2 Isoform 2 of Caspase-5 OS=Homo sapiens GN=CASP5 # P49662 Caspase-4 OS=Homo sapiens GN=CASP4 PE=1 SV=1 # P51878 Caspase-5 OS=Homo sapiens GN=CASP5 PE=1 SV=3 # P49662-2 Isoform 2 of Caspase-4 OS=Homo sapiens GN=CASP4 # A0A087WZP8 Caspase OS=Homo sapiens GN=CASP4 PE=1 SV=1 #	3
WC*EYGLTFTEK	C76;C76	1.524959354	A0A0A0MR02 P45880	A0A0A0MR02 Voltage-dependent anion-selective channel protein 2 (Fragment) OS=Homo sapiens GN=VDAC2 PE=1 SV=1 # P45880 Voltage-dependent anion-selective channel protein 2 OS=Homo sapiens GN=VDAC2 PE=1 SV=2 #	4
EENVGLHQTLDQTLNELNC*I	C283;C109;C247	1.51793486	P67936 K7EPB9 P67936	P67936-2 Isoform 2 of Tropomyosin alpha-4 chain OS=Homo sapiens GN=TPM4 # K7EPB9 Tropomyosin alpha-4 chain (Fragment) OS=Homo sapiens GN=TPM4 PE=1 SV=1 # P67936 Tropomyosin alpha-4 chain OS=Homo sapiens GN=TPM4 PE=1 SV=3 #	2

AYHEQLSVAEITNAC*FEPAN QMVK	C295	1.514009541	Q13748 P68363 Q71U36 P68366	Q13748 Tubulin alpha-3C/D chain OS=Homo sapiens GN=TUBA3C PE=1 SV=3 # P68363 Tubulin alpha-1B chain OS=Homo sapiens GN=TUBA1B PE=1 SV=1 # Q71U36 Tubulin alpha-1A chain OS=Homo sapiens GN=TUBA1A PE=1 SV=1 # P68366 Tubulin alpha-4A chain OS=Homo sapiens GN=TUBA4A PE=1 SV=1 #	4
IIC*SAGLSLLAEER	C195;C107	1.51272167	Q9BV86 S4R338	Q9BV86 N-terminal Xaa-Pro-Lys N-methyltransferase 1 OS=Homo sapiens GN=NTMT1 PE=1 SV=3 # S4R338 N-terminal Xaa-Pro-Lys N-methyltransferase 1 OS=Homo sapiens GN=NTMT1 PE=1 SV=1 #	4
VC*TLAIIDPGDSDIIR	C92;C92	1.51256941	P62888 E5RI99	P62888 60S ribosomal protein L30 OS=Homo sapiens GN=RPL30 PE=1 SV=2 # E5RI99 60S ribosomal protein L30 (Fragment) OS=Homo sapiens GN=RPL30 PE=1 SV=1 #	4
QTISNAC*GTIGLIHAIANNK	C95;C95	1.507609085	P15374	P15374 Ubiquitin carboxyl-terminal hydrolase isozyme L3 OS=Homo sapiens GN=UCHL3 PE=1 SV=1 # contaminant_UBIQUITIN10 no description#	2
NWYIQATC*ATSGDGLYEGL DWLSNQLR	C159	1.499682366	P84077	P84077 ADP-ribosylation factor 1 OS=Homo sapiens GN=ARF1 PE=1 SV=2 #	4
IGFPETTEEELEEIASENSDC* IFPSAPDVKA	C353;C340	1.498251604	Q9Y3F4 Q9Y3F4	Q9Y3F4-2 Isoform 2 of Serine-threonine kinase receptor-associated protein OS=Homo sapiens GN=STRAP # Q9Y3F4 Serine-threonine kinase receptor-associated protein OS=Homo sapiens GN=STRAP PE=1 SV=1 #	4
TIIPLISQC*TPK	C212	1.49266	P40926	P40926 Malate dehydrogenase# mitochondrial OS=Homo sapiens GN=MDH2 PE=1 SV=3 #	2
LVVVDFSATWC*GPCK	C32	1.491556053	P10599	P10599 Thioredoxin OS=Homo sapiens GN=TXN PE=1 SV=3 #	4
SEGTYC*CGPVPVR	C370	1.490169059	P21980	P21980 Protein-glutamine gamma-glutamyltransferase 2 OS=Homo sapiens GN=TGM2 PE=1 SV=2 #	3
LLPAITILGC*R	C389;C442	1.479029592	Q96IJ6 Q96IJ6	Q96IJ6 Mannose-1-phosphate guanyltransferase alpha OS=Homo sapiens GN=GMPPA PE=1 SV=1 # Q96IJ6-2 Isoform 2 of Mannose-1-phosphate guanyltransferase alpha OS=Homo sapiens GN=GMPPA #	4
VPAFEGDDGFC*VFESNAIAY YVSNEELR	C68;C118	1.478916116	P26641 P26641	P26641 Elongation factor 1-gamma OS=Homo sapiens GN=EEF1G PE=1 SV=3 # P26641-2 Isoform 2 of Elongation factor 1-gamma OS=Homo sapiens GN=EEF1G #	4

NESC*SENYTTDFIYQLYSEE GK	C641	1.477165197	Q01813	Q01813 ATP-dependent 6-phosphofructokinase# platelet type OS=Homo sapiens GN=PFKP PE=1 SV=2 #	3
KTPC*GEGSK	C70;C70	1.476518081	P60866 P60866	P60866 40S ribosomal protein S20 OS=Homo sapiens GN=RPS20 PE=1 SV=1 # P60866-2 Isoform 2 of 40S ribosomal protein S20 OS=Homo sapiens GN=RPS20 #	4
WAELLPLLQQC*QVVR	C30	1.472192443	P13489	P13489 Ribonuclease inhibitor OS=Homo sapiens GN=RNH1 PE=1 SV=2 #	4
VQENSAYIC*SR	C585	1.469243856	Q9Y3T9	Q9Y3T9 Nucleolar complex protein 2 homolog OS=Homo sapiens GN=NOC2L PE=1 SV=4 #	3
MGVEAVIALLEATPDTPAC*V VSLNGN	C343	1.4683	Q01813	Q01813 ATP-dependent 6-phosphofructokinase# platelet type OS=Homo sapiens GN=PFKP PE=1 SV=2 #	2
VAASC*GAIQYIPTELDQVR	C134	1.466280912	Q7L2H7	Q7L2H7 Eukaryotic translation initiation factor 3 subunit M OS=Homo sapiens GN=EIF3M PE=1 SV=1 #	4
AGQC*VIGLQMGTNK	C164;C153;C185; C155	1.464570529	Q99439 B4DDF4 B4DUT8 A0A087X271	Q99439 Calponin-2 OS=Homo sapiens GN=CNN2 PE=1 SV=4 # B4DDF4 Calponin OS=Homo sapiens GN=CNN2 PE=1 SV=1 # B4DUT8 Calponin OS=Homo sapiens GN=CNN2 PE=1 SV=1 # A0A087X271 Calponin (Fragment) OS=Homo sapiens GN=CNN2 PE=1 SV=1 #	3
VQEAPIDEHWIIEC*NDGVFQ R	C91	1.452702304	Q14353	Q14353 Guanidinoacetate N-methyltransferase OS=Homo sapiens GN=GAMT PE=1 SV=1 #	2
GPC*IIYNEDNGIIK	C208	1.438966627	P36578	P36578 60S ribosomal protein L4 OS=Homo sapiens GN=RPL4 PE=1 SV=5 #	2
INISEGNC*PER	C54;C54;C54	1.427355517	Q15366 Q15366 Q15365	Q15366-3 Isoform 3 of Poly(rC)-binding protein 2 OS=Homo sapiens GN=PCBP2 # Q15366-6 Isoform 6 of Poly(rC)-binding protein 2 OS=Homo sapiens GN=PCBP2 # Q15365 Poly(rC)-binding protein 1 OS=Homo sapiens GN=PCBP1 PE=1 SV=2 #	4
VLVTTNVC*AR	C361;C302;C392; C393;C310	1.424474823	I3L0H8 Q9NUU7 Q9NUU7 F6QDS0 I3L352	I3L0H8 ATP-dependent RNA helicase DDX19A OS=Homo sapiens GN=DDX19A PE=1 SV=1 # Q9NUU7-2 Isoform 2 of ATP-dependent RNA helicase DDX19A OS=Homo sapiens GN=DDX19A # Q9NUU7 ATP-dependent RNA helicase DDX19A OS=Homo sapiens GN=DDX19A PE=1 SV=1 # F6QDS0 HCG2043426# isoform CRA_b OS=Homo sapiens GN=hCG_2043426 PE=1 SV=1 # I3L352 ATP-dependent RNA helicase DDX19A (Fragment) OS=Homo sapiens GN=DDX19A PE=1 SV=1 #	2

SWC*PDCVQAEPVVR	C43	1.410010449	Q9BRA2	Q9BRA2 Thioredoxin domain-containing protein 17 OS=Homo sapiens GN=TXNDC17 PE=1 SV=1 #	4
AVC*MLSNTTAVAEAWAR	C376	1.409286361	Q9BQE3 F5H5D3	Q9BQE3 Tubulin alpha-1C chain OS=Homo sapiens GN=TUBA1C PE=1 SV=1 # F5H5D3 Tubulin alpha-1C chain OS=Homo sapiens GN=TUBA1C PE=1 SV=1 #	4
NYLPAINGIVFLVDC*ADHSR	C102	1.407052077	Q9NR31	Q9NR31 GTP-binding protein SAR1a OS=Homo sapiens GN=SAR1A PE=1 SV=1 #	4
FAC*HSASLTVR	C145	1.399133944	Q15233	Q15233 Non-POU domain-containing octamer-binding protein OS=Homo sapiens GN=NONO PE=1 SV=4 #	2
AGAIAPC*EVTVPAQNTGLGP EK	C119;C119	1.398761333	P05388 Q8NHW5	P05388 60S acidic ribosomal protein P0 OS=Homo sapiens GN=RPLP0 PE=1 SV=1 # Q8NHW5 60S acidic ribosomal protein P0-like OS=Homo sapiens GN=RPLP0P6 PE=5 SV=1 #	3
LTWHSC*PEDEAQ	C177	1.393198104	Q13185	Q13185 Chromobox protein homolog 3 OS=Homo sapiens GN=CBX3 PE=1 SV=4 #	2
YWLC*AATGPSIK	C249	1.389666495	P63244	P63244 Receptor of activated protein C kinase 1 OS=Homo sapiens GN=RACK1 PE=1 SV=3 #	4
C*LLIHPNPESALNEEAGR	C118;C147	1.387414531	Q16763 K7EPJ1	Q16763 Ubiquitin-conjugating enzyme E2 S OS=Homo sapiens GN=UBE2S PE=1 SV=2 # K7EPJ1 Ubiquitin-conjugating enzyme E2 S (Fragment) OS=Homo sapiens GN=UBE2S PE=1 SV=1 #	3
GC*LLYGPPGTGK	C184;C170	1.38664574	A0A087X2I1 P62333	A0A087X2I1 26S protease regulatory subunit 10B OS=Homo sapiens GN=PSMC6 PE=1 SV=1 # P62333 26S protease regulatory subunit 10B OS=Homo sapiens GN=PSMC6 PE=1 SV=1 #	4
ITAFVPNDGC*LNFIEENDEVL VAGFGR	C90;C90	1.382669234	P62266 D6RD47	P62266 40S ribosomal protein S23 OS=Homo sapiens GN=RPS23 PE=1 SV=3 # D6RD47 40S ribosomal protein S23 OS=Homo sapiens GN=RPS23 PE=1 SV=1 #	4
YFNPTGAHASGC*IGEDPQGI PNNLMPYVSQVAIGR	C196	1.379572402	Q14376	Q14376 UDP-glucose 4-epimerase OS=Homo sapiens GN=GALE PE=1 SV=2 #	3
LVFLAC*CVAPTNPR	C301	1.375913763	Q14566	Q14566 DNA replication licensing factor MCM6 OS=Homo sapiens GN=MCM6 PE=1 SV=1 #	3
IVGIGYNGMPNGC*SDDVLP WR	C71 C60;M67	1.371645666	P32321 P32321	P32321 Deoxycytidylate deaminase OS=Homo sapiens GN=DCTD PE=1 SV=2 # P32321-2 Isoform 2 of Deoxycytidylate deaminase OS=Homo sapiens GN=DCTD #	3
LNISFPATGC*QK	C12	1.361978108	P62753	P62753 40S ribosomal protein S6 OS=Homo sapiens GN=RPS6 PE=1 SV=1 #	4

LC*LNICVGESGDR	C21;C19;C20	1.358918589	P62913 Q5VVC8 P62913	P62913 60S ribosomal protein L11 OS=Homo sapiens GN=RPL11 PE=1 SV=2 # Q5VVC8 60S ribosomal protein L11 (Fragment) OS=Homo sapiens GN=RPL11 PE=1 SV=1 # P62913-2 Isoform 2 of 60S ribosomal protein L11 OS=Homo sapiens GN=RPL11 #	3
NC*LTNFHGMDLTR	C96;C76	1.35668724	P61247 D6RG13	P61247 40S ribosomal protein S3a OS=Homo sapiens GN=RPS3A PE=1 SV=2 # D6RG13 40S ribosomal protein S3a (Fragment) OS=Homo sapiens GN=RPS3A PE=1 SV=1 #	4
RPLNPLASGQGTSEENTFYS WLEGLC*VEK	C241	1.355504645	Q96HE7	Q96HE7 ERO1-like protein alpha OS=Homo sapiens GN=ERO1A PE=1 SV=2 #	3
NIC*FTVWDVGGQDR	C62	1.346008644	P18085	P18085 ADP-ribosylation factor 4 OS=Homo sapiens GN=ARF4 PE=1 SV=3 #	4
C*GFLPGNEK	C80;C106;C91	1.345303439	H0YM70 A0A087X1Z3 Q9UL46	H0YM70 Proteasome activator complex subunit 2 OS=Homo sapiens GN=PSME2 PE=1 SV=1 # A0A087X1Z3 Proteasome activator complex subunit 2 OS=Homo sapiens GN=PSME2 PE=1 SV=1 # Q9UL46 Proteasome activator complex subunit 2 OS=Homo sapiens GN=PSME2 PE=1 SV=4 #	2
C*FIVGADNVGSK	C27;C27	1.328104159	P05388 Q8NHW5	P05388 60S acidic ribosomal protein P0 OS=Homo sapiens GN=RPLP0 PE=1 SV=1 # Q8NHW5 60S acidic ribosomal protein P0-like OS=Homo sapiens GN=RPLP0P6 PE=5 SV=1 #	3
VPTANVSVVDLTC*R	C247	1.323420436	P04406	P04406 Glyceraldehyde-3-phosphate dehydrogenase OS=Homo sapiens GN=GAPDH PE=1 SV=3 #	2
TIGGGDDSFTTFFC*ETGAGK	C54	1.320963834	P68366	P68366 Tubulin alpha-4A chain OS=Homo sapiens GN=TUBA4A PE=1 SV=1 #	3
LGEWVGLC*K	C92	1.318965219	P25398	P25398 40S ribosomal protein S12 OS=Homo sapiens GN=RPS12 PE=1 SV=3 #	3
CPEALFQPSFLGMESC*GIHE TTFNSIMK	C272 C272;M269	1.31666736	P63261 P60709	P63261 Actin# cytoplasmic 2 OS=Homo sapiens GN=ACTG1 PE=1 SV=1 # P60709 Actin# cytoplasmic 1 OS=Homo sapiens GN=ACTB PE=1 SV=1 #	4
GPAVGIDLGTTYSC*VGVFQH GK	C17;C17	1.314064419	P11142 P11142	P11142 Heat shock cognate 71 kDa protein OS=Homo sapiens GN=HSPA8 PE=1 SV=1 # P11142-2 Isoform 2 of Heat shock cognate 71 kDa protein OS=Homo sapiens GN=HSPA8 #	2

VQVSDPESTVAVAFTPTIPHC*SMATLIGLSIK	C55;C93;C93	1.313560885	J3KS95 Q9Y3D0 H3BNV7	J3KS95 Mitotic spindle-associated MMXD complex subunit MIP18 (Fragment) OS=Homo sapiens GN=FAM96B PE=1 SV=1 # Q9Y3D0 Mitotic spindle-associated MMXD complex subunit MIP18 OS=Homo sapiens GN=FAM96B PE=1 SV=1 # H3BNV7 Mitotic spindle-associated MMXD complex subunit MIP18 (Fragment) OS=Homo sapiens GN=FAM96B PE=1 SV=1 #	3
TATAVAHC*K	C25	1.307537972	P62249	P62249 40S ribosomal protein S16 OS=Homo sapiens GN=RPS16 PE=1 SV=2 #	4
AAAPAPEEEMDEC*EQALAAEPK	C266;C316	1.301732419	P26641 P26641	P26641 Elongation factor 1-gamma OS=Homo sapiens GN=EEF1G PE=1 SV=3 # P26641-2 Isoform 2 of Elongation factor 1-gamma OS=Homo sapiens GN=EEF1G #	4
YTIVVSATASDAAPLQYLAPYSGC*SMGEYFR	C294	1.299557045	P25705 P25705 P25705	P25705 ATP synthase subunit alpha# mitochondrial OS=Homo sapiens GN=ATP5A1 PE=1 SV=1 # P25705-3 Isoform 3 of ATP synthase subunit alpha# mitochondrial OS=Homo sapiens GN=ATP5A1 # P25705-2 Isoform 2 of ATP synthase subunit alpha# mitochondrial OS=Homo sapiens GN=ATP5A1 #	2
VIGSGC*NLDSAR	C192;C164;C163	1.29911654	P00338 P07195 P00338	P00338-3 Isoform 3 of L-lactate dehydrogenase A chain OS=Homo sapiens GN=LDHA # P07195 L-lactate dehydrogenase B chain OS=Homo sapiens GN=LDHB PE=1 SV=2 # P00338 L-lactate dehydrogenase A chain OS=Homo sapiens GN=LDHA PE=1 SV=2 #	4
FLSQIESDC*LALLQVR	C794	1.292508337	P52789	P52789 Hexokinase-2 OS=Homo sapiens GN=HK2 PE=1 SV=2 #	2
ECISIHVGQAGVQIGNACWELYC*LEHGIQPDGQMPSDK	C25	1.29227859	Q13748 P68363 Q9BQE3 F5H5D3 Q71U36	Q13748 Tubulin alpha-3C/D chain OS=Homo sapiens GN=TUBA3C PE=1 SV=3 # P68363 Tubulin alpha-1B chain OS=Homo sapiens GN=TUBA1B PE=1 SV=1 # Q9BQE3 Tubulin alpha-1C chain OS=Homo sapiens GN=TUBA1C PE=1 SV=1 # F5H5D3 Tubulin alpha-1C chain OS=Homo sapiens GN=TUBA1C PE=1 SV=1 # Q71U36 Tubulin alpha-1A chain OS=Homo sapiens GN=TUBA1A PE=1 SV=1 #	3
TC*DISFSDPDDLLNFK	C47	1.292165	P61081	P61081 NEDD8-conjugating enzyme Ubc12 OS=Homo sapiens GN=UBE2M PE=1 SV=1 #	2
ECPSDEC*GAGVFMASHFDR	C126	1.288782552	P62979	P62979 Ubiquitin-40S ribosomal protein S27a OS=Homo sapiens GN=RPS27A PE=1 SV=2 #	2
EC*LPLIIFLR	C41	1.288277976	P62701	P62701 40S ribosomal protein S4# X isoform OS=Homo sapiens GN=RPS4X PE=1 SV=2 #	4

LVVPASQC*GSLIGK	C109;C109	1.279579492	Q15366 Q15366	Q15366-3 Isoform 3 of Poly(rC)-binding protein 2 OS=Homo sapiens GN=PCBP2 # Q15366-6 Isoform 6 of Poly(rC)-binding protein 2 OS=Homo sapiens GN=PCBP2 #	3
GILLYGPPGC*GK	C259;C264	1.278870043	I3L0N3 P46459	I3L0N3 Vesicle-fusing ATPase OS=Homo sapiens GN=NSF PE=1 SV=1 # P46459 Vesicle-fusing ATPase OS=Homo sapiens GN=NSF PE=1 SV=3 #	3
PMC*IPPSYADLGK	C13 C13;M12	1.269337736	A0A0A0MR02 P45880	A0A0A0MR02 Voltage-dependent anion-selective channel protein 2 (Fragment) OS=Homo sapiens GN=VDAC2 PE=1 SV=1 # P45880 Voltage-dependent anion-selective channel protein 2 OS=Homo sapiens GN=VDAC2 PE=1 SV=2 #	4
TYAIC*GAIR	C56;C56;C56	1.267648453	Q8WVC2 Q9BYK1 P63220	Q8WVC2 40S ribosomal protein S21 OS=Homo sapiens GN=RPS21 PE=1 SV=1 # Q9BYK1 40S ribosomal protein S21 OS=Homo sapiens GN=RPS21 PE=1 SV=1 # P63220 40S ribosomal protein S21 OS=Homo sapiens GN=RPS21 PE=1 SV=1 #	4
FLYEC*PWR	C622	1.262639931	P11498	P11498 Pyruvate carboxylase# mitochondrial OS=Homo sapiens GN=PC PE=1 SV=2 #	2
C*SEGSFLLTTFPR	C119;C208	1.260415	Q15233 Q15233	Q15233-2 Isoform 2 of Non-POU domain-containing octamer-binding protein OS=Homo sapiens GN=NONO # Q15233 Non-POU domain-containing octamer-binding protein OS=Homo sapiens GN=NONO PE=1 SV=4 #	2
AFAFVTFADDQIAQSLC*GEDLIIK	C244;C244;C244;C244;C244	1.254381535	A0A087X260 A0A087WYY0 B1AKP7 Q13148 G3V162	A0A087X260 TAR DNA-binding protein 43 OS=Homo sapiens GN=TARDBP PE=1 SV=1 # A0A087WYY0 TAR DNA-binding protein 43 OS=Homo sapiens GN=TARDBP PE=1 SV=1 # B1AKP7 TAR DNA-binding protein 43 OS=Homo sapiens GN=TARDBP PE=1 SV=1 # Q13148 TAR DNA-binding protein 43 OS=Homo sapiens GN=TARDBP PE=1 SV=1 # G3V162 TAR DNA binding protein# isoform CRA_d OS=Homo sapiens GN=TARDBP PE=1 SV=1 #	3
GC*TATLGNFAK	C229	1.251823686	P15880	P15880 40S ribosomal protein S2 OS=Homo sapiens GN=RPS2 PE=1 SV=2 #	3
IHMGSC*AENTAK	C196	1.249579008	P24752	P24752 Acetyl-CoA acetyltransferase# mitochondrial OS=Homo sapiens GN=ACAT1 PE=1 SV=1 #	4

GSDC*GIVNVNIPTSGAEIGG AFGGEK	C450;C478;C414; C414;C441	1.24202753	P49419 P49419 P49419 F8VS02 A0A140T9V3	P49419-2 Isoform 2 of Alpha-aminoadipic semialdehyde dehydrogenase OS=Homo sapiens GN=ALDH7A1 # P49419 Alpha-aminoadipic semialdehyde dehydrogenase OS=Homo sapiens GN=ALDH7A1 PE=1 SV=5 # P49419-4 Isoform 4 of Alpha-aminoadipic semialdehyde dehydrogenase OS=Homo sapiens GN=ALDH7A1 # F8VS02 Alpha-aminoadipic semialdehyde dehydrogenase OS=Homo sapiens GN=ALDH7A1 PE=1 SV=1 # A0A140T9V3 Alpha-aminoadipic semialdehyde dehydrogenase OS=Homo sapiens GN=ALDH7A1 PE=1 SV=1 #	3
LDVGNFSWGSEC*CTR	C71	1.24091994	P62241	P62241 40S ribosomal protein S8 OS=Homo sapiens GN=RPS8 PE=1 SV=2 #	4
VELC*SFSGYK	C6;C6;C6	1.229350102	C9JNW5 C9JXB8 P83731	C9JNW5 60S ribosomal protein L24 OS=Homo sapiens GN=RPL24 PE=1 SV=1 # C9JXB8 60S ribosomal protein L24 OS=Homo sapiens GN=RPL24 PE=1 SV=1 # P83731 60S ribosomal protein L24 OS=Homo sapiens GN=RPL24 PE=1 SV=1 #	2
NC*IVLIDSTPYR	C100	1.223595686	P62241	P62241 40S ribosomal protein S8 OS=Homo sapiens GN=RPS8 PE=1 SV=2 #	4
VPADTEVVC*APPTAYIDFAR	C42;C79	1.222077433	P60174 P60174	P60174-1 Isoform 2 of Triosephosphate isomerase OS=Homo sapiens GN=TPI1 # P60174 Triosephosphate isomerase OS=Homo sapiens GN=TPI1 PE=1 SV=3 #	2
FIC*TTSAIQNR	C20	1.21976927	P53396	P53396 ATP-citrate synthase OS=Homo sapiens GN=ACLY PE=1 SV=3 #	4
WNDNC*PSWNTIDPEER	C301	1.21147732	P17655	P17655 Calpain-2 catalytic subunit OS=Homo sapiens GN=CAPN2 PE=1 SV=6 #	4
LISPNLGVVFFNAC*EAASR	C316;C342	1.211285933	Q66K74 Q66K74	Q66K74-2 Isoform 2 of Microtubule-associated protein 1S OS=Homo sapiens GN=MAP1S # Q66K74 Microtubule-associated protein 1S OS=Homo sapiens GN=MAP1S PE=1 SV=2 #	3
TIAEC*LADELINAAK	C172;C193;C172	1.200717187	P46782 M0R0R2 M0R0F0	P46782 40S ribosomal protein S5 OS=Homo sapiens GN=RPS5 PE=1 SV=4 # M0R0R2 40S ribosomal protein S5 OS=Homo sapiens GN=RPS5 PE=1 SV=1 # M0R0F0 40S ribosomal protein S5 (Fragment) OS=Homo sapiens GN=RPS5 PE=1 SV=1 #	4
EC*PSDECGAGVFMASHFDR	C121	1.198095053	P62979	P62979 Ubiquitin-40S ribosomal protein S27a OS=Homo sapiens GN=RPS27A PE=1 SV=2 #	3
VVMALGDYMGASCHAC*IGG TNVR	C134	1.197409199	P60842	P60842 Eukaryotic initiation factor 4A-I OS=Homo sapiens GN=EIF4A1 PE=1 SV=1 #	3

HELQANC*YEEVKDR	C177;C122;C139; C139	1.191814614	E9PK25 G3V1A4 P23528 E9PP50	E9PK25 Cofilin-1 OS=Homo sapiens GN=CFL1 PE=1 SV=1 # G3V1A4 Cofilin 1 (Non-muscle)# isoform CRA_a OS=Homo sapiens GN=CFL1 PE=1 SV=1 # P23528 Cofilin-1 OS=Homo sapiens GN=CFL1 PE=1 SV=3 # E9PP50 Cofilin-1 (Fragment) OS=Homo sapiens GN=CFL1 PE=1 SV=7 #	4
VSDTVVEPYNATLSVHQLVE NTDETYCIDNEALYDIC*FR	C211;C211;C211; C193;C211	1.189085	P68371 Q9BVA1 P04350 Q5JP53 Q9BUF5	P68371 Tubulin beta-4B chain OS=Homo sapiens GN=TUBB4B PE=1 SV=1 # Q9BVA1 Tubulin beta-2B chain OS=Homo sapiens GN=TUBB2B PE=1 SV=1 # P04350 Tubulin beta-4A chain OS=Homo sapiens GN=TUBB4A PE=1 SV=2 # Q5JP53 Tubulin beta chain OS=Homo sapiens GN=TUBB PE=1 SV=1 # Q9BUF5 Tubulin beta-6 chain OS=Homo sapiens GN=TUBB6 PE=1 SV=1 #	2
YEAAFPFLSPC*GR	C143;C98	1.187401751	H0YF29 Q6P1X6	H0YF29 UPF0598 protein C8orf82 (Fragment) OS=Homo sapiens GN=C8orf82 PE=1 SV=1 # Q6P1X6 UPF0598 protein C8orf82 OS=Homo sapiens GN=C8orf82 PE=1 SV=2 #	4
ALNALC*DGLIDELNQALK	C62	1.18723479	P30084	P30084 Enoyl-CoA hydratase# mitochondrial OS=Homo sapiens GN=ECHS1 PE=1 SV=4 #	4
LGGSLIVAFEGC*PV	C146;C163	1.18623817	P60981 P60981	P60981-2 Isoform 2 of Destrin OS=Homo sapiens GN=DSTN # P60981 Destrin OS=Homo sapiens GN=DSTN PE=1 SV=3 #	4
TWYVQATC*ATQGTGLYEGL DWLSNELSK	C159	1.185623235	P18085	P18085 ADP-ribosylation factor 4 OS=Homo sapiens GN=ARF4 PE=1 SV=3 #	4
HSMNPFC*EIAVEEAVR	C133;M38 C42;M129 C42	1.184643524	P38117 P38117 M0QY67	P38117 Electron transfer flavoprotein subunit beta OS=Homo sapiens GN=ETFB PE=1 SV=3 # P38117-2 Isoform 2 of Electron transfer flavoprotein subunit beta OS=Homo sapiens GN=ETFB # M0QY67 Electron transfer flavoprotein subunit beta (Fragment) OS=Homo sapiens GN=ETFB PE=1 SV=1 #	2
GVLLYGPPGC*GK	C137	1.183741509	Q8NBU5	Q8NBU5 ATPase family AAA domain-containing protein 1 OS=Homo sapiens GN=ATAD1 PE=1 SV=1 #	2

VSDTVVEPYNATLSVHQLVENTDETYC*IDNEALYDICFR	C201;C201;C201;C201;C164;C183;C201	1.178339005	P07437 P68371 Q9BVA1 P04350 K7ESM5 Q5JP53 Q9BUF5	P07437 Tubulin beta chain OS=Homo sapiens GN=TUBB PE=1 SV=2 # P68371 Tubulin beta-4B chain OS=Homo sapiens GN=TUBB4B PE=1 SV=1 # Q9BVA1 Tubulin beta-2B chain OS=Homo sapiens GN=TUBB2B PE=1 SV=1 # P04350 Tubulin beta-4A chain OS=Homo sapiens GN=TUBB4A PE=1 SV=2 # K7ESM5 Tubulin beta-6 chain (Fragment) OS=Homo sapiens GN=TUBB6 PE=1 SV=1 # Q5JP53 Tubulin beta chain OS=Homo sapiens GN=TUBB PE=1 SV=1 # Q9BUF5 Tubulin beta-6 chain OS=Homo sapiens GN=TUBB6 PE=1 SV=1 #	4
FDPTQFQDC*IIQGLTETGTDLEAVAK	C35;C67;C39	1.176229718	Q7L1Q6 Q7L1Q6 Q7L1Q6	Q7L1Q6 Basic leucine zipper and W2 domain-containing protein 1 OS=Homo sapiens GN=BZW1 PE=1 SV=1 # Q7L1Q6-3 Isoform 3 of Basic leucine zipper and W2 domain-containing protein 1 OS=Homo sapiens GN=BZW1 # Q7L1Q6-4 Isoform 4 of Basic leucine zipper and W2 domain-containing protein 1 OS=Homo sapiens GN=BZW1 #	4
TIQFVDWC*PTGFK	C347;C347;C417;C371;C347	1.173131675	Q13748 Q9BQE3 F5H5D3 C9J2C0 Q71U36	Q13748 Tubulin alpha-3C/D chain OS=Homo sapiens GN=TUBA3C PE=1 SV=3 # Q9BQE3 Tubulin alpha-1C chain OS=Homo sapiens GN=TUBA1C PE=1 SV=1 # F5H5D3 Tubulin alpha-1C chain OS=Homo sapiens GN=TUBA1C PE=1 SV=1 # C9J2C0 Tubulin alpha-8 chain (Fragment) OS=Homo sapiens GN=TUBA8 PE=1 SV=1 # Q71U36 Tubulin alpha-1A chain OS=Homo sapiens GN=TUBA1A PE=1 SV=1 #	4
IIPGFMC*QGGDFTR	C62 C62;M61	1.165426078	F8WE65 C9J5S7 P62937	F8WE65 Peptidyl-prolyl cis-trans isomerase OS=Homo sapiens GN=PPIA PE=1 SV=1 # C9J5S7 Peptidyl-prolyl cis-trans isomerase OS=Homo sapiens GN=PPIA PE=1 SV=1 # P62937 Peptidyl-prolyl cis-trans isomerase A OS=Homo sapiens GN=PPIA PE=1 SV=2 #	4
KC*STPEEIK	C6;C23	1.164373221	P60981 P60981	P60981-2 Isoform 2 of Destrin OS=Homo sapiens GN=DSTN # P60981 Destrin OS=Homo sapiens GN=DSTN PE=1 SV=3 #	2

NFYGGNGIVGAQVPLGAGIALAC*K	C181;C219;C188	1.163597672	P08559 P08559 P08559	P08559 Pyruvate dehydrogenase E1 component subunit alpha# somatic form# mitochondrial OS=Homo sapiens GN=PDHA1 PE=1 SV=3 # P08559-4 Isoform 4 of Pyruvate dehydrogenase E1 component subunit alpha# somatic form# mitochondrial OS=Homo sapiens GN=PDHA1 # P08559-2 Isoform 2 of Pyruvate dehydrogenase E1 component subunit alpha# somatic form# mitochondrial OS=Homo sapiens GN=PDHA1 #	4
SSC*LFCLPSFK	C29	1.151448318	Q9UNA3	Q9UNA3 Alpha-1#4-N-acetylglucosaminyltransferase OS=Homo sapiens GN=A4GNT PE=2 SV=1 #	2
ALANVNIGSLIC*NVGAGGPAPAAGAAPAGGPAPSTAAAPAEEK	C61	1.150056294	P05386	P05386 60S acidic ribosomal protein P1 OS=Homo sapiens GN=RPLP1 PE=1 SV=1 #	4
WLSDEC*TNAVVNFLSR	C345;C350;C380	1.149225	O75521 A0A0C4DGA2 O75521	O75521-2 Isoform 2 of Enoyl-CoA delta isomerase 2# mitochondrial OS=Homo sapiens GN=ECI2 # A0A0C4DGA2 Enoyl-CoA delta isomerase 2# mitochondrial OS=Homo sapiens GN=ECI2 PE=1 SV=1 # O75521 Enoyl-CoA delta isomerase 2# mitochondrial OS=Homo sapiens GN=ECI2 PE=1 SV=4 #	2
GIDQC*IPLFVEAALER	C757	1.147271891	O95373	O95373 Importin-7 OS=Homo sapiens GN=IPO7 PE=1 SV=1 #	3
LPACVVDC*GTGYTK	C12	1.142319122	P61158	P61158 Actin-related protein 3 OS=Homo sapiens GN=ACTR3 PE=1 SV=3 #	2
VTDGALVVVDCVSGVC*VQTETVLR	C136	1.141082024	P13639	P13639 Elongation factor 2 OS=Homo sapiens GN=EEF2 PE=1 SV=4 #	4
NTVLC*NVVEQFLQADLAR	C70	1.136312284	Q14258	Q14258 E3 ubiquitin/ISG15 ligase TRIM25 OS=Homo sapiens GN=TRIM25 PE=1 SV=2 #	2
TGC*TFPEKPDFH	C318;C353;C336	1.134421105	P55263 P55263 P55263	P55263-4 Isoform 4 of Adenosine kinase OS=Homo sapiens GN=ADK # P55263 Adenosine kinase OS=Homo sapiens GN=ADK PE=1 SV=2 # P55263-2 Isoform 2 of Adenosine kinase OS=Homo sapiens GN=ADK #	4
VDEFPLC*GHMVSDEYEQLSSEALEAAR	C49	1.125416339	X1WI28 P27635	X1WI28 60S ribosomal protein L10 (Fragment) OS=Homo sapiens GN=RPL10 PE=1 SV=6 # P27635 60S ribosomal protein L10 OS=Homo sapiens GN=RPL10 PE=1 SV=4 #	4
VNQAIWLLC*TGAR	C155;C176;C155	1.123764124	P46782 M0R0R2 M0R0F0	P46782 40S ribosomal protein S5 OS=Homo sapiens GN=RPS5 PE=1 SV=4 # M0R0R2 40S ribosomal protein S5 OS=Homo sapiens GN=RPS5 PE=1 SV=1 # M0R0F0 40S ribosomal protein S5 (Fragment) OS=Homo sapiens GN=RPS5 PE=1 SV=1 #	4

IINDNATYC*R	C211	1.122849333	O00567	O00567 Nucleolar protein 56 OS=Homo sapiens GN=NOP56 PE=1 SV=4 #	2
NMMAAC*DPR	C303;M299 C303;M646 C303;M281 C285;M299 C650;M299 C303	1.118740212	Q13509 P68371 Q9BVA1 A0A0B4J269 P04350 Q5JP53 Q9BUF5	Q13509 Tubulin beta-3 chain OS=Homo sapiens GN=TUBB3 PE=1 SV=2 # P68371 Tubulin beta-4B chain OS=Homo sapiens GN=TUBB4B PE=1 SV=1 # Q9BVA1 Tubulin beta-2B chain OS=Homo sapiens GN=TUBB2B PE=1 SV=1 # A0A0B4J269 Uncharacterized protein OS=Homo sapiens PE=1 SV=1 # P04350 Tubulin beta-4A chain OS=Homo sapiens GN=TUBB4A PE=1 SV=2 # Q5JP53 Tubulin beta chain OS=Homo sapiens GN=TUBB PE=1 SV=1 # Q9BUF5 Tubulin beta-6 chain OS=Homo sapiens GN=TUBB6 PE=1 SV=1 #	4
QMFEPVSC*TFTYLLGDR	C34 C34;M28	1.111785505	O95571 M0QXB5	O95571 Persulfide dioxygenase ETHE1# mitochondrial OS=Homo sapiens GN=ETHE1 PE=1 SV=2 # M0QXB5 Persulfide dioxygenase ETHE1# mitochondrial OS=Homo sapiens GN=ETHE1 PE=1 SV=1 #	4
SIQFVDWC*PTGFK	C347;C347	1.111776695	P68363 P68366	P68363 Tubulin alpha-1B chain OS=Homo sapiens GN=TUBA1B PE=1 SV=1 # P68366 Tubulin alpha-4A chain OS=Homo sapiens GN=TUBA4A PE=1 SV=1 #	4
IGLIQFC*LSAPK	C252	1.11010728	P50991	P50991 T-complex protein 1 subunit delta OS=Homo sapiens GN=CCT4 PE=1 SV=4 #	3
AFQYVETHGEVC*PANWTPD SPTIKPSPAASK	C229;C211	1.098279255	P30048 P30048	P30048 Thioredoxin-dependent peroxide reductase# mitochondrial OS=Homo sapiens GN=PRDX3 PE=1 SV=3 # P30048-2 Isoform 2 of Thioredoxin-dependent peroxide reductase# mitochondrial OS=Homo sapiens GN=PRDX3 #	3
IC*DQWDALGSLTHSR	C499	1.098126183	O43707	O43707 Alpha-actinin-4 OS=Homo sapiens GN=ACTN4 PE=1 SV=2 #	2
GNHEC*ASINR	C138;C126;C127	1.090452677	P62136 P62140 P62136	P62136-2 Isoform 2 of Serine/threonine-protein phosphatase PP1-alpha catalytic subunit OS=Homo sapiens GN=PPP1CA # P62140 Serine/threonine-protein phosphatase PP1-beta catalytic subunit OS=Homo sapiens GN=PPP1CB PE=1 SV=3 # P62136 Serine/threonine-protein phosphatase PP1-alpha catalytic subunit OS=Homo sapiens GN=PPP1CA PE=1 SV=1 #	2
NLVFSSSATVYGNPQYLPLD EAHPTGGC*TNPYGK	C153	1.083760079	Q14376	Q14376 UDP-glucose 4-epimerase OS=Homo sapiens GN=GALE PE=1 SV=2 #	2

C*PEALFQPSFLGMESCGIHETTFNSIMK	C257	1.081955502	P63261 P60709	P63261 Actin# cytoplasmic 2 OS=Homo sapiens GN=ACTG1 PE=1 SV=1 # P60709 Actin# cytoplasmic 1 OS=Homo sapiens GN=ACTB PE=1 SV=1 #	4
YMAC*CLLYR	C385;M313 C315 C315;M320 C282;M383 C322;M313 C315;M313 C315;M280	1.08153113	P68363 Q9BQE3 A6NHL2 F5H5D3 Q71U36 A6NHL2 P68366	P68363 Tubulin alpha-1B chain OS=Homo sapiens GN=TUBA1B PE=1 SV=1 # Q9BQE3 Tubulin alpha-1C chain OS=Homo sapiens GN=TUBA1C PE=1 SV=1 # A6NHL2-2 Isoform 2 of Tubulin alpha chain-like 3 OS=Homo sapiens GN=TUBAL3 # F5H5D3 Tubulin alpha-1C chain OS=Homo sapiens GN=TUBA1C PE=1 SV=1 # Q71U36 Tubulin alpha-1A chain OS=Homo sapiens GN=TUBA1A PE=1 SV=1 # A6NHL2 Tubulin alpha chain-like 3 OS=Homo sapiens GN=TUBAL3 PE=1 SV=2 # P68366 Tubulin alpha-4A chain OS=Homo sapiens GN=TUBA4A PE=1 SV=1 #	4
NQSFC*PTVNLDK	C70;C70	1.080792356	P46776 E9PLL6	P46776 60S ribosomal protein L27a OS=Homo sapiens GN=RPL27A PE=1 SV=2 # E9PLL6 60S ribosomal protein L27a OS=Homo sapiens GN=RPL27A PE=1 SV=1 #	4
TVLCGTC*GQPADK	C479;C492;C187; C591;C591;C561	1.07875	P02545 P02545 A0A0C4DGC5 P02545 P02545 P02545	P02545-4 Isoform 4 of Prelamin-A/C OS=Homo sapiens GN=LMNA # P02545-5 Isoform 5 of Prelamin-A/C OS=Homo sapiens GN=LMNA # A0A0C4DGC5 Prelamin-A/C (Fragment) OS=Homo sapiens GN=LMNA PE=1 SV=1 # P02545-6 Isoform 6 of Prelamin-A/C OS=Homo sapiens GN=LMNA # P02545 Prelamin-A/C OS=Homo sapiens GN=LMNA PE=1 SV=1 # P02545-3 Isoform ADelta10 of Prelamin-A/C OS=Homo sapiens GN=LMNA #	2
LVVPATQC*GSLIGK	C109	1.066076401	Q15365	Q15365 Poly(rC)-binding protein 1 OS=Homo sapiens GN=PCBP1 PE=1 SV=2 #	4
LVAFC*PFASSQVALENANAVSEGVVHEDLR	C52	1.065344508	O00567	O00567 Nucleolar protein 56 OS=Homo sapiens GN=NOP56 PE=1 SV=4 #	4
AYHEQLTVAEITNAC*FEPANQMVK		1.064331352		Tubulin alpha-1C chain OS=Homo sapiens GN=TUBA1C PE=1 SV=1 #	4
EFC*SYLQYLEYLSQNRPPPNAYELFAK	C278;C261	1.063184484	O14744 O14744	O14744 Protein arginine N-methyltransferase 5 OS=Homo sapiens GN=PRMT5 PE=1 SV=4 # O14744-2 Isoform 2 of Protein arginine N-methyltransferase 5 OS=Homo sapiens GN=PRMT5 #	2

CPEVEELVFSHFVIC*NDTQETLR	C2610;C2635;C2634	1.058392694	Q7Z7G8 Q7Z7G8 Q7Z7G8	Q7Z7G8-2 Isoform 2 of Vacuolar protein sorting-associated protein 13B OS=Homo sapiens GN=VPS13B # Q7Z7G8 Vacuolar protein sorting-associated protein 13B OS=Homo sapiens GN=VPS13B PE=1 SV=2 # Q7Z7G8-6 Isoform 6 of Vacuolar protein sorting-associated protein 13B OS=Homo sapiens GN=VPS13B #	2
SYC*AEIAHNVSSK	C96;C114;C96	1.055074707	P62910 F8W727 D3YTB1	P62910 60S ribosomal protein L32 OS=Homo sapiens GN=RPL32 PE=1 SV=2 # F8W727 60S ribosomal protein L32 OS=Homo sapiens GN=RPL32 PE=1 SV=1 # D3YTB1 60S ribosomal protein L32 (Fragment) OS=Homo sapiens GN=RPL32 PE=1 SV=1 #	4
YGAVDPLLALLAVPDMSSLAC*GYLR	C223	1.053334172	P52292	P52292 Importin subunit alpha-1 OS=Homo sapiens GN=KPNA2 PE=1 SV=1 #	4
IEEDVVVTDSGIELLTC*VPR	C403;C467	1.051111126	P12955 P12955	P12955-3 Isoform 3 of Xaa-Pro dipeptidase OS=Homo sapiens GN=PEPD # P12955 Xaa-Pro dipeptidase OS=Homo sapiens GN=PEPD PE=1 SV=3 #	4
SAGAC*TAAAFLK	C462;C431	1.050568434	P28838 P28838	P28838 Cytosol aminopeptidase OS=Homo sapiens GN=LAP3 PE=1 SV=3 # P28838-2 Isoform 2 of Cytosol aminopeptidase OS=Homo sapiens GN=LAP3 #	3
IISNASC*TTNCLAPLAK	C152	1.049621226	P04406	P04406 Glyceraldehyde-3-phosphate dehydrogenase OS=Homo sapiens GN=GAPDH PE=1 SV=3 #	4
TDICQGALGDC*WLLAAIASLTLNEEILAR	C105	1.048621049	P17655	P17655 Calpain-2 catalytic subunit OS=Homo sapiens GN=CAPN2 PE=1 SV=6 #	3
YMACC*LLYR	C316;M280 C316;M320 C316 C323;M313 C283;M313	1.038903906	P68363 A6NHL2 Q71U36 A6NHL2 P68366	P68363 Tubulin alpha-1B chain OS=Homo sapiens GN=TUBA1B PE=1 SV=1 # A6NHL2-2 Isoform 2 of Tubulin alpha chain-like 3 OS=Homo sapiens GN=TUBAL3 # Q71U36 Tubulin alpha-1A chain OS=Homo sapiens GN=TUBA1A PE=1 SV=1 # Tubulin alpha-1C chain OS=Homo sapiens GN=TUBA1C PE=1 SV=1 # A6NHL2 Tubulin alpha chain-like 3 OS=Homo sapiens GN=TUBAL3 PE=1 SV=2 # P68366 Tubulin alpha-4A chain OS=Homo sapiens GN=TUBA4A PE=1 SV=1 #	3
YAYLNVVGMVGSIDNDFC*GTDMTIGTDSALHR	C179	1.033937038	Q01813	Q01813 ATP-dependent 6-phosphofructokinase# platelet type OS=Homo sapiens GN=PFKP PE=1 SV=2 #	3
STFFNVLTNSQASAENFPFC*TIDPNESR	C75;C55	1.033312954	J3KQ32 Q9NTK5	J3KQ32 Obg-like ATPase 1 OS=Homo sapiens GN=OLA1 PE=1 SV=1 # Q9NTK5 Obg-like ATPase 1 OS=Homo sapiens GN=OLA1 PE=1 SV=2 #	4

AYHEQLSVAEITSSC*FEPNSQMVK	C53	1.031208644	V9GZ17 C9J2C0 Q9NY65	V9GZ17 Tubulin alpha-8 chain (Fragment) OS=Homo sapiens GN=TUBA8 PE=1 SV=1 # C9J2C0 Tubulin alpha-8 chain (Fragment) OS=Homo sapiens GN=TUBA8 PE=1 SV=1 # Q9NY65 Tubulin alpha-8 chain OS=Homo sapiens GN=TUBA8 PE=1 SV=1 #	3
TVGVQGDC*R	C523	1.030536693	P49915	P49915 GMP synthase [glutamine-hydrolyzing] OS=Homo sapiens GN=GMPS PE=1 SV=1 #	2
ECENCDC*LQGFQLTHSLGGGTGSGMGTLLISK	C129;C476	1.028255763	Q13509 A0A0B4J269	Q13509 Tubulin beta-3 chain OS=Homo sapiens GN=TUBB3 PE=1 SV=2 # A0A0B4J269 Uncharacterized protein OS=Homo sapiens PE=1 SV=1 #	2
VWNLANC*K	C182	1.022539	P63244	P63244 Receptor of activated protein C kinase 1 OS=Homo sapiens GN=RACK1 PE=1 SV=3 #	4
FFACAPNYSYAALCEC*LR	C513	1.021705429	Q96RS6	Q96RS6 NudC domain-containing protein 1 OS=Homo sapiens GN=NUDCD1 PE=1 SV=2 #	2
VC*ENIPIVLCGNK	C112;C130;C129;C108	1.014693017	P62826 J3KQE5 B5MDF5 F5H018	P62826 GTP-binding nuclear protein Ran OS=Homo sapiens GN=RAN PE=1 SV=3 # J3KQE5 GTP-binding nuclear protein Ran (Fragment) OS=Homo sapiens GN=RAN PE=1 SV=1 # B5MDF5 GTP-binding nuclear protein Ran OS=Homo sapiens GN=RAN PE=1 SV=1 # F5H018 GTP-binding nuclear protein Ran (Fragment) OS=Homo sapiens GN=RAN PE=1 SV=7 #	3
AITIAGIPQSIIEC*VK	C158;C158	1.01293287	Q15366 Q15366	Q15366-3 Isoform 3 of Poly(rC)-binding protein 2 OS=Homo sapiens GN=PCBP2 # Q15366-6 Isoform 6 of Poly(rC)-binding protein 2 OS=Homo sapiens GN=PCBP2 #	2
VTEDENDEPIEIPSEDDGTVLLSTVTAQFPGAC*GLR	C39;C39;C39;C39;C39	1.008762615	A0A087X260 A0A087WYY0 B1AKP7 Q13148 G3V162	A0A087X260 TAR DNA-binding protein 43 OS=Homo sapiens GN=TARDBP PE=1 SV=1 # A0A087WYY0 TAR DNA-binding protein 43 OS=Homo sapiens GN=TARDBP PE=1 SV=1 # B1AKP7 TAR DNA-binding protein 43 OS=Homo sapiens GN=TARDBP PE=1 SV=1 # Q13148 TAR DNA-binding protein 43 OS=Homo sapiens GN=TARDBP PE=1 SV=1 # G3V162 TAR DNA binding protein# isoform CRA_d OS=Homo sapiens GN=TARDBP PE=1 SV=1 #	2
C*WDPSPQAYFTLPR	C354;C348	1.008601832	O14641 I3L2N2	O14641 Segment polarity protein dishevelled homolog DVL-2 OS=Homo sapiens GN=DVL2 PE=1 SV=1 # I3L2N2 Segment polarity protein dishevelled homolog DVL-2 OS=Homo sapiens GN=DVL2 PE=1 SV=1 #	3

MYGISLC*QAILDETKGDYEK	C324	1.00686105	P04083	P04083 Annexin A1 OS=Homo sapiens GN=ANXA1 PE=1 SV=2 #	4
LC*YVALDFEQEMATVASSSSLEK	C917	1.006757047	A5A3E0	A5A3E0 POTE ankyrin domain family member F OS=Homo sapiens GN=POTEF PE=1 SV=2 #	3
CC*SGAIIVLTK	C424	1.004791186	P14618	P14618 Pyruvate kinase PKM OS=Homo sapiens GN=PKM PE=1 SV=4 #	2
CPALYWLSGLTC*TEQNFISK	C27;C56	1.004253173	X6RA14 P10768	X6RA14 S-formylglutathione hydrolase OS=Homo sapiens GN=ESD PE=1 SV=1 # P10768 S-formylglutathione hydrolase OS=Homo sapiens GN=ESD PE=1 SV=2 #	4
ELDLSNNC*LGDAGILQLVESVR	C409	0.997783509	P13489	P13489 Ribonuclease inhibitor OS=Homo sapiens GN=RNH1 PE=1 SV=2 #	3
YAIC*SALAASALPALVMSK	C125	0.988946737	P36578	P36578 60S ribosomal protein L4 OS=Homo sapiens GN=RPL4 PE=1 SV=5 #	4
NTGIIC*TIGPASR	C49;C49	0.983275335	P14618 P14618	P14618-2 Isoform M1 of Pyruvate kinase PKM OS=Homo sapiens GN=PKM # P14618 Pyruvate kinase PKM OS=Homo sapiens GN=PKM PE=1 SV=4 #	4
C*GETAFIAPQCEMIPIEWVCR	C81	0.983204366	P22234	P22234 Multifunctional protein ADE2 OS=Homo sapiens GN=PAICS PE=1 SV=3 #	3
LLAC*IASR	C174	0.979250421	P62241	P62241 40S ribosomal protein S8 OS=Homo sapiens GN=RPS8 PE=1 SV=2 #	3
MC*LFAGFQR	C575 C594;M574	0.97815	Q00839 Q00839	Q00839 Heterogeneous nuclear ribonucleoprotein U OS=Homo sapiens GN=HNRNPU PE=1 SV=6 # Q00839-2 Isoform Short of Heterogeneous nuclear ribonucleoprotein U OS=Homo sapiens GN=HNRNPU #	2
FMTPVIQDNPSGWGPC*AVPEQFR	C19 C19;M5	0.968583908	O15371 O15371	O15371-2 Isoform 2 of Eukaryotic translation initiation factor 3 subunit D OS=Homo sapiens GN=EIF3D # O15371-3 Isoform 3 of Eukaryotic translation initiation factor 3 subunit D OS=Homo sapiens GN=EIF3D #	4
AHEILPNLVCC*SAK	C149	0.966364707	P50990	P50990 T-complex protein 1 subunit theta OS=Homo sapiens GN=CCT8 PE=1 SV=4 #	2
NAFAC*FDEEATGTIQEDYLR	C108;C114;C109	0.965203804	P19105 J3QRS3 O14950	P19105 Myosin regulatory light chain 12A OS=Homo sapiens GN=MYL12A PE=1 SV=2 # J3QRS3 Myosin regulatory light chain 12A OS=Homo sapiens GN=MYL12A PE=1 SV=1 # O14950 Myosin regulatory light chain 12B OS=Homo sapiens GN=MYL12B PE=1 SV=2 #	2

C*CFLCMVCR	C33;C33;C33	0.953614922	Q16527 F8VQR7 F8VW96	Q16527 Cysteine and glycine-rich protein 2 OS=Homo sapiens GN=CSRP2 PE=1 SV=3 # F8VQR7 Cysteine and glycine-rich protein 2 OS=Homo sapiens GN=CSRP2 PE=1 SV=1 # F8VW96 Cysteine and glycine-rich protein 2 OS=Homo sapiens GN=CSRP2 PE=1 SV=1 #	2
QGEYGLASIC*NGGGGASAM LIQK	C413	0.953529366	P24752	P24752 Acetyl-CoA acetyltransferase# mitochondrial OS=Homo sapiens GN=ACAT1 PE=1 SV=1 #	3
ITSC*IFQLLQEAGIK	C63	0.953130587	P22234	P22234 Multifunctional protein ADE2 OS=Homo sapiens GN=PAICS PE=1 SV=3 #	4
DSNNLC*LHFNPR	C43	0.952567491	P09382	P09382 Galectin-1 OS=Homo sapiens GN=LGALS1 PE=1 SV=2 #	2
VIEINPYLLGTMSGC*AADCQ YWER	C116;C120;C120	0.950677241	P28062 X5D2R7 P28062	P28062-2 Isoform 2 of Proteasome subunit beta type-8 OS=Homo sapiens GN=PSMB8 # X5D2R7 Proteasome subunit beta type OS=Homo sapiens GN=PSM8 PE=1 SV=1 # P28062 Proteasome subunit beta type-8 OS=Homo sapiens GN=PSMB8 PE=1 SV=3 #	4
AGSDGESIGNC*PFSQR	C35	0.947923603	Q9Y696	Q9Y696 Chloride intracellular channel protein 4 OS=Homo sapiens GN=CLIC4 PE=1 SV=4 #	4
LYYFQYPC*YQEGLR	C130	0.94582	Q9NRW3	Q9NRW3 DNA dC- dU-editing enzyme APOBEC-3C OS=Homo sapiens GN=APOBEC3C PE=1 SV=2 #	2
ATDYPC*LLILDPQNEFETLR	C145	0.92958589	Q9NVG8	Q9NVG8 TBC1 domain family member 13 OS=Homo sapiens GN=TBC1D13 PE=1 SV=3 #	2
SGEEDFESLASQFSDC*SSA K	C113;C113	0.926673471	K7EMU7 Q13526	K7EMU7 Peptidylprolyl isomerase OS=Homo sapiens GN=PIN1 PE=1 SV=1 # Q13526 Peptidyl-prolyl cis-trans isomerase NIMA-interacting 1 OS=Homo sapiens GN=PIN1 PE=1 SV=1 #	4
LDINLLDNVVNC*LYHGEGAQ QR	C34	0.918419997	O14980	O14980 Exportin-1 OS=Homo sapiens GN=XPO1 PE=1 SV=1 #	4
GLGTDEDSLIEIIC*SR	C151;C133	0.917905188	P07355 P07355	P07355-2 Isoform 2 of Annexin A2 OS=Homo sapiens GN=ANXA2 # P07355 Annexin A2 OS=Homo sapiens GN=ANXA2 PE=1 SV=2 #	3
YNFFTGC*PK	C364	0.91642993	Q99832	Q99832 T-complex protein 1 subunit eta OS=Homo sapiens GN=CCT7 PE=1 SV=2 #	3
GTPEQPQC*GFSNAVVQILR	C67	0.913922743	Q86SX6	Q86SX6 Glutaredoxin-related protein 5# mitochondrial OS=Homo sapiens GN=GLRX5 PE=1 SV=2 #	4
C*CSGAIIVLTK	C423	0.900454475	P14618	P14618 Pyruvate kinase PKM OS=Homo sapiens GN=PKM PE=1 SV=4 #	2

GNFTLPEVAEC*FDEITYVEL QK	C648;C629	0.900166667	Q00839 Q00839	Q00839 Heterogeneous nuclear ribonucleoprotein U OS=Homo sapiens GN=HNRNPU PE=1 SV=6 # Q00839-2 Isoform Short of Heterogeneous nuclear ribonucleoprotein U OS=Homo sapiens GN=HNRNPU #	3
VLLSICSLLC*DPNPDDPLVPE IAR	C113;C111;C111; C105;C82;C82;C1 11;C82;C112;C11 1	0.899517736	P61077 P61077 P61077 H9KV45 P62837 D6RAH7 A0A0A0MQU3 D6RFM0 A0A087WY85 P62837	P61077-3 Isoform 3 of Ubiquitin-conjugating enzyme E2 D3 OS=Homo sapiens GN=UBE2D3 # P61077 Ubiquitin-conjugating enzyme E2 D3 OS=Homo sapiens GN=UBE2D3 PE=1 SV=1 # P61077-2 Isoform 2 of Ubiquitin-conjugating enzyme E2 D3 OS=Homo sapiens GN=UBE2D3 # H9KV45 Ubiquitin-conjugating enzyme E2 D3 OS=Homo sapiens GN=UBE2D3 PE=1 SV=1 # P62837-2 Isoform 2 of Ubiquitin-conjugating enzyme E2 D2 OS=Homo sapiens GN=UBE2D2 # D6RAH7 Ubiquitin-conjugating enzyme E2 D3 OS=Homo sapiens GN=UBE2D3 PE=1 SV=1 # A0A0A0MQU3 Ubiquitin-conjugating enzyme E2 D2 OS=Homo sapiens GN=UBE2D2 PE=1 SV=1 # D6RFM0 Ubiquitin-conjugating enzyme E2 D2 (Fragment) OS=Homo sapiens GN=UBE2D2 PE=3 SV=1 # A0A087WY85 Ubiquitin-conjugating enzyme E2 D3 OS=Homo sapiens GN=UBE2D3 PE=1 SV=1 # P62837 Ubiquitin-conjugating enzyme E2 D2 OS=Homo sapiens GN=UBE2D2 PE=1 SV=1 #	2
VIGIEC*SSISDYAVK	C73;C119;C101;C 109;C95;C91	0.894987156	E9PKG1 H7C2I1 Q99873 Q99873 Q99873 Q99873	E9PKG1 Protein arginine N-methyltransferase 1 OS=Homo sapiens GN=PRMT1 PE=1 SV=1 # H7C2I1 Protein arginine N-methyltransferase 1 OS=Homo sapiens GN=PRMT1 PE=1 SV=1 # Q99873-4 Isoform 4 of Protein arginine N-methyltransferase 1 OS=Homo sapiens GN=PRMT1 # Q99873 Protein arginine N-methyltransferase 1 OS=Homo sapiens GN=PRMT1 PE=1 SV=2 # Q99873-2 Isoform 2 of Protein arginine N-methyltransferase 1 OS=Homo sapiens GN=PRMT1 # Q99873-3 Isoform 3 of Protein arginine N-methyltransferase 1 OS=Homo sapiens GN=PRMT1 #	3
VDDEILGFISEATPLGGIQAAS TESC*NQQLDLALCR	C561	0.888263773	P42166	P42166 Lamina-associated polypeptide 2# isoform alpha OS=Homo sapiens GN=TMPO PE=1 SV=2 #	3

INPYMSSPC*HIEMILTEK	C144 C144;M102 C144;M140 C134;M140 C106;M140 C106;M130	0.886489038	J3KRX5 P18621 J3QLC8 A0A087WXM6 A0A0A0MRF8 A0A0A6YYL6 P18621 J3QQT2 P18621	J3KRX5 60S ribosomal protein L17 (Fragment) OS=Homo sapiens GN=RPL17 PE=3 SV=1 # P18621-2 Isoform 2 of 60S ribosomal protein L17 OS=Homo sapiens GN=RPL17 # J3QLC8 60S ribosomal protein L17 OS=Homo sapiens GN=RPL17 PE=1 SV=1 # A0A087WXM6 60S ribosomal protein L17 (Fragment) OS=Homo sapiens GN=RPL17 PE=3 SV=1 # A0A0A0MRF8 Protein RPL17-C18orf32 OS=Homo sapiens GN=RPL17-C18orf32 PE=3 SV=1 # A0A0A6YYL6 Protein RPL17-C18orf32 OS=Homo sapiens GN=RPL17-C18orf32 PE=3 SV=1 # P18621 60S ribosomal protein L17 OS=Homo sapiens GN=RPL17 PE=1 SV=3 # J3QQT2 60S ribosomal protein L17 (Fragment) OS=Homo sapiens GN=RPL17 PE=3 SV=1 # P18621-3 Isoform 3 of 60S ribosomal protein L17 OS=Homo sapiens GN=RPL17 #	3
FSFCC*SPEPEAEAEAAAGP GPCER	C27;C27	0.885556557	E7EMC7 Q13501	E7EMC7 Sequestosome-1 OS=Homo sapiens GN=SQSTM1 PE=1 SV=1 # Q13501 Sequestosome-1 OS=Homo sapiens GN=SQSTM1 PE=1 SV=1 #	3
FPEELTQTFMSC*NLITGMFQ R	C389 C339;M387	0.878301162	P26641 P26641	P26641 Elongation factor 1-gamma OS=Homo sapiens GN=EEF1G PE=1 SV=3 # P26641-2 Isoform 2 of Elongation factor 1-gamma OS=Homo sapiens GN=EEF1G #	3
EITSLDTENIDEILNNADVALV NFYADWC*R	C58	0.870859303	Q9BS26	Q9BS26 Endoplasmic reticulum resident protein 44 OS=Homo sapiens GN=ERP44 PE=1 SV=1 #	3
GMYGIENEVFLSLPC*ILNAR	C294	0.863438215	P07195	P07195 L-lactate dehydrogenase B chain OS=Homo sapiens GN=LDHB PE=1 SV=2 #	3
HFTNETLLDILFYNSPTYC*QT	C548;C548	0.862061236	Q9Y6Y8 Q9Y6Y8	Q9Y6Y8 SEC23-interacting protein OS=Homo sapiens GN=SEC23IP PE=1 SV=1 # Q9Y6Y8-2 Isoform 2 of SEC23-interacting protein OS=Homo sapiens GN=SEC23IP #	2
GAFC*DLVWSDPEDVDTWAI SPR	C192;C229	0.860242004	O00743 O00743	O00743 Serine/threonine-protein phosphatase 6 catalytic subunit OS=Homo sapiens GN=PPP6C PE=1 SV=1 # O00743-3 Isoform 3 of Serine/threonine-protein phosphatase 6 catalytic subunit OS=Homo sapiens GN=PPP6C #	3

VILITPTPLC*ETAWEEQCIIQGCK	C137;C112;C24;C24;C117;C24	0.860127696	Q2TAA2 C9JE02 C9JDY4 Q2TAA2 H7C5G1 C9J5J2	Q2TAA2 Isoamyl acetate-hydrolyzing esterase 1 homolog OS=Homo sapiens GN=IAH1 PE=1 SV=1 # C9JE02 Isoamyl acetate-hydrolyzing esterase 1 homolog OS=Homo sapiens GN=IAH1 PE=1 SV=1 # C9JDY4 Isoamyl acetate-hydrolyzing esterase 1 homolog (Fragment) OS=Homo sapiens GN=IAH1 PE=1 SV=1 # Q2TAA2-2 Isoform 2 of Isoamyl acetate-hydrolyzing esterase 1 homolog OS=Homo sapiens GN=IAH1 # H7C5G1 Isoamyl acetate-hydrolyzing esterase 1 homolog (Fragment) OS=Homo sapiens GN=IAH1 PE=1 SV=1 # C9J5J2 Isoamyl acetate-hydrolyzing esterase 1 homolog (Fragment) OS=Homo sapiens GN=IAH1 PE=1 SV=1 #	4
LC*PGGQLPFLLYGTEVHTDTNK	C59	0.859036231	O00299	O00299 Chloride intracellular channel protein 1 OS=Homo sapiens GN=CLIC1 PE=1 SV=4 #	2
SSPGLSDTIFC*R	C27	0.850550509	Q9H8M7	Q9H8M7 Protein FAM188A OS=Homo sapiens GN=FAM188A PE=1 SV=1 #	2
LGTDESC*FNMILATR	C363;C341	0.8489	P20073 P20073	P20073 Annexin A7 OS=Homo sapiens GN=ANXA7 PE=1 SV=3 # P20073-2 Isoform 2 of Annexin A7 OS=Homo sapiens GN=ANXA7 #	2
AAQGPPAPAVPPNTDVMAC*TQTALLQK	C146;C152;C115	0.839221231	H0YEB6 O60232 G3V1B8	H0YEB6 Sjoegren syndrome/scleroderma autoantigen 1 (Fragment) OS=Homo sapiens GN=SSSCA1 PE=1 SV=1 # O60232 Sjoegren syndrome/scleroderma autoantigen 1 OS=Homo sapiens GN=SSSCA1 PE=1 SV=1 # G3V1B8 Sjoegren syndrome/scleroderma autoantigen 1 OS=Homo sapiens GN=SSSCA1 PE=1 SV=1 #	3
FLENTPSSLNIEDIEDLFSLAQYYC*SK	C283;C283	0.834200124	Q9NUY8 Q9NUY8	Q9NUY8 TBC1 domain family member 23 OS=Homo sapiens GN=TBC1D23 PE=1 SV=3 # Q9NUY8-2 Isoform 2 of TBC1 domain family member 23 OS=Homo sapiens GN=TBC1D23 #	3
C*TPSVISFGSK	C34;C34	0.818805	Q92598 Q92598	Q92598 Heat shock protein 105 kDa OS=Homo sapiens GN=HSPH1 PE=1 SV=1 # Q92598-2 Isoform Beta of Heat shock protein 105 kDa OS=Homo sapiens GN=HSPH1 #	2
YDC*GEEILITVLSAMTEEAAVAIK	C159	0.81497789	P63241 P63241	P63241-2 Isoform 2 of Eukaryotic translation initiation factor 5A-1 OS=Homo sapiens GN=EIF5A # P63241 Eukaryotic translation initiation factor 5A-1 OS=Homo sapiens GN=EIF5A PE=1 SV=2 #	4
EGTDSSQGIPQLVSNISAC*QVIAEAVR	C29	0.81309742	Q99832	Q99832 T-complex protein 1 subunit eta OS=Homo sapiens GN=CCT7 PE=1 SV=2 #	4

QAVLGAGLPISTPC*TTINK	C119	0.810549874	P24752	P24752 Acetyl-CoA acetyltransferase# mitochondrial OS=Homo sapiens GN=ACAT1 PE=1 SV=1 #	4
SMKAC*VSETLSMLGQHFGQ LLELALTR	C215;C168;C167; C168;C168;C168	0.81014	Q1MX18 Q1MX18 A0A0A0MSI1 Q1MX18 Q1MX18 Q1MX18	Q1MX18 Protein inscuteable homolog OS=Homo sapiens GN=INSC PE=1 SV=1 # Q1MX18-4 Isoform 4 of Protein inscuteable homolog OS=Homo sapiens GN=INSC # A0A0A0MSI1 Protein inscuteable homolog OS=Homo sapiens GN=INSC PE=4 SV=1 # Q1MX18-6 Isoform 6 of Protein inscuteable homolog OS=Homo sapiens GN=INSC # Q1MX18-5 Isoform 5 of Protein inscuteable homolog OS=Homo sapiens GN=INSC # Q1MX18-2 Isoform 2 of Protein inscuteable homolog OS=Homo sapiens GN=INSC #	2
LNIISNLDC*VNEVIGIR	C402;C275;C402; C390	0.797213544	P30154 P30154 P30154 P30153	P30154-2 Isoform 2 of Serine/threonine-protein phosphatase 2A 65 kDa regulatory subunit A beta isoform OS=Homo sapiens GN=PPP2R1B # P30154-5 Isoform 5 of Serine/threonine-protein phosphatase 2A 65 kDa regulatory subunit A beta isoform OS=Homo sapiens GN=PPP2R1B # P30154 Serine/threonine-protein phosphatase 2A 65 kDa regulatory subunit A beta isoform OS=Homo sapiens GN=PPP2R1B PE=1 SV=3 # P30153 Serine/threonine-protein phosphatase 2A 65 kDa regulatory subunit A alpha isoform OS=Homo sapiens GN=PPP2R1A PE=1 SV=4 #	2
IAVYSC*PFDGMITETK	C244	0.796255653	P50990	P50990 T-complex protein 1 subunit theta OS=Homo sapiens GN=CCT8 PE=1 SV=4 #	3
ILYSQC*GDVMR	C32;C33;C20;C32 ;C125;C32;C33;C 32	0.795647878	G3V1V0 G8JLA2 F8VPF3 P60660 B7Z6Z4 P60660 J3KND3 F8W1R7	G3V1V0 Myosin light polypeptide 6 OS=Homo sapiens GN=MYL6 PE=1 SV=1 # G8JLA2 Myosin light polypeptide 6 OS=Homo sapiens GN=MYL6 PE=1 SV=1 # F8VPF3 Myosin light polypeptide 6 (Fragment) OS=Homo sapiens GN=MYL6 PE=1 SV=1 # P60660-2 Isoform Smooth muscle of Myosin light polypeptide 6 OS=Homo sapiens GN=MYL6 # B7Z6Z4 Myosin light polypeptide 6 OS=Homo sapiens GN=MYL6 PE=1 SV=1 # P60660 Myosin light polypeptide 6 OS=Homo sapiens GN=MYL6 PE=1 SV=2 # J3KND3 Myosin light polypeptide 6 OS=Homo sapiens GN=MYL6 PE=1 SV=1 # F8W1R7 Myosin light polypeptide 6 OS=Homo sapiens GN=MYL6 PE=1 SV=1 #	3
IC*EPGYSPTYK	C211	0.789064684	P07858	P07858 Cathepsin B OS=Homo sapiens GN=CTSB PE=1 SV=3 #	3

LLLC*GGAPLSATTQR	C450	0.788176623	O95573	O95573 Long-chain-fatty-acid--CoA ligase 3 OS=Homo sapiens GN=ACSL3 PE=1 SV=3 #	4
GDLENAFLNLVQC*IQNKPLY FADR	C280;C262	0.784733555	P07355 P07355	P07355-2 Isoform 2 of Annexin A2 OS=Homo sapiens GN=ANXA2 # P07355 Annexin A2 OS=Homo sapiens GN=ANXA2 PE=1 SV=2 #	2
QSLLFC*PK	C27	0.78171687	Q56VL3	Q56VL3 OCIA domain-containing protein 2 OS=Homo sapiens GN=OCIAD2 PE=1 SV=1 #	4
WTLGFC*DER	C78	0.77880088	O95336	O95336 6-phosphogluconolactonase OS=Homo sapiens GN=PGLS PE=1 SV=2 #	2
LNLPINIIGLAPLC*ENMPSGK	C335	0.77415	P28838 P28838	P28838 Cytosol aminopeptidase OS=Homo sapiens GN=LAP3 PE=1 SV=3 # P28838-2 Isoform 2 of Cytosol aminopeptidase OS=Homo sapiens GN=LAP3 #	2
LTTPTYGDLNHLVSATMSGV TTC*LR	C239;C239;C239; C221	0.769376471	P68371 Q9BVA1 P04350 Q5JP53	P68371 Tubulin beta-4B chain OS=Homo sapiens GN=TUBB4B PE=1 SV=1 # Q9BVA1 Tubulin beta-2B chain OS=Homo sapiens GN=TUBB2B PE=1 SV=1 # P04350 Tubulin beta-4A chain OS=Homo sapiens GN=TUBB4A PE=1 SV=2 # Q5JP53 Tubulin beta chain OS=Homo sapiens GN=TUBB PE=1 SV=1 #	4
AEGSDVANAVLDGADC*IMLS GETAK	C358;C358	0.74969315	P14618 P14618	P14618-2 Isoform M1 of Pyruvate kinase PKM OS=Homo sapiens GN=PKM # P14618 Pyruvate kinase PKM OS=Homo sapiens GN=PKM PE=1 SV=4 #	2
LESLLQSMEMAHSGSLRDEL C*LDFPCDSPEK	C259;C386;C388; C389;C183;C321; C394;C270	0.739561178	B7Z4D2 Q9NX95 Q9NX95 Q9NX95 B3KRD1 Q9NX95 A0A0C4DG86 Q9NX95	B7Z4D2 Syntabulin OS=Homo sapiens GN=SYBU PE=1 SV=1 # Q9NX95-4 Isoform 4 of Syntabulin OS=Homo sapiens GN=SYBU # Q9NX95-3 Isoform 3 of Syntabulin OS=Homo sapiens GN=SYBU # Q9NX95 Syntabulin OS=Homo sapiens GN=SYBU PE=1 SV=2 # B3KRD1 Syntabulin OS=Homo sapiens GN=SYBU PE=1 SV=1 # Q9NX95-2 Isoform 2 of Syntabulin OS=Homo sapiens GN=SYBU # A0A0C4DG86 Syntabulin OS=Homo sapiens GN=SYBU PE=1 SV=1 # Q9NX95-5 Isoform 5 of Syntabulin OS=Homo sapiens GN=SYBU #	4
QPPWC*DPLGPFVVGGEDLD PFGPR	C185;C185	0.734520716	Q5QPM7 Q92530	Q5QPM7 Proteasome inhibitor PI31 subunit OS=Homo sapiens GN=PSMF1 PE=1 SV=2 # Q92530 Proteasome inhibitor PI31 subunit OS=Homo sapiens GN=PSMF1 PE=1 SV=2 #	3
ASVGFGGSC*FQK	C276	0.729984174	O60701	O60701 UDP-glucose 6-dehydrogenase OS=Homo sapiens GN=UGDH PE=1 SV=1 #	2

LC*DFGVSGQLIDSMANSFVGTR	C114	0.724924892	G5E9C7 H3BRW9 Q02750 Q02750 P36507	G5E9C7 Dual-specificity mitogen-activated protein kinase kinase 2 OS=Homo sapiens GN=MAP2K2 PE=1 SV=1 # H3BRW9 Dual-specificity mitogen-activated protein kinase kinase 1 OS=Homo sapiens GN=MAP2K1 PE=1 SV=1 # Q02750 Dual specificity mitogen-activated protein kinase kinase 1 OS=Homo sapiens GN=MAP2K1 PE=1 SV=2 # Q02750-2 Isoform 2 of Dual specificity mitogen-activated protein kinase kinase 1 OS=Homo sapiens GN=MAP2K1 # P36507 Dual specificity mitogen-activated protein kinase kinase 2 OS=Homo sapiens GN=MAP2K2 PE=1 SV=1 #	4
VFIMDNC*EELIPEYLNFIR	C496;M371 C374	0.719115	P07900 P07900	P07900-2 Isoform 2 of Heat shock protein HSP 90-alpha OS=Homo sapiens GN=HSP90AA1 # P07900 Heat shock protein HSP 90-alpha OS=Homo sapiens GN=HSP90AA1 PE=1 SV=5 #	2
IC*PVEFNPNFVAR	C33;C33;C33	0.706979375	Q9UI30 Q9UI30 F5GX77	Q9UI30 Multifunctional methyltransferase subunit TRM112-like protein OS=Homo sapiens GN=TRMT112 PE=1 SV=1 # Q9UI30-2 Isoform 2 of Multifunctional methyltransferase subunit TRM112-like protein OS=Homo sapiens GN=TRMT112 # F5GX77 Multifunctional methyltransferase subunit TRM112-like protein OS=Homo sapiens GN=TRMT112 PE=1 SV=1 #	4
LVSSPCC*IVTSTYGWTANMER	C590	0.691623325	P08238	P08238 Heat shock protein HSP 90-beta OS=Homo sapiens GN=HSP90AB1 PE=1 SV=4 #	2
LSGSC*SAPSLAAPDGSAPSAPR	C100	0.68981153	Q92529	Q92529 SHC-transforming protein 3 OS=Homo sapiens GN=SHC3 PE=1 SV=1 #	2
LECVEPNC*R	C77;C77;C113;C77;C77	0.665297873	P83881 Q969Q0 J3KQN4 H7BZ11 H0Y5B4	P83881 60S ribosomal protein L36a OS=Homo sapiens GN=RPL36A PE=1 SV=2 # Q969Q0 60S ribosomal protein L36a-like OS=Homo sapiens GN=RPL36AL PE=1 SV=3 # J3KQN4 60S ribosomal protein L36a OS=Homo sapiens GN=RPL36A PE=3 SV=1 # H7BZ11 Protein RPL36A-HNRNPH2 OS=Homo sapiens GN=RPL36A-HNRNPH2 PE=3 SV=2 # H0Y5B4 60S ribosomal protein L36a OS=Homo sapiens GN=RPL36A PE=3 SV=2 #	2
AGAVVAVPTDTLYGLACAASC*SAALR	C99	0.657549876	Q86U90	Q86U90 YrdC domain-containing protein# mitochondrial OS=Homo sapiens GN=YRDC PE=1 SV=1 #	2
EAVFPFQPGSVAEVC*ITFDQANLTVK	C89	0.631160522	P09382	P09382 Galectin-1 OS=Homo sapiens GN=LGALS1 PE=1 SV=2 #	3

AQNTWGC*GNSLR	C410;C423;C148;C522;C522;C522	0.627997067	P02545 P02545 A0A0C4DGC5 P02545 P02545 P02545	P02545-4 Isoform 4 of Prelamin-A/C OS=Homo sapiens GN=LMNA # P02545-5 Isoform 5 of Prelamin-A/C OS=Homo sapiens GN=LMNA # A0A0C4DGC5 Prelamin-A/C (Fragment) OS=Homo sapiens GN=LMNA PE=1 SV=1 # P02545-6 Isoform 6 of Prelamin-A/C OS=Homo sapiens GN=LMNA # P02545 Prelamin-A/C OS=Homo sapiens GN=LMNA PE=1 SV=1 # P02545-3 Isoform ADelta10 of Prelamin-A/C OS=Homo sapiens GN=LMNA #	2
RPTEIC*ADPQFIIGGATR	C82	0.612197205	P17655	P17655 Calpain-2 catalytic subunit OS=Homo sapiens GN=CAPN2 PE=1 SV=6 #	3
LVSSPC*CIVTSTYGWTANMER	C589	0.601278417	P08238	P08238 Heat shock protein HSP 90-beta OS=Homo sapiens GN=HSP90AB1 PE=1 SV=4 #	2
AC*QSIYPLHDVFVR	C164;C164;C201;C181	0.59401614	D6RB09 D6RAT0 P61247 D6RG13	D6RB09 40S ribosomal protein S3a (Fragment) OS=Homo sapiens GN=RPS3A PE=1 SV=7 # D6RAT0 40S ribosomal protein S3a OS=Homo sapiens GN=RPS3A PE=1 SV=1 # P61247 40S ribosomal protein S3a OS=Homo sapiens GN=RPS3A PE=1 SV=2 # D6RG13 40S ribosomal protein S3a (Fragment) OS=Homo sapiens GN=RPS3A PE=1 SV=1 #	3
FALAC*NASDK	C68;C171	0.588308518	A0A087WVY3 P35250	A0A087WVY3 Replication factor C subunit 2 OS=Homo sapiens GN=RFC2 PE=1 SV=1 # P35250 Replication factor C subunit 2 OS=Homo sapiens GN=RFC2 PE=1 SV=3 #	2
LC*VQNSPQEAR	C150;C150;C150;C150;C141	0.577172785	P33240 P33240 E7EWR4 E9PID8 A0A0A0MT56	P33240-2 Isoform 2 of Cleavage stimulation factor subunit 2 OS=Homo sapiens GN=CSTF2 # P33240 Cleavage stimulation factor subunit 2 OS=Homo sapiens GN=CSTF2 PE=1 SV=1 # E7EWR4 Cleavage stimulation factor subunit 2 OS=Homo sapiens GN=CSTF2 PE=1 SV=1 # E9PID8 Cleavage stimulation factor subunit 2 OS=Homo sapiens GN=CSTF2 PE=1 SV=1 # A0A0A0MT56 Cleavage stimulation factor subunit 2 (Fragment) OS=Homo sapiens GN=CSTF2 PE=1 SV=1 #	2
HFVLDEC*DK	C197	0.576451232	O00148	O00148 ATP-dependent RNA helicase DDX39A OS=Homo sapiens GN=DDX39A PE=1 SV=2 #	2

KSQTGILLGVC*SK	C798;C798;C798;C798	0.56261	Q12923 Q12923 Q12923 Q12923	Q12923-2 Isoform 2 of Tyrosine-protein phosphatase non-receptor type 13 OS=Homo sapiens GN=PTPN13 # Q12923-4 Isoform 4 of Tyrosine-protein phosphatase non-receptor type 13 OS=Homo sapiens GN=PTPN13 # Q12923-3 Isoform 3 of Tyrosine-protein phosphatase non-receptor type 13 OS=Homo sapiens GN=PTPN13 # Q12923 Tyrosine-protein phosphatase non-receptor type 13 OS=Homo sapiens GN=PTPN13 PE=1 SV=2 #	3
NHLLPDIVTC*VQSSR	C184	0.516804965	Q9BSD7	Q9BSD7 Cancer-related nucleoside-triphosphatase OS=Homo sapiens GN=NTPCR PE=1 SV=1 #	2
YREVHYVLLDPSC*SGSGEMVR	C124	0.516260701	Q63ZY6	Q63ZY6-2 Isoform 2 of Putative methyltransferase NSUN5C OS=Homo sapiens GN=NSUN5P2 #	2
RTWCEVYLALDVLFC*TSSIVHLCAISLDR	C96;C96	0.503798826	P18089 A2RUS0	P18089 Alpha-2B adrenergic receptor OS=Homo sapiens GN=ADRA2B PE=1 SV=3 # A2RUS0 Adrenergic# alpha-2B-# receptor OS=Homo sapiens GN=ADRA2B PE=1 SV=1 #	2
YVDIAIPC*NNK	C168;C163;C163	0.501630032	A0A0C4DG17 C9J9K3 P08865	A0A0C4DG17 40S ribosomal protein SA OS=Homo sapiens GN=RPSA PE=1 SV=1 # C9J9K3 40S ribosomal protein SA (Fragment) OS=Homo sapiens GN=RPSA PE=1 SV=7 # P08865 40S ribosomal protein SA OS=Homo sapiens GN=RPSA PE=1 SV=4 #	2
C*EGINISGNFYR	C37	0.491930647	M0QYS1	M0QYS1 60S ribosomal protein L13a (Fragment) OS=Homo sapiens GN=RPL13A PE=1 SV=2 #	3
NCGC*LGASPNLEQLQEENLK	C34	0.468619766	P54136	P54136 Arginine--tRNA ligase# cytoplasmic OS=Homo sapiens GN=RARS PE=1 SV=2 #	3
FSPNSSNPIIVSC*GWDK	C168	0.46616048	P63244	P63244 Receptor of activated protein C kinase 1 OS=Homo sapiens GN=RACK1 PE=1 SV=3 #	3
YAC*GLWGLSPASR	C457	0.456650098	Q15637	Q15637-6 Isoform 6 of Splicing factor 1 OS=Homo sapiens GN=SF1 #	3
VTAVIPC*FPYAR	C24;C91;C91;C91	0.45559904	P60891 P11908 P60891 P11908	P60891-2 Isoform 2 of Ribose-phosphate pyrophosphokinase 1 OS=Homo sapiens GN=PRPS1 # P11908-2 Isoform 2 of Ribose-phosphate pyrophosphokinase 2 OS=Homo sapiens GN=PRPS2 # P60891 Ribose-phosphate pyrophosphokinase 1 OS=Homo sapiens GN=PRPS1 PE=1 SV=2 # P11908 Ribose-phosphate pyrophosphokinase 2 OS=Homo sapiens GN=PRPS2 PE=1 SV=2 #	3
HLYTLDGGDIINALC*FSPNR	C240	0.441329151	P63244	P63244 Receptor of activated protein C kinase 1 OS=Homo sapiens GN=RACK1 PE=1 SV=3 #	2

YAGLSTC*FR	C300;C300	0.419141837	Q5T5C7 P49591	Q5T5C7 Serine--tRNA ligase# cytoplasmic OS=Homo sapiens GN=SARS PE=1 SV=1 # P49591 Serine--tRNA ligase# cytoplasmic OS=Homo sapiens GN=SARS PE=1 SV=3 #	3
EDPTVSALLTSEKDWQGFLE LYLQNSPEAC*DYGL	C237	0.396445644	P78417	P78417 Glutathione S-transferase omega-1 OS=Homo sapiens GN=GSTO1 PE=1 SV=2 #	3
LAPILC*DGTATFVDLVPGFR	C568;C568	0.383025	O43264 O43264	O43264 Centromere/kinetochore protein zw10 homolog OS=Homo sapiens GN=ZW10 PE=1 SV=3 # O43264-2 Isoform 2 of Centromere/kinetochore protein zw10 homolog OS=Homo sapiens GN=ZW10 #	2
ILLNACC*PGWVR	C227	0.380693253	P16152	P16152 Carbonyl reductase [NADPH] 1 OS=Homo sapiens GN=CBR1 PE=1 SV=3 #	3
VMALQEAC*EAYLVGLFEDTN LCAIHAK	C97	0.360452206	P68431	P68431 Histone H3.1 OS=Homo sapiens GN=HIST1H3A PE=1 SV=2 #	4
QC*MMFSATLSK	C223	0.356931813	O00148	O00148 ATP-dependent RNA helicase DDX39A OS=Homo sapiens GN=DDX39A PE=1 SV=2 #	2
HNLSC*SFDVVSPVAGLRVIY PAPR	C813;C813;C813	0.356793307	P98161 P98161 P98161	P98161-2 Isoform 2 of Polycystin-1 OS=Homo sapiens GN=PKD1 # P98161-3 Isoform 3 of Polycystin-1 OS=Homo sapiens GN=PKD1 # P98161 Polycystin-1 OS=Homo sapiens GN=PKD1 PE=1 SV=3 #	3
CAIIPSDMLHISTNC*R	C220;M207 C214;M207 C214;M183 C245;M246 C253 C190;M238	0.312112763	Q8N9N5 Q8N9N5 Q8N9N5 Q8N9N5 Q8N9N5 Q8N9N5 Q8N9N5	Q8N9N5-5 Isoform 5 of Protein BANP OS=Homo sapiens GN=BANP # Q8N9N5-4 Isoform 4 of Protein BANP OS=Homo sapiens GN=BANP # Q8N9N5-6 Isoform 6 of Protein BANP OS=Homo sapiens GN=BANP # Q8N9N5-2 Isoform 2 of Protein BANP OS=Homo sapiens GN=BANP # Q8N9N5-3 Isoform 3 of Protein BANP OS=Homo sapiens GN=BANP # Q8N9N5 Protein BANP OS=Homo sapiens GN=BANP PE=1 SV=3 # Q8N9N5-7 Isoform 7 of Protein BANP OS=Homo sapiens GN=BANP #	3
LVILANNC*PALR	C52;C52	0.289325333	P62888 E5RI99	P62888 60S ribosomal protein L30 OS=Homo sapiens GN=RPL30 PE=1 SV=2 # E5RI99 60S ribosomal protein L30 (Fragment) OS=Homo sapiens GN=RPL30 PE=1 SV=1 #	2

GC*GTVLLSGPR	C136;C134;C134;C105;C113	0.269627662	J3QQ67 G3V203 Q07020 Q07020 H0YHA7	J3QQ67 60S ribosomal protein L18 (Fragment) OS=Homo sapiens GN=RPL18 PE=1 SV=1 # G3V203 60S ribosomal protein L18 OS=Homo sapiens GN=RPL18 PE=1 SV=1 # Q07020 60S ribosomal protein L18 OS=Homo sapiens GN=RPL18 PE=1 SV=2 # Q07020-2 Isoform 2 of 60S ribosomal protein L18 OS=Homo sapiens GN=RPL18 # H0YHA7 60S ribosomal protein L18 (Fragment) OS=Homo sapiens GN=RPL18 PE=1 SV=1 #	3
SVHVGQAGVQMGNAC*WELYCLEHGIQPDGQMPSDK	C20	0.254604414	P68366	P68366 Tubulin alpha-4A chain OS=Homo sapiens GN=TUBA4A PE=1 SV=1 #	3
C*LAQEVNIPDWIVDLR	C140; C140	0.248885652	Q9Y4W2 Q9Y4W2	Q9Y4W2 Ribosomal biogenesis protein LAS1L OS=Homo sapiens GN=LAS1L PE=1 SV=2 # Q9Y4W2-2 Isoform 2 of Ribosomal biogenesis protein LAS1L OS=Homo sapiens GN=LAS1L #	2
VC*ATLPSTVAVTSVCWSPK	C186;C186;C186;C186;C186	0.198163633	P35658 P35658 P35658 P35658 P35658	P35658-4 Isoform 4 of Nuclear pore complex protein Nup214 OS=Homo sapiens GN=NUP214 # P35658 Nuclear pore complex protein Nup214 OS=Homo sapiens GN=NUP214 PE=1 SV=2 # P35658-2 Isoform 2 of Nuclear pore complex protein Nup214 OS=Homo sapiens GN=NUP214 # P35658-3 Isoform 3 of Nuclear pore complex protein Nup214 OS=Homo sapiens GN=NUP214 # P35658-5 Isoform 5 of Nuclear pore complex protein Nup214 OS=Homo sapiens GN=NUP214 #	3
ACFC*IDNEALYDICFR	C201	0.17486	Q9H4B7	Q9H4B7 Tubulin beta-1 chain OS=Homo sapiens GN=TUBB1 PE=1 SV=1 #	2
LQSAMALFAC*KTLGLK	C3702;M83 C88 C3695;M3697	0.122540503	Q8NCM8 Q8NCM8 H0YDE0	Q8NCM8 Cytoplasmic dynein 2 heavy chain 1 OS=Homo sapiens GN=DYNC2H1 PE=1 SV=4 # Q8NCM8-2 Isoform 2 of Cytoplasmic dynein 2 heavy chain 1 OS=Homo sapiens GN=DYNC2H1 # H0YDE0 Cytoplasmic dynein 2 heavy chain 1 (Fragment) OS=Homo sapiens GN=DYNC2H1 PE=1 SV=1 #	2
YVLC*TAPR	C370;C360;C405	0.1029566	J3KQ69 P25205 P25205	J3KQ69 DNA replication licensing factor MCM3 OS=Homo sapiens GN=MCM3 PE=1 SV=2 # P25205 DNA replication licensing factor MCM3 OS=Homo sapiens GN=MCM3 PE=1 SV=3 # P25205-2 Isoform 2 of DNA replication licensing factor MCM3 OS=Homo sapiens GN=MCM3 #	2

QC*TGLQGFLVFHSFGGGTG SGFTSLLMER	C129	0.083267384	P68363 Q71U36 P68366	P68363 Tubulin alpha-1B chain OS=Homo sapiens GN=TUBA1B PE=1 SV=1 # Q71U36 Tubulin alpha-1A chain OS=Homo sapiens GN=TUBA1A PE=1 SV=1 # Tubulin alpha-1C chain OS=Homo sapiens GN=TUBA1C PE=1 SV=1 # P68366 Tubulin alpha-4A chain OS=Homo sapiens GN=TUBA4A PE=1 SV=1 #	3
MAC*GLVASNLNLKPGECLR	C3	0.079174557	P09382	P09382 Galectin-1 OS=Homo sapiens GN=LGALS1 PE=1 SV=2 #	2
LLDLVQQSC*NYK	C34;C30	0.068348467	B1AHD1 P55769	B1AHD1 NHP2-like protein 1 OS=Homo sapiens GN=SNU13 PE=1 SV=1 # P55769 NHP2-like protein 1 OS=Homo sapiens GN=SNU13 PE=1 SV=3 #	2
C*NASFRMTSDLVYHMR	C630	0.066469032	Q9NQV8	Q9NQV8 PR domain zinc finger protein 8 OS=Homo sapiens GN=PRDM8 PE=1 SV=3 #	3
LPYHLGDDAEEGEVSDEDSA DEIEDEC*KFK	C454;C472;C472; C472	0.056717511	Q4KWH8 Q4KWH8 Q4KWH8 Q4KWH8	Q4KWH8-2 Isoform 2 of 1-phosphatidylinositol 4#5-bisphosphate phosphodiesterase eta-1 OS=Homo sapiens GN=PLCH1 # Q4KWH8 1-phosphatidylinositol 4#5-bisphosphate phosphodiesterase eta-1 OS=Homo sapiens GN=PLCH1 PE=1 SV=1 # Q4KWH8-4 Isoform 4 of 1-phosphatidylinositol 4#5-bisphosphate phosphodiesterase eta-1 OS=Homo sapiens GN=PLCH1 # Q4KWH8-3 Isoform 3 of 1-phosphatidylinositol 4#5-bisphosphate phosphodiesterase eta-1 OS=Homo sapiens GN=PLCH1 #	2
DQVAALEMIC*SNPVTVISGK	C466	0.025347347	Q8NG08	Q8NG08 DNA helicase B OS=Homo sapiens GN=HELB PE=1 SV=2 #	2
HC*DC*LQGFQLTHSLGGGT GSGMGTLLISK	C129 C127	0.01961142	Q9BUF5	Q9BUF5 Tubulin beta-6 chain OS=Homo sapiens GN=TUBB6 PE=1 SV=1 #	3
EC*ENCDCLQGFQLTHSLGG GTGSGMGTLLISK	C124;C471	0.017982906	Q13509 A0A0B4J269	Q13509 Tubulin beta-3 chain OS=Homo sapiens GN=TUBB3 PE=1 SV=2 # A0A0B4J269 Uncharacterized protein OS=Homo sapiens PE=1 SV=1 #	3
QSRTC*STQVC*R	C3687 C3692;C3688 C3693	0.012542589	A2VEC9 A0A096LNW2	A2VEC9 SCO-spondin OS=Homo sapiens GN=SSPO PE=2 SV=1 # A0A096LNW2 SCO-spondin OS=Homo sapiens GN=SSPO PE=4 SV=1 #	3
KQC*QQLQTAIAEAEQR	C383	0.010957646	Q5XKE5	Q5XKE5 Keratin# type II cytoskeletal 79 OS=Homo sapiens GN=KRT79 PE=1 SV=2 #	2
CEHC*DCLQGFQLTHSLGGG TGSGMGTLLISK	C127	0.01007	Q9BUF5	Q9BUF5 Tubulin beta-6 chain OS=Homo sapiens GN=TUBB6 PE=1 SV=1 #	2
CEHCDC*LQGFQLTHSLGGG TGSGMGTLLISK	C129	0.01007	Q9BUF5	Q9BUF5 Tubulin beta-6 chain OS=Homo sapiens GN=TUBB6 PE=1 SV=1 #	2

NIFLVAATLRPETMFGQTNC* WVR	C305	0.010039467	Q9P2J5	Q9P2J5 Leucine--tRNA ligase# cytoplasmic OS=Homo sapiens GN=LARS PE=1 SV=2 #	2
C*QGDCAGALSWAR	C303;C303	0.009814785	Q8N271 Q8N271	Q8N271-2 Isoform 2 of Prominin-2 OS=Homo sapiens GN=PROM2 # Q8N271 Prominin-2 OS=Homo sapiens GN=PROM2 PE=1 SV=1 #	2
MEAGGC*MDSEHMVMSFR	C6;REVERSE	0.004926459	U3KQV1	U3KQV1 E3 SUMO-protein ligase PIAS3 (Fragment) OS=Homo sapiens GN=PIAS3 PE=4 SV=1 # Reverse_sp|P01775|HV314_HUMAN Ig heavy chain V-III region LAY OS=Homo sapiens PE=1 SV=1 #	2
FFAFWGQDINNLTTPLEC*GR ESR	C735	0.003570728	Q8NCN5	Q8NCN5 Pyruvate dehydrogenase phosphatase regulatory subunit# mitochondrial OS=Homo sapiens GN=PDPR PE=1 SV=2 #	2
C*PEALFQPCFLGMESCGIHE TTFNSIMK	C957;C957;C920; C957	0.001334166	A5A3E0 Q6S8J3 P0CG39 P0CG38	A5A3E0 POTE ankyrin domain family member F OS=Homo sapiens GN=POTEF PE=1 SV=2 # Q6S8J3 POTE ankyrin domain family member E OS=Homo sapiens GN=POTEE PE=1 SV=3 # P0CG39 POTE ankyrin domain family member J OS=Homo sapiens GN=POTEJ PE=3 SV=1 # P0CG38 POTE ankyrin domain family member I OS=Homo sapiens GN=POTEI PE=3 SV=1 #	2

Table 2. Structures of cysteine-reactive covalent ligands screened against FAK1

Compound Name	Compound Structure
DKM 2-31	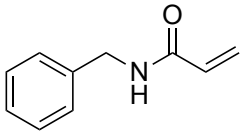
DKM 2-32	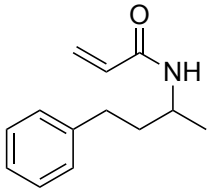
DKM 2-33	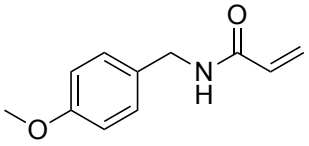
DKM 2-34	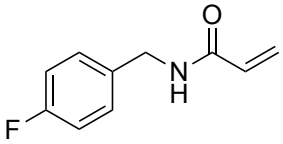
DKM 2-37	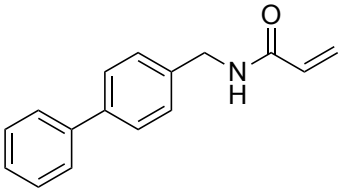
DKM 2-39	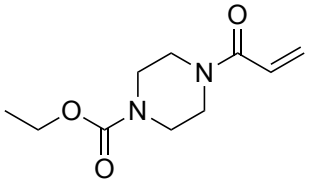
DKM 2-40	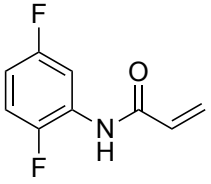

DKM 2-42	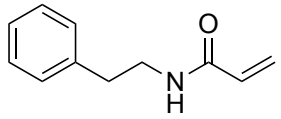
DKM 2-43	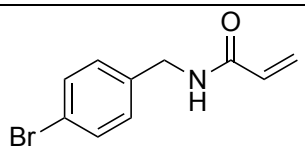
DKM 2-47	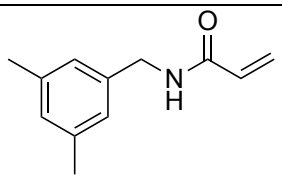
DKM 2-48	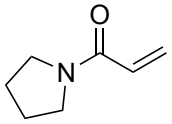
DKM 2-49	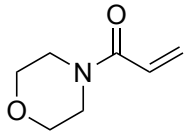
DKM 2-50	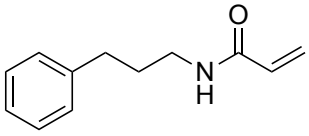
DKM 2-52	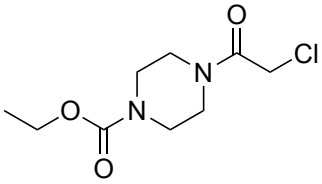

DKM 2-58	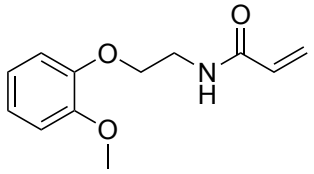
DKM 2-59	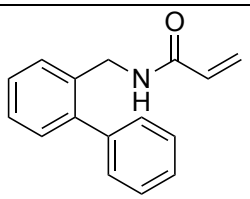
DKM 2-60	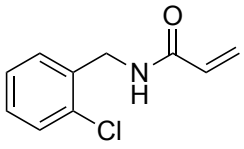
DKM 2-62	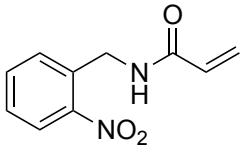
DKM 2-67	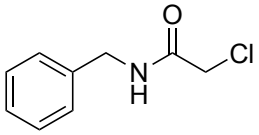
DKM 2-71	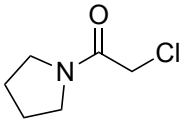
DKM 2-72	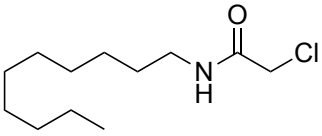

DKM 2-76	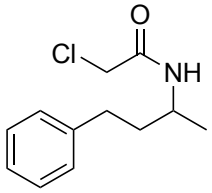
DKM 2-79	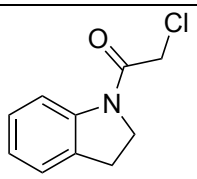
DKM 2-80	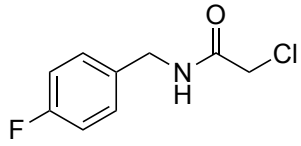
DKM 2-83	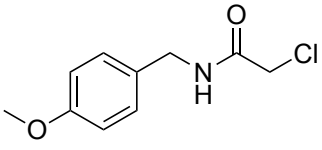
DKM 2-84	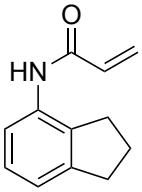
DKM 2-85	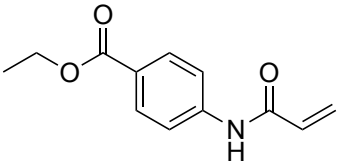
DKM 2-86	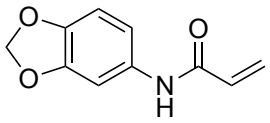

DKM 2-87	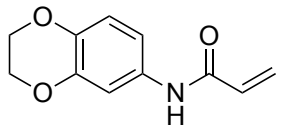
DKM 2-90	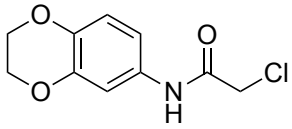
DKM 2-91	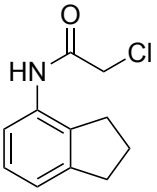
DKM 2-93	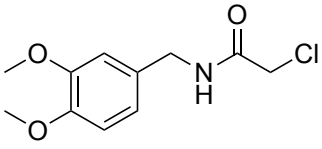
DKM 2-94	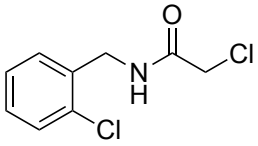
DKM 2-95	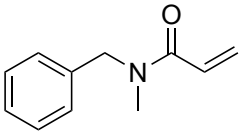 (Two rotamers in equal amounts)
DKM 2-97	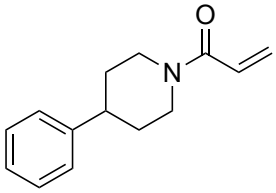

DKM 2-98	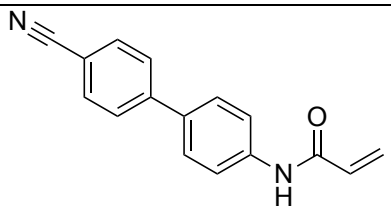
DKM 2-100	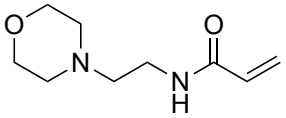
DKM 2-101	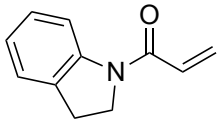
DKM 2-102	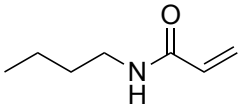
DKM 2-103	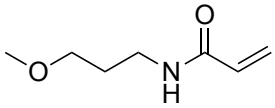
DKM 2-106	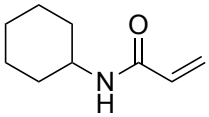
DKM 2-107	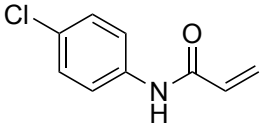

DKM 2-108	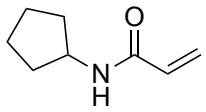
DKM 2-109	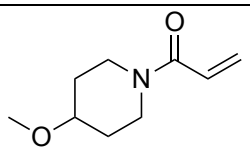
DKM 2-110	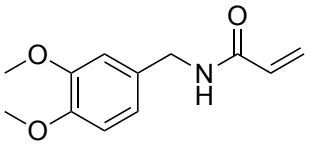
DKM 2-111	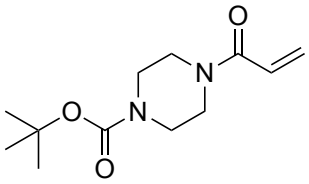
DKM 2-113	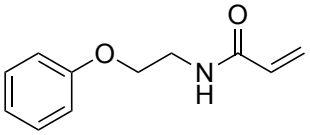
DKM 2-114	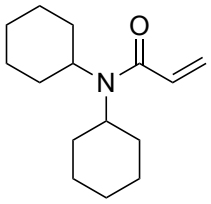
DKM 2-116	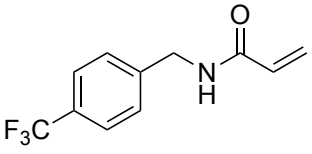

DKM 2-117	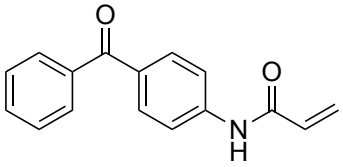
DKM 2-119	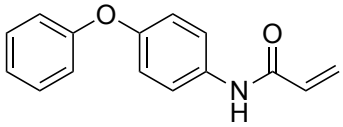
DKM 2-120	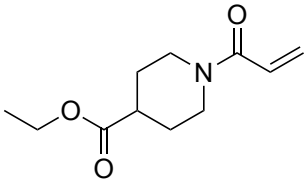
DKM 3-3	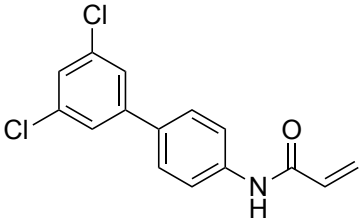
DKM 3-4	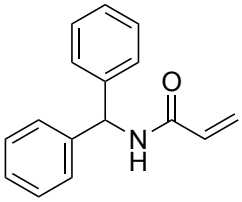
DKM 3-5	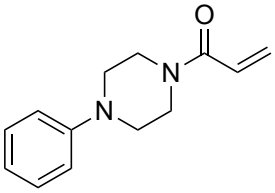
DKM 3-7	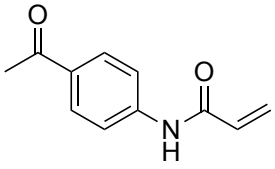

DKM 3-8	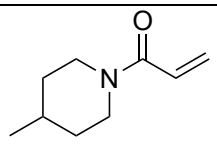
DKM 3-9	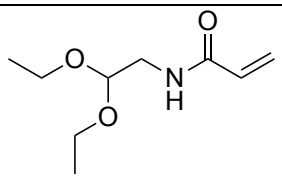
DKM 3-10	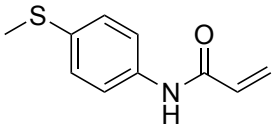
DKM 3-11	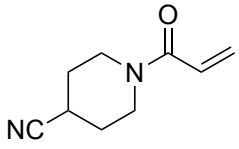
DKM 3-12	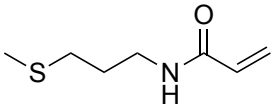
DKM 3-13	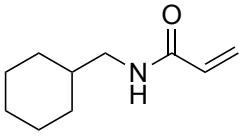
DKM 3-15	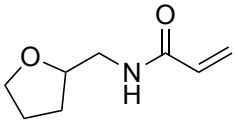

DKM 3-16	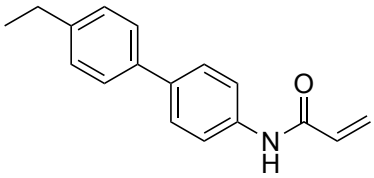
DKM 3-22	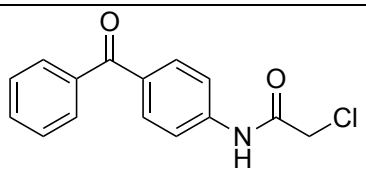
DKM 3-29	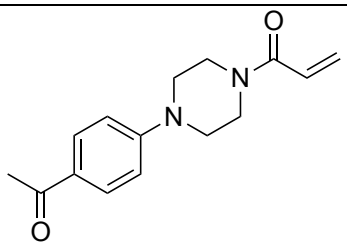
DKM 3-30	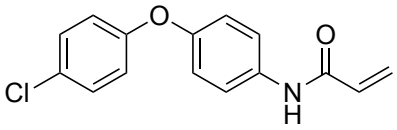
DKM 3-31	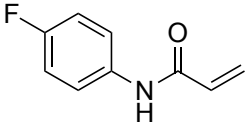
DKM 3-32	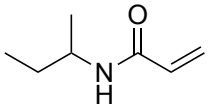
DKM 3-36	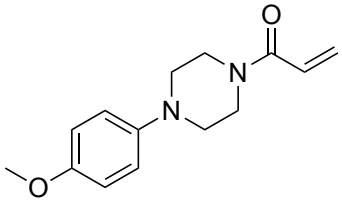
DKM 3-41	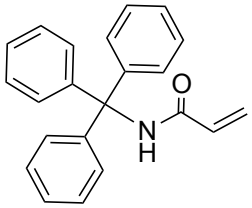

DKM 3-42	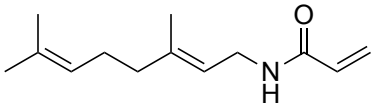
DKM 3-43	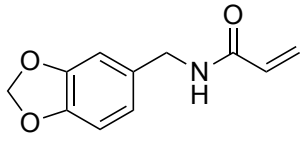
DKM 3-70	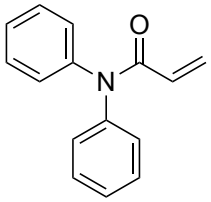
TRH 1-12	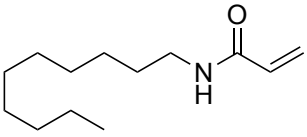
TRH 1-13	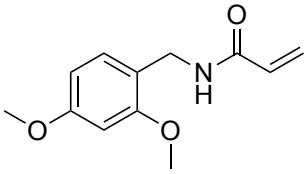
TRH 1-17	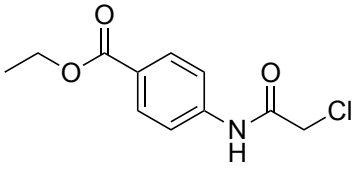
TRH 1-19	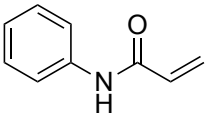

TRH 1-20	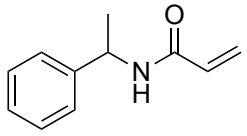
TRH 1-23	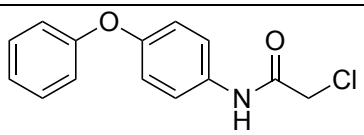
TRH 1-27	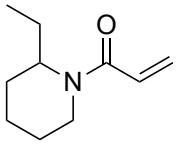
TRH 1-32	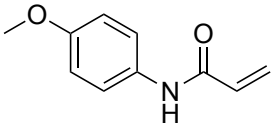
TRH 1-50	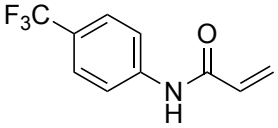
TRH 1-51	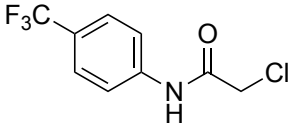
TRH 1-53	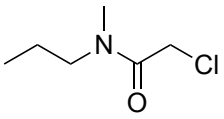

TRH 1-54	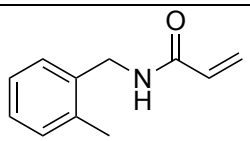
TRH 1-55	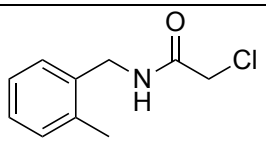
TRH 1-56	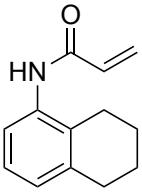
TRH 1-57	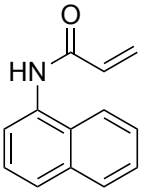
TRH 1-58	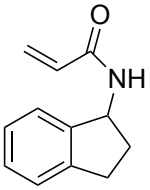
TRH 1-59	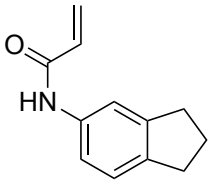
TRH 1-60	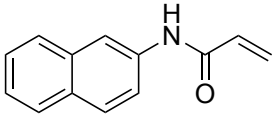

TRH 1-65	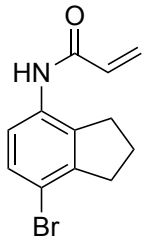
TRH 1-68	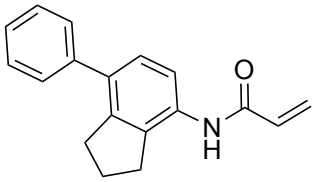
TRH 1-70	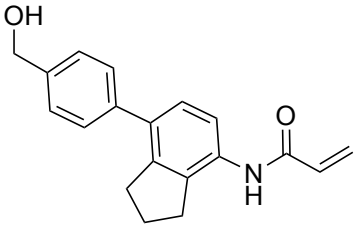
TRH 1-74	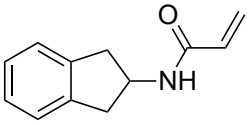
TRH 1-78	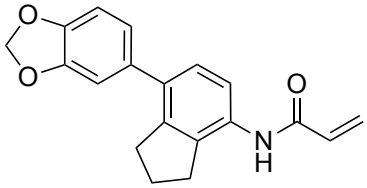
TRH 1-115	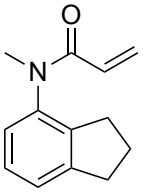
TRH 1-129	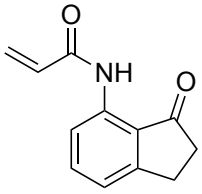

TRH 1-133	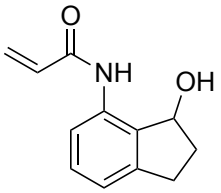
TRH 1-134	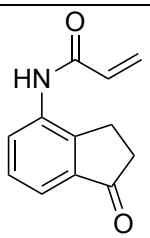
TRH 1-135	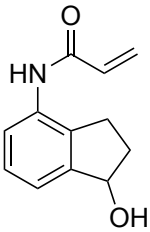
TRH 1-140	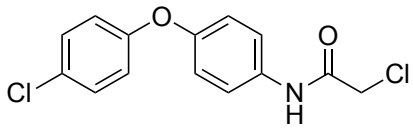
TRH 1-143	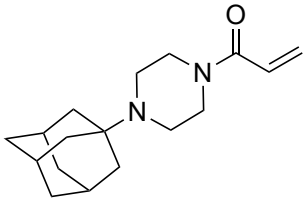
TRH 1-145	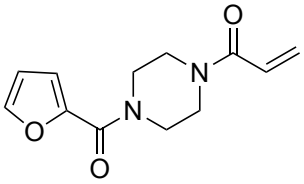
TRH 1-149	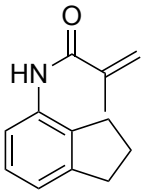

TRH 1-152	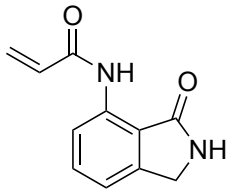
TRH 1-155	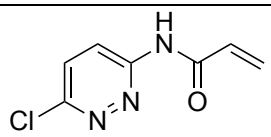
TRH 1-156	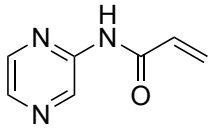
TRH 1-160	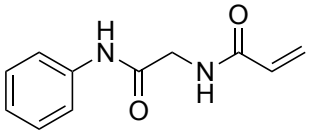
TRH 1-162	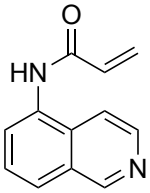
TRH 1-163	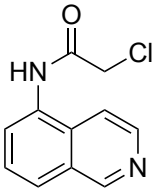
TRH 1-167	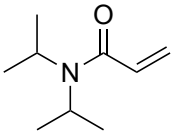
TRH 1-168	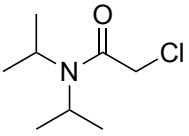

TRH 1-170	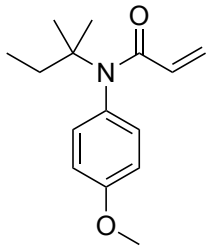
TRH 1-171	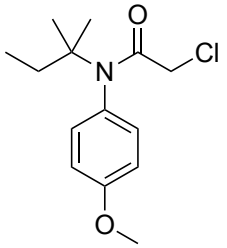
TRH 1-176	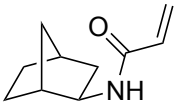 (racemic)
TRH 1-177	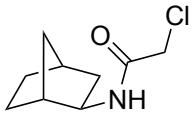 (racemic)
TRH 1-178	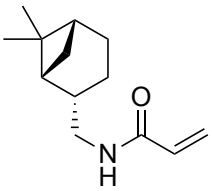
TRH 1-179	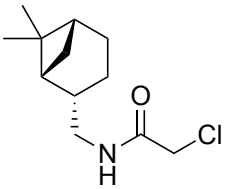
TRH 1-189	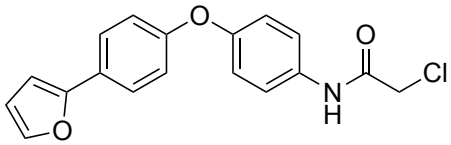

TRH 1-191	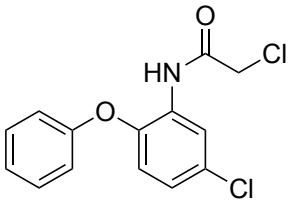
TRH 1-194	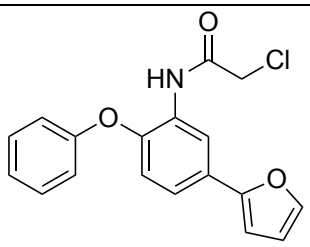
TRH 1-196	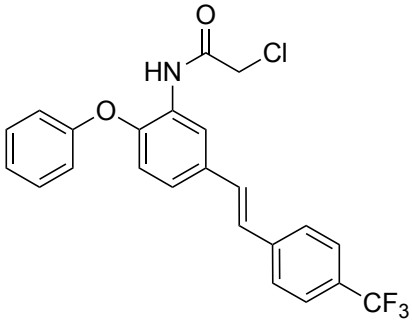
YP 1-1	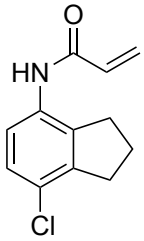
YP 1-16	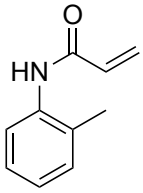
YP 1-18	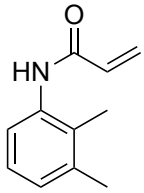
YP 1-19	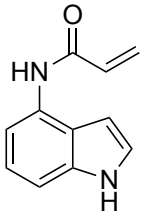

YP 1-22	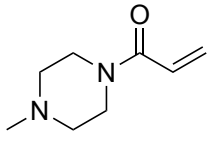
YP 1-23	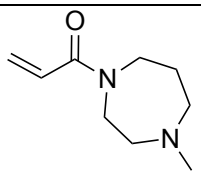
YP 1-24	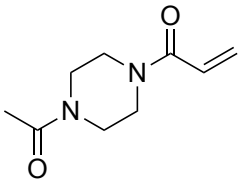
YP 1-25	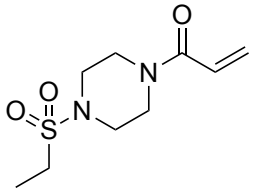
YP 1-26	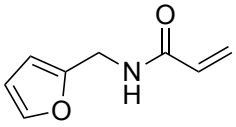
YP 1-31	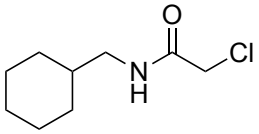
YP 1-36	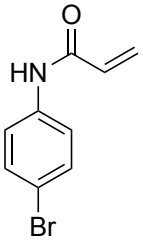

YP 1-37	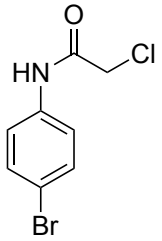
YP 1-38	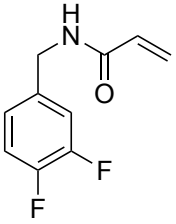
YP 1-39	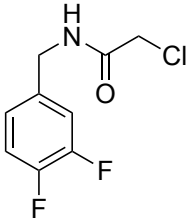
YP 1-40	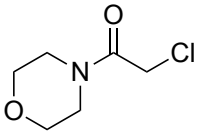
YP 1-42	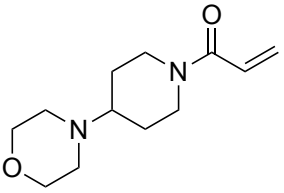
YP 1-44	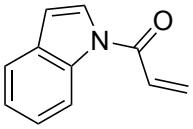
YP 1-38	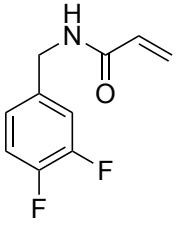

IGA 1-12	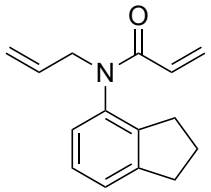
IGA 1-14	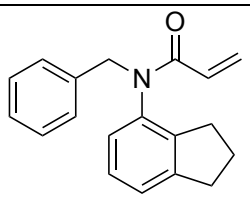
IGA 1-15	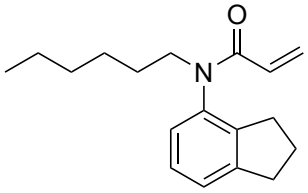
IGA 1-26	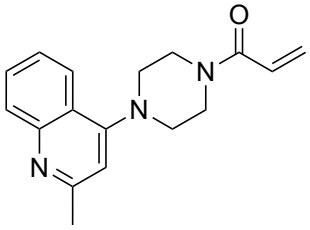

Supporting Methods

General synthetic methods

Chemicals and reagents were purchased from major commercial suppliers and used without further purification. Reactions were performed under a nitrogen atmosphere unless otherwise noted. Silica gel flash column chromatography was performed using EMD or Sigma Aldrich silica gel 60 (230-400 mesh). Proton and carbon nuclear magnetic resonance (^{1}H NMR and ^{13}C NMR) data was acquired on a Bruker AVB 400, AVQ 400, or AV 600 spectrometer at the University of California, Berkeley. High resolution mass spectrum were obtained from the QB3 mass spectrometry facility at the University of California, Berkeley using positive or negative electrospray ionization (+ESI or -ESI). Yields are reported as a single run.

General Procedure A

The amine (1 eq.) was dissolved in DCM (5 mL/mmol) and cooled to 0^{o}C. To the solution was added acryloyl chloride (1.2 eq.) followed by triethylamine (1.2 eq.). The solution was warmed to room temperature and stirred overnight. The solution was then washed with brine and the crude product was purified by silica gel chromatography (and recrystallization if necessary) to afford the corresponding acrylamide.

General Procedure B

The amine (1 eq.) was dissolved in DCM (5 mL/mmol) and cooled to 0^{o}C. To the solution was added chloroacetyl chloride (1.2 eq.) followed by triethylamine (1.2 eq.). The solution was warmed to room temperature and stirred overnight. The solution was then washed with brine and the crude product was purified by silica gel chromatography (and recrystallization if necessary) to afford the corresponding chloroacetamide.

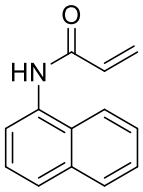

***N*-(naphthalene-1-yl)acrylamide (TRH-1-57).**

To a solution of 1-naphthylamine (294 mg, 2.0 mmol) in dichloromethane (10 mL) was added acryloyl chloride (0.20 mL, 2.4 mmol) followed by triethylamine (248 mg, 2.4 mmol) at 0˚ C under N_2 atmosphere. The reaction mixture was allowed to warm to room temperature and was stirred for 16 hours. The solution was washed twice with brine, and the resulting crude was purified by silica gel chromatography (30% to 40% ethyl acetate in hexanes) and recrystallized from toluene to yield 173 mg of white solid (44% yield).

^{1}H NMR (400MHz, MeOD): δ 7.96-7.94 (m, 1H), 7.88-7.86 (m, 1H), 7.76 (d, *J* = 8.1 Hz, 1H), 7.64 (d, *J* = 7.3 Hz, 1H), 7.52-7.44 (m, 3H), 6.43 (dd, *J* = 16.9, 10.4 Hz, 1H), 6.41 (dd, *J* = 16.9, 1.5 Hz, 1H), 5.82 (dd, *J* = 10.1, 1.0 Hz, 1H).

^{13}C NMR (100MHz, MeOD): δ 167.3, 135.7, 133.9, 132.1, 129.9, 129.4, 128.2, 127.7, 127.3, 127.2, 126.4, 123.8, 123.3.

HRMS (+ESI): Calculated: 198.0913 ($C_{13}H_{12}NO$). Observed: 198.0912.

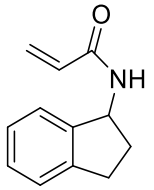

N-(2,3-dihydro-1*H*-inden-1-yl)acrylamide (TRH-1-58).
To a solution of 1-aminoindan (274 mg, 2.0 mmol) in dichloromethane (10 mL) was added acryloyl chloride (0.20 mL, 2.4 mmol) followed by triethylamine (276 mg, 2.4 mmol) at 0˚ C under N_2 atmosphere. After stirring for 20 minutes, the reaction mixture was allowed to warm to room temperature and was stirred for 28 hours. The solution was washed twice with brine, and the resulting crude was purified by silica gel chromatography (20%-40% ethyl acetate in hexanes) to yield 238 mg of white solid (62% yield).
^{1}H NMR (400MHz, $CDCl_3$): δ 7.22-7.11 (m, 4H), 6.76 (d, *J* = 7.8 Hz, 1H), 6.23-6.13 (m, 2H), 5.56 (dd, *J* = 3.5, 8.1 Hz, 1H), 5.40 (q, *J* = 7.9 Hz, 1H), 2.95-2.88 (m, 1H), 2.84-2.76 (m, 1H), 2.51-2.43 (m, 1H), 1.83-1.74 (m, 1H).
^{13}C NMR (100MHz, $CDCl_3$): δ 165.5, 143.2, 143.1, 130.9, 127.8,126.6, 126.3, 124.6, 124.0, 54.5, 33.7, 30.2.
HRMS (+ESI): Calculated: 188.1070 ($C_{12}H_{14}NO$). Observed: 188.1068.

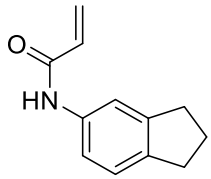

***N*-(2,3-dihydro-1*H*-inden-5-yl)acrylamide (TRH-1-59).**
To a solution of 5-aminoindan (269 mg, 2.0 mmol) in dichloromethane (10 mL) was added acryloyl chloride (0.20 mL, 2.4 mmol) followed by triethylamine (270 mg, 2.4 mmol) at 0˚ C under N_2 atmosphere. The reaction mixture was allowed to warm to room temperature and was stirred for 20 hours. The solution was washed twice with brine, and the resulting crude was purified by silica gel chromatography (40% ethyl acetate in hexanes) to yield 129 mg of white solid (34% yield).
^{1}H NMR (400MHz, $CDCl_3$): δ 8.87 (s, 1H), 7.54 (s, 1H), 7.31 (d, *J* = 7.6 Hz, 1H), 7.11 (d, *J* = 7.8 Hz, 1H), 6.40 (d, *J* = 5.6 Hz, 2H), 5.66 (t, *J* = 5.6 Hz, 1H), 2.87-2.80 (m, 4H), 2.04 (t, *J* = 7.2 Hz, 2H).
^{13}C NMR (100MHz, $CDCl_3$): δ 164.4, 144.9, 140.4, 136.0, 131.6, 127.0, 124.3, 118.8, 117.0, 32.9, 32.4, 25.6.
HRMS (+ESI): Calculated: 188.1070 ($C_{12}H_{14}NO$). Observed: 188.1068.

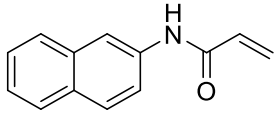

***N*-(naphthalene-2-yl)acrylamide (TRH-1-60).**

To a solution of 2-naphthylamine (289 mg, 2.0 mmol) in dichloromethane (10 mL) was added acryloyl chloride (0.20 mL, 2.4 mmol) followed by triethylamine (269 mg, 2.4 mmol) at 0˚ C under N_2 atmosphere. After 15 minutes, the reaction mixture was allowed to warm to room temperature and was stirred for 16 hours. The solution was washed twice with 5% citric acid and once with brine, and the resulting crude was purified by silica gel chromatography (30% ethyl acetate in hexanes) to yield 266 mg of an off-white solid (67% yield).
^{1}H NMR (400MHz, MeOD): δ 8.25 (d, *J* = 1.8 Hz, 1H), 7.73-7.69 (m, 3H), 5.54 (dd, *J* = 2.1, 8.8 Hz, 1H), 7.39-7.34 (m, 1H), 7.33-7.29 (m, 1H), 6.44 (dd, *J* = 9.7, 17.0 Hz, 1H), 6.36 (dd, *J* = 2.2, 17.0 Hz, 1H), 5.72 (dd, *J* = 2.2, 9.7 Hz, 1H).
^{13}C NMR (100MHz, MeOD): δ 166.2, 137.1, 135.1, 132.4, 132.1, 129.5, 128.6, 128.5, 127.9, 127.4, 126.1, 121.1, 118.1.
HRMS (+ESI): Calculated: 198.0913 ($C_{13}H_{12}NO$). Observed: 198.0912.

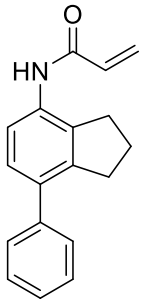

N-(7-phenyl-2,3-dihydro-1*H*-inden-4-yl)acrylamide (TRH-1-68).

To a solution of *N*-(7-bromo-2,3-dihydro-1*H*-inden-4yl)acrylamide (**TRH-1-65**, 56 mg, 0.2 mmol) in a solution of dioxane and water (4:1 dioxane:water, 2.1 mL) was added sequentially phenylboronic acid (55 mg, 0.4 mmol), potassium carbonate (78 mg, 0.5 mmol), and tetrakis(triphenylphosphine)palladium(0) (26 mg, 10 mol%). The reaction mixture was heated to a reflux and was stirred overnight. The reaction was diluted with water (20 mL) and extracted with DCM (3x20 mL). The combined organics were evaporated and the resulting crude was purified by silica gel chromatography (10% to 50% ethyl acetate in hexanes) then recrystallized from toluene to give 11 mg of white solid (20% yield).

^{1}H NMR (400MHz, MeOD): δ 7.48 (d, *J* = 8.2 Hz, 1H), 7.40-7.39 (m, 4H), 7.33-7.27 (m, 1H), 7.16 (d, *J* = 8.2 Hz, 1H), 6.53 (dd, *J* = 10.2, 17.0 Hz, 1H), 6.36 (dd, *J* = 1.7, 17.0 Hz, 1H), 5.77 (dd, *J* =1.7, 10.2 Hz, 1H), 2.96 (t, *J*= 7.3 Hz, 2H), 2.91 (t, *J* = 7.3 Hz, 2H), 2.04 (quint, *J* = 7.3 Hz, 2H).

^{13}C NMR (100MHz, MeOD): δ 166.3, 144.2, 142.4, 139.2, 133.8, 132.2, 129., 129.3, 128.2, 127.9, 127.8, 123.0, 34.3, 32.1, 26.6.

HRMS (+ESI): Calculated: 264.1383 ($C_{18}H_{18}NO$). Observed: 264.1381.

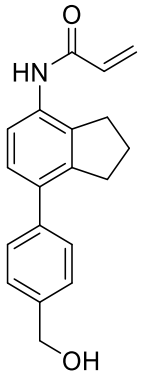

***N*-(7-(4-(hydroxymethyl)phenyl)-2,3-dihydro-1*H*-4-yl)acrylamide (TRH-1-70).**

To a solution of *N*-(7-bromo-2,3-dihydro-1*H*-inden-4yl)acrylamide (**TRH-1-65**, 56 mg, 0.2 mmol) in a solution of dioxane and water (4:1 dioxane:water, 2.1 mL) under nitrogen atmosphere was added sequentially 4-(hydroxymethyl)phenylboronic acid (66 mg, 0.4 mmol), potassium carbonate (78 mg, 0.5 mmol), and tetrakis(triphenylphosphine)palladium(0) (26 mg, 10 mol%). The reaction mixture was heated to a reflux and stirred overnight. The reaction was diluted with water (20 mL) and extracted with DCM (3x20 mL). The combined organics were dried with magnesium sulfate, filtered, and evaporated, and the resulting crude was purified by silica gel chromatography (20% to 50% ethyl acetate in hexanes) to give 16 mg of white solid (26% yield).

^{1}H NMR (400MHz, MeOD): δ 7.47 (d, *J* = 8.1 Hz, 1H), 7.41-7.38 (m, 4H), 7.15 (d, *J* = 8.2 Hz, 1H), 6.52 (dd, *J* = 10.2, 16.9 Hz, 1H), 6.36 (d, *J* = 17.0 Hz, 1H), 5.77 (d, *J* = 10.5 Hz, 1H), 4.63 (s, 2H), 2.95 (t, *J* = 7.1 Hz, 2H), 2.90 (t, *J* = 7.2 Hz, 2H), 2.03 (t, *J* = 7.3 Hz, 2H).

^{13}C NMR (100MHz, MeOD): δ 166.3, 144.1, 141.4, 139.2, 136.9, 133.8, 132.2, 129.5, 128.5,128.2, 128.0, 127.9, 123.0, 65.0, 34.3, 32.0, 26.6.

HRMS (+ESI): Calculated: 294.1489 ($C_{19}H_{20}NO_2$). Observed: 294.1486.

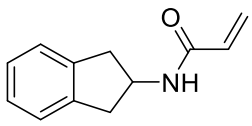

***N*-(2,3-dihydro-1*H*-inden-2-yl)acrylamide (TRH-1-74).**

To a solution of 2-aminoindan (253 mg, 2.0 mmol) in dichloromethane (10 mL) was added acryloyl chloride (0.19 mL, 2.4 mmol) followed by triethylamine (222 mg, 2.4 mmol) at 0˚ C under N_2 atmosphere. The reaction mixture was allowed to warm to room temperature after 15 minutes and was stirred for 23 hours. The solution was washed twice with brine, and the resulting crude was purified by silica gel chromatography (40% ethyl acetate in hexanes) to yield 126 mg of an off-white solid (35% yield).

^{1}H NMR (400MHz, $CDCl_3$): δ 7.23-7.16 (m, 4H), 6.27 (dd, *J* = 1.3, 17.0 Hz, 1H), 6.10 (s, 1H), 6.04 (dd, *J* = 10.3, 17.0 Hz, 1H), 5.60 (dd, *J* = 1.3, 10.3 Hz, 1H), 4.82-4.75 (m, 1H), 3.32 (dd, *J* = 7.1, 16.2 Hz, 2H), 2.84 (dd, *J* = 4.4, 16.1 Hz, 2H).

^{13}C NMR (100MHz, $CDCl_3$): δ 165.4 ,140.9, 130.9, 126.8, 126.5, 124.9, 50.7, 40.1.

HRMS (+ESI): Calculated: 188.1070 ($C_{12}H_{14}NO$). Observed: 188.1068.

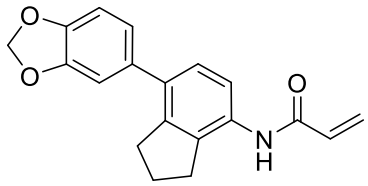

***N*-(7-(benzo[*d*][1,3]dioxol-5-yl)-2,3-dihydro-1*H*-inden-4-yl)acrylamide (TRH-1-78).**
To a solution of N-(7-bromo-2,3-dihydro-1H-inden-4yl)acrylamide (**TRH-1-65**, 55 mg, 0.2 mmol) in a mixture of dioxane and water (4:1 dioxane:water, 2.1 mL) under nitrogen atmosphere was added sequentially 3,4-(methylenedioxy)phenylboronic acid (70 mg, 0.4 mmol), potassium carbonate (74 mg, 0.5 mmol), and tetrakis(triphenylphosphine)palladium(0) (24 mg, 10 mol%). The reaction mixture was heated to a reflux and stirred overnight. The reaction was diluted with water (20 mL) and extracted with DCM (3x20 mL). The combined organics were dried with magnesium sulfate, filtered, and evaporated, and the resulting crude was purified by silica gel chromatography (0% to 25% ethyl acetate in hexanes) to give 7 mg of white solid (11% yield).

^{1}H NMR (600 MHz, $CDCl_3$): δ 7.93 (d, *J* = 7.0 Hz, 1H), 7.18 (d, *J* = 8.2 Hz, 1H), 7.10 (s, 1H), 6.90 (s, 1H), 6.86 (t, *J* = 8.1 Hz, 2H), 6.45 (d, *J* = 16.8 Hz, 1H), 6.30 (dd, *J* = 10.3, 16.8 Hz, 1H), 5.79 (d, *J* = 10.2 Hz, 1H), 3.00 (t, *J* = 7.3 Hz, 2H), 2.88 (t, *J* = 7.3 Hz, 2H), 2.10 (quint, 7.3 Hz, 2H).
^{13}C NMR (150 MHz, $CDCl_3$): δ 147.7, 146.7, 142.84, 142.81, 135.2, 134.9, 132.8, 131.3, 127.9, 127.8, 122.1, 119.8, 109.2, 108.3, 101.2, 36.8, 33.5, 30.5, 25.4.
HRMS (-ESI): Calculated: 306.1136 ($C_{19}H_{16}NO_3$). Observed: 306.1130.

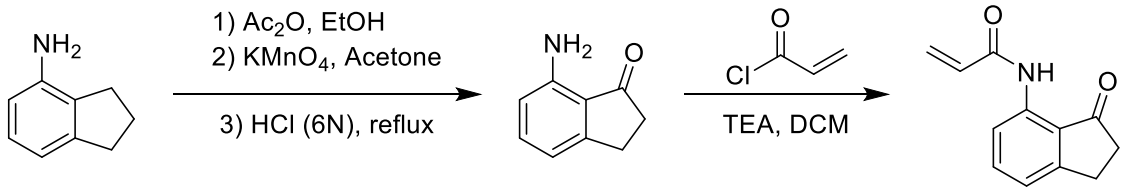

***N*-(3-oxo-2,3-dihydro-1*H*-inden-4-yl)acrylamide (TRH-1-129)**
To a solution of 4-aminoindan (1.0 g, 7.5 mmol) in ethanol (20 mL) at 0 °C was added acetic anhydride (1.4 mL, 15.0 mmol). The solution was raised to room temperature and stirred overnight, after which the solvent was evaporated. The residue was then dissolved in acetone (50 mL) to which was added 15% aqueous magnesium sulfate (1.2 g in 6.75 mL of water) followed by potassium permanganate (3.4 g, 17.0 mmol), and the resulting solution was stirred for 24 hours. The reaction filtered through a pad of celite, eluting with chloroform and then water. The eluent was separated, and the aqueous layer was extracted several times with additional chloroform. The combined organics

were dried over magnesium sulfate, filtered and evaporated. The residue was then dissolved in a 6N HCl solution (20 mL) and heated to 90 °C. After stirring for 5 hours, the solution was cooled, neutralized with small portions of potassium carbonate, and extracted with ethyl acetate. The combined organics were dried with magnesium sulfate, filtered, and evaporated to give 610 mg (55% over 3 steps) of crude **7-aminoindan-1-one** which was used without further purification.
To a solution of 7-aminoindan-1-one in dichloromethane (15 mL) was added acryloyl chloride (0.39 mL, 4.8 mmol) followed by triethylamine (0.67 mL, 4.8 mmol) at 0˚ C under N_2 atmosphere. The reaction mixture was allowed to warm to room temperature and was stirred overnight. The solution was washed 1M HCl solution (2x) and brine, and the resulting crude was purified by silica gel chromatography (10% to 20% ethyl acetate in hexanes) to yield 390 mg of white solid (47% yield, 26% combined over 4 steps).
^{1}H NMR (400MHz, $CDCl_3$): δ 10.64 (s, 1H), 8.45 (d, *J* = 8.2 Hz, 1H), 7.55 (t, *J* = 7.9 Hz, 1H), 7.12 (d, *J* = 7.6 Hz, 1H), 6.45 (dd, *J* = 1.0, 17.0 Hz, 1H), 6.33 (dd, *J* = 10.1, 17.0 Hz, 1H), 5.82 (dd, *J* = 1.0, 10.1 Hz, 1H), 3.11 (t, *J* = 11.5 Hz, 2H), 2.74-2.71 (m, 2H).
^{13}C NMR (100MHz, $CDCl_3$): δ 209.3, 164.4, 155.9, 138.7, 137.0, 131.7, 128.0, 123.1, 120.8, 116.9, 36.5, 25.5.
HRMS (+ESI): Calculated: 202.0863 ($C_{12}H_{12}NO_2$). Observed: 202.0860.

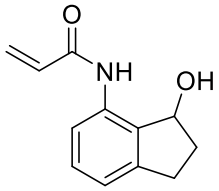

***N*-(3-hydroxy-2,3-dihydro-1*H*-inden-4-yl)acrylamide (TRH-1-133).**
To a solution of *N*-(3-oxo-2,3-dihydro-1*H*-inden-4-yl)acrylamide (**TRH-1-129**, 201 mg, 1.0 mmol) in anhydrous methanol (7 mL) under nitrogen atmosphere was added sodium borohydride (46.1 mg, 1.2 mmol). After 30 minutes of stirring, the reaction was quenched with saturated sodium bicarbonate solution and extracted three times with DCM. The combined organics were dried with magnesium sulfate, filtered, and concentrated. Crude was purified by silica gel chromatography (30 to 50% ethyl acetate in hexanes) to give 190 mg of the product as a white solid (94% yield).
^{1}H NMR (400 MHz, $CDCl_3$): δ 8.93 (s, 1H), 7.98 (d, *J* = 7.8 Hz, 1H), 7.19 (t, *J* = 7.9 Hz, 1H), 6.95 (d, *J* = 7.4 Hz, 1H), 6.29 (d, *J* = 16.8 Hz, 1H), 6.15 (dd, *J* = 10.2, 16.9 Hz, 1H), 5.66 (d, *J* = 10.2 Hz, 1H), 5.32 (q, *J* = 6.9 Hz, 1H), 3.60 (d, *J* = 6.7 Hz, 1H), 2.96 (ddd, *J* = 2.4, 9.0, 15.7 Hz), 2.73 (quint, *J* = 8.1 Hz, 1H), 2.56-2.48 (m, 1H), 1.96-1.86 (m, 1H).
^{13}C NMR (100 MHz, $CDCl_3$): δ 164.1, 143,7 ,135.6, 132.8, 131.6, 129.5, 127.3, 121.0, 118.5, 76.2, 36.0, 29.8.
HRMS (-ESI): Calculated: 202.0874 ($C_{12}H_{12}NO_2$). Observed: 202.0874.

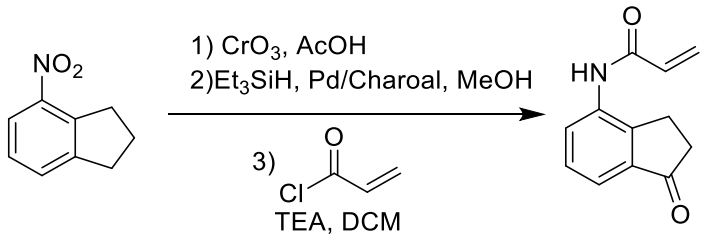

***N*-(1-oxo-2,3-dihydro-1*H*-inden-4-yl)acrylamide (TRH-1-134).**

To a solution of 4-nitroindan (5.38 g, 33 mmol) in acetic acid (250 mL) was slowly added chromium trioxide (8.95 g, 90 mmol). After stirring for 24 hours, the reaction was neutralized with 2M NaOH and extracted five times with ethyl acetate. The combined organics were washed with a saturated sodium bicarbonate solution and brine, then dried over magnesium sulfate, filtered, and concentrated. The crude material was purified by silica gel chromatography (10-20% ethyl acetate in hexanes) to give 1.26 g (ca. 7.1 mmol) of 4-nitroindanone as a white solid.

This intermediate was combined with palladium on activated charcoal (125 mg, 10 wt%) dissolved in anhydrous methanol (21 mL) under the atmosphere of a nitrogen balloon. Triethylsilane (11.3 mL, 71 mmol) was slowly added by addition funnel over the course of 10 minutes while the reaction was stirred under the cooling of a room temperature water bath. After an additional 20 minutes of stirring, the reaction mixture was filtered through a pad of celite and subsequently concentrated to give crude 4-aminoindanone which was used without further purification.

This final intermediate was then dissolved in DCM (21 mL) under N_2 atmosphere and cooled to 0^{o}C, after which acryloyl chloride (0.77 mL, 9.5 mmol) and triethylamine (1.19 mL, 8.5 mmol) were slowly added. The reaction was allowed to warm to room temperature while stirring overnight, at which point the reaction was washed twice with brine, dried with magnesium sulfate, filtered, and concentrated. The crude was purified by silica gel chromatography (30-50% ethyl acetate in hexanes) to give 989 mg of a white solid (15% yield over 3 steps).

^{1}H NMR (400 MHz, $CDCl_3$): δ 8.20 (d, *J* = 5.8 Hz, 1H), 7.63 (s, 1H), 7.56 (d, *J* = 7.5 Hz, 1H), 7.39 (t, *J* = 7.7 Hz, 1H), 6.48 (d, *J* = 16.7 Hz, 1H), 6.37 (dd, *J* = 10.0 Hz, 16.8 Hz, 1H), 5.83 (d, *J* = 10.1 Hz, 1H), 3.04 (t, *J* = 5.6 Hz, 2H), 2.70 (t, *J* = 5.7 Hz, 2H).

^{13}C NMR (100 MHz, $CDCl_3$): δ 206.3, 163.9, 146.0, 138.0, 135.4, 130.7, 128.8, 128.7, 127.6, 120.4, 36.1, 23.4.

HRMS (-ESI): Calculated: 200.0717 ($C_{12}H_{10}NO_2$). Observed: 200.0715.

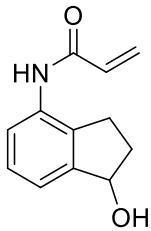

***N*-(1-hydroxy-2,3-dihydro-1*H*-inden-4-yl)acrylamide (TRH-1-135).**

To a solution of *N*-(1-oxo-2,3-dihydro-1*H*-inden-4-yl)acrylamide (**TRH-1-134**, 1.26 g, 6.25 mmol) in anhydrous methanol (50 mL) under nitrogen atmosphere was added sodium borohydride (292.7 mg, 7.7 mmol). After 30 minutes of stirring, the reaction was

quenched with water and the methanol was removed *in vacuo*. The residue was saturated with NaCl and extracted five times with a 2:1 chloroform:methanol solution. The combined organics were dried over 3 angstrom molecular sieves, filtered, and concentrated. The crude material was purified by silica gel chromatography (40 to 70% ethyl acetate in hexanes) to give 1.05 g of the product as a white solid (83% yield).
^{1}H NMR (400 MHz, MeOD): δ 7.50 (dd, *J* = 2.3, 6.3 Hz, 1H), 7.25-7.20 (m, 2H), 6.51 (dd, *J* = 10.2, 17.0 Hz, 1H), 6.35 (dd, *J* = 1.7, 17.0 Hz, 1H), 5.77 (dd, *J* = 1.7, 10.2 Hz, 1H), 5.17 (t, *J* = 6.3 Hz, 1H), 2.97 (ddd, *J* = 4.5, 8.6, 16.2, 1H), 2.74 (quint, *J* = 7.8 Hz, 1H), 2.47-2.39 (m, 1H), 1.95-1.86 (m, 1H).
^{13}C NMR (100 MHz, MeOD): δ 166.3, 148.0, 137.8, 134.8, 132.1, 128.3, 127.9, 124.0, 122.7, 76.9, 36.1, 28.6.
HRMS (-ESI): Calculated: 202.0874 ($C_{12}H_{12}NO_2$). Observed: 202.0872.

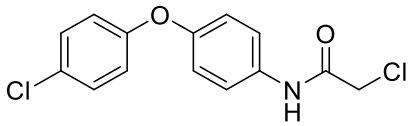

2-Chloro-*N*-(4-(4-chlorophenoxy)phenyl)acetamide (TRH-1-140).
To a solution 4-(4-chlorophenoxy)aniline (446 mg, 2.0 mmol) in dichloromethane (10 mL) was added chloroacetyl chloride (0.39 mL, 4.8 mmol) followed by triethylamine (0.67 mL, 4.8 mmol) at 0˚ C under N_2 atmosphere. After stirring for 35 minutes, the reaction mixture was allowed to warm to room temperature and was stirred for 27 hours. The solution was washed twice with brine, dried with magnesium sulfate, and the resulting crude was purified by silica gel chromatography (30% to 50% ethyl acetate in hexanes) to yield 533 mg of an off-white solid (89% yield).
^{1}H NMR (400 MHz, $CDCl_3$): δ 8.33 (s, 1H), 7.52-7.48 (m, 2H), 7.29-7.25 (m, 2H), 6.99-6.96 (m, 2H), 6.93-6.89 (m, 2H), 4.17 (s, 2H)
^{13}C NMR (100 MHz, $CDCl_3$): δ 164.1, 156.0, 154.0, 132.5, 129.8, 128.4, 122.2, 119.9, 119.6, 42.9.
HRMS (-ESI): Calculated: 294.0094 ($C_{14}H_{10}NO_2Cl_2$). Observed: 294.0094.

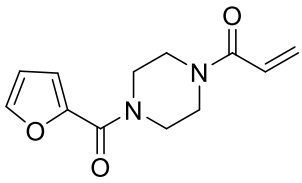

1-(4-(furan-2-carbonyl)piperazin-1-yl)prop-2-en-1-one (TRH-1-145).
To a solution 1-(2-furoyl)piperazine (362 mg, 2.0 mmol) in dichloromethane (10 mL) was added acryloyl chloride (0.20 mL, 2.4 mmol) followed by triethylamine (0.34 mL, 2.4 mmol) at 0˚ C under N_2 atmosphere. After stirring for 20 minutes, the reaction mixture was allowed to warm to room temperature and was stirred for 24 hours. The solution was washed twice with brine, dried with magnesium sulfate, and the resulting crude was purified by silica gel chromatography (70% to 100% ethyl acetate in hexanes) to yield 446 mg of yellow solid (95% yield).

^{1}H NMR (400 MHz, $CDCl_3$): δ 7.53 (m, 1H), 7.06 (dd, *J* = 0.7, 3.5 Hz, 1H), 6.61 (dd, *J* = 10.5, 16.8 Hz, 1H), 6.52 (dd, *J* = 1.8, 3.5 Hz, 1H), 6.33 (dd, *J* = 1.9, 16.8 Hz, 1H), 5.75 (dd, *J* = 1.9, 10.5 Hz, 1H), 3.84-3.67 (m, 8H).
^{13}C NMR (100 MHz, $CDCl_3$): δ 165.5, 159.1, 147.5, 144.0, 128.5, 127.1, 117.0, 111.5, 45.6, 41.9.
HRMS (+ESI): Calculated: 235.1077 ($C_{12}H_{15}N_2O_3$). Observed: 235.1075.

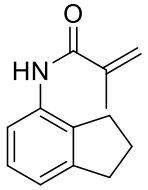

***N*-(2,3-dihydro-1*H*-inden-4-yl)methacrylamide (TRH-1-149).**
To a solution 4-aminoindan (0.24 mL, 2.0 mmol) in dichloromethane (10 mL) was added methacryloyl chloride (0.23 mL, 2.4 mmol) followed by triethylamine (0.34 mL, 2.4 mmol) at 0˚ C under N_2 atmosphere. After stirring for 20 minutes, the reaction mixture was allowed to warm to room temperature and was stirred for 3.5 hours. The solution was washed twice with brine, dried with magnesium sulfate, and the resulting crude was purified by silica gel chromatography (35% to 40% ethyl acetate in hexanes) to yield 378 mg of off-white solid (94% yield).
^{1}H NMR (400 MHz, $CDCl_3$): δ 7.72 (d, *J* = 8.0 Hz, 1H), 7.55 (s, 1H), 7.12 (t, *J* = 7.7 Hz, 1H), 7.01 (d, *J* = 7.4 Hz, 1H), 5.79 (s, 1H), 5.42 (s, 1H), 2.93 (t, *J* = 7.5 Hz, 2H), 2.79 (t, *J* =7.4 Hz, 2H), 7.12-2.06 (m, 2H), 2.04 (s, 3H).
^{13}C NMR (100 MHz, $CDCl_3$): δ 166.3, 145.1, 140.6, 134.5, 133.7, 127.0, 120.7, 119.8, 118.9, 33.1, 29.9, 24.7, 18.6.
HRMS (+ESI): Calculated: 202.1226 ($C_{13}H_{16}NO$). Observed: 202.1224.

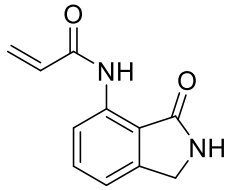

***N*-(3-oxoisoindolin-4-yl)acrylamide (TRH-1-152).**
To a solution of 7-aminoisoindolin-1-one (99 mg, 0.67 mmol) in dichloromethane (4 mL) was added acryloyl chloride (0.07 mL, 0.8 mmol) followed by triethylamine (0.11 mL, 0.8 mmol) at 0˚ C under N_2 atmosphere. After stirring for 20 minutes, the reaction mixture was allowed to warm to room temperature and was stirred overnight. The solution was washed twice with brine, dried with magnesium sulfate, and the resulting crude was purified by silica gel chromatography (50 to 60% ethyl acetate in hexanes) to yield 58 mg of a white solid (43% yield).
^{1}H NMR (400 MHz, $CDCl_3$): δ 10.50 (s, 1H), 8.58 (d, *J* = 8.2 Hz, 1H), 7.55 (t, *J* = 7.9 Hz, 1H), 7.15 (d, *J* = 7.5 Hz, 1H), 6.82 (s, 1H), 6.46 (dd, *J* = 1.3, 17.0 Hz, 1H), 6.36 (dd, *J* = 10.0, 17.0 Hz, 1H), 5.81 (dd, *J* = 1.3, 10.0 Hz, 1H), 4.46 (s, 2H).
^{13}C NMR (100 MHz, $CDCl_3$): δ 172.9, 164.2, 143.9, 138.2, 133.8, 131.8, 127.8, 118.0, 117.7, 117.6, 45.6.

HRMS (+ESI): Calculated: 203.0815 ($C_{11}H_{11}N_2O_2$). Observed: 203.0814.

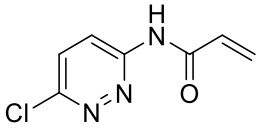

***N*-(6-chloropyridazin-3-yl)acrylamide (TRH-1-155).**

To a solution 3-amino-6-chloropyridazine (261 mg, 2.0 mmol) in dichloromethane (10 mL) was added acryloyl chloride (0.20 mL, 2.4 mmol) followed by triethylamine (0.34 mL, 2.4 mmol) at 0˚ C under N_2 atmosphere. After stirring for 20 minutes, the reaction mixture was allowed to warm to room temperature and was stirred overnight. The solution was washed twice with brine, dried with magnesium sulfate, and the resulting crude was purified by silica gel chromatography (40% to 50% ethyl acetate in hexanes) to yield 23 mg of a pale-yellow solid (6% yield).

^{1}H NMR (400 MHz, $CDCl_3$): δ 10.06 (s, 1H), 8.70 (d, *J* = 9.4 Hz, 1H), 7.57 (d, *J* = 9.4 Hz, 1H), 6.73 (dd, *J* = 10.2, 16.8 Hz, 1H) 6.56 (dd, *J* = 1.2, 16.8, 1H), 5.94 (dd, *J* = 1.2, 10.2 Hz, 1H).

^{13}C NMR (100 MHz, $CDCl_3$): δ 164.8, 155.2, 152.3, 130.7, 130.4, 130.3, 122.0.

HRMS (+ESI): Calculated: 182.0127 ($C_7H_5N_3OCl$). Observed: 182.0126.

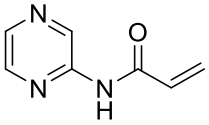

***N*-(Pyrazin-2-yl)acrylamide (TRH-1-156).**

To a solution of aminopyrazine (192 mg, 2.0 mmol) in dichloromethane (10 mL) was added acryloyl chloride (0.20 mL, 2.4 mmol) followed by triethylamine (0.34 mL, 2.4 mmol) at 0˚ C under N_2 atmosphere. After stirring for 20 minutes, the reaction mixture was allowed to warm to room temperature and was stirred overnight. The solution was washed twice with brine, dried with magnesium sulfate, and the resulting crude was purified by silica gel chromatography (50% to 70% ethyl acetate in hexanes) to yield 22 mg of white solid (7% yield).

^{1}H NMR (600 MHz, $CDCl_3$): δ 9.65 (d, *J* = 1.3 Hz, 1H), 8.38 (d, *J* = 2.5 Hz, 1H), 8.27 (dd, *J* = 1.6, 2.5 Hz, 1H), 8.19 (s, 1H), 6.54 (dd, *J* = 0.8, 16.9 Hz, 1H), 6.33 (dd, *J* = 10.3, 16.9 Hz, 1H), 5.90 (dd, *J* = 0.8, 10.3 Hz, 1H).

^{13}C NMR (150 MHz, $CDCl_3$): δ 163.5, 148.2, 142.2, 140.6, 137.4, 130.2, 129.8.

HRMS (+ESI): Calculated: 150.0662 ($C_7H_8N_3O$). Observed: 150.0660.

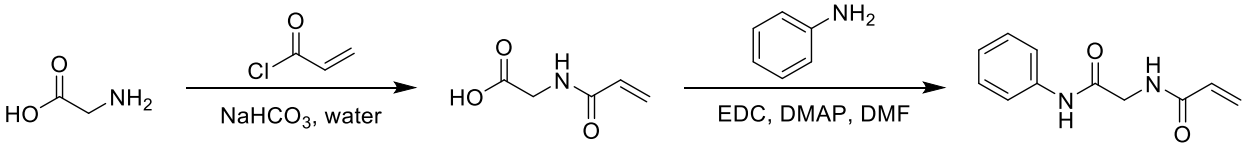

***N*-(2-oxo-2-(phenylamino)ethyl)acrylamide (TRH-1-160).**

To a solution of glycine (1.50 g, 20.0 mmol) and sodium bicarbonate (1.70 g, 20.2 mmol) in water (30 mL) at 0˚ C was slowly added acryloyl chloride (2.45 mL, 30.2 mmol). After stirring for 3.5 hours, the reaction was extracted 3 times with ethyl acetate. The combined organics were dried over magnesium sulfate, filtered, and concentrated

to give an oil. The oil was treated with hexanes causing a white solid to crash out which was collected by gravity filtration to give 124 mg of crude acryloylglycine of which 58 mg (47% of the crude material) was used immediately without further purification.
This solid (ca. 0.45 mmol) was dissolved in DMF (2.5 mL) and a solution of N-(3-dimethylaminopropyl)-N′-ethylcarbodiimide hydrochloride (104 mg, 0.54 mmol) and 4-dimethylaminopyridine (68 mg, 0.56 mmol) in DMF (2.5 mL) was added followed by aniline (0.050 mL, 0.54 mmol). The solution was stirred overnight, diluted with ethyl acetate, and washed with both a saturated solution of sodium bicarbonate and brine. The organics were then dried over magnesium sulfate, filtered, and concentrated, and the resulting crude was purified by silica gel chromatography (30-60% ethyl acetate in hexanes) to give 19 mg of the title compound as a white solid (1% yield over two steps).

^{1}H NMR (400 MHz, MeOD): δ 7.56-7.53 (m, 2H), 7.30 (t, *J* = 8.0 Hz, 2H), 7.08 (t, *J* = 7.4 Hz, 1H), 6.35 (dd, *J* = 9.9, 17.1 Hz, 1H), 6.26 (dd, *J* = 2.0, 17.1 Hz, 1H), 5.71 (dd, *J* = 2.0, 9.9 Hz, 1H), 4.08 (s, 2H).
^{13}C NMR (100 MHz, MeOD): δ 169.4, 168.6, 139.5, 131.7, 129.8, 127.2, 125.3, 121.2, 44.0.
HRMS (-ESI): Calculated: 203.0826 ($C_{11}H_{11}N_2O_2$). Observed: 203.0825.

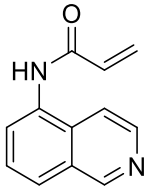

***N*-(isoquinolin-5-yl)acrylamide (TRH-1-162).**
To a solution of 5-aminoisoquinoline (287 mg, 2.0 mmol) in dichloromethane (10 mL) was added acryloyl chloride (0.20 mL, 2.4 mmol) followed by triethylamine (0.34 mL, 2.4 mmol) at 0˚ C under N_2 atmosphere. After stirring for 20 minutes, the reaction mixture was allowed to warm to room temperature and was stirred overnight. The solution was washed with brine, and the resulting aqueous layer was extracted with a 2:1 chloroform:methanol solution. The resulting crude was purified by chromatography on basic alumina (50% ethyl acetate in hexanes to 4% ethanol in ethyl acetate) to yield 43 mg of a yellow solid (11% yield).
^{1}H NMR (400 MHz, MeOD): δ 9.23 (s, 1H), 8.45 (d, *J* = 6.1 Hz, 1H), 8.03 (d, *J* = 7.5 Hz, 1H), 7.97 (d, *J* = 8.2 Hz, 1H), 7.88 (d, *J* = 6.1 Hz, 1H), 7.68 (t, *J* = 7.9 Hz, 1H), 6.66 (dd, *J* = 10.2, 17.0 Hz, 1H), 6.47 (dd, *J* = 1.5, 17.0 Hz, 1H), 5.88 (dd, *J* = 1.7, 10.2 Hz, 1H).
^{13}C NMR (100 MHz, MeOD): δ 167.1, 153.5, 143.0, 133.6, 132.4, 131.9, 130.6, 128.7, 127.9, 127.1, 117.2.
HRMS (+ESI): Calculated: 199.0866 ($C_{12}H_{11}N_2O$). Observed: 199.0863.

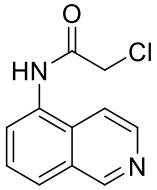

2-Chloro-*N*-(isoquinolin-5-yl)acetamide (TRH-1-163).

To a solution 5-aminoisoquinoline (289 mg, 2.0 mmol) in dichloromethane (10 mL) was added chloroacetyl chloride (0.19 mL, 2.4 mmol) followed by triethylamine (0.34 mL, 2.4 mmol) at 0˚ C under N_2 atmosphere. After stirring for 20 minutes, the reaction mixture was allowed to warm to room temperature and was stirred overnight. The solution was washed with saturated sodium bicarbonate solution and brine, dried with magnesium sulfate, and the resulting crude was purified by chromatography on basic alumina (30% ethyl acetate in hexanes to 4% ethanol in ethyl acetate) to yield 157 mg of yellow solid (36% yield).
^{1}H NMR (600 MHz, MeOD): δ 9.26 (s, 1H), 8.48 (d, *J* = 6.1 Hz, 1H), 8.03 (d, *J* = 8.2 Hz, 1H), 7.98 (d, *J* = 7.4 Hz, 1H), 7.91 (d, *J* = 6.1 Hz, 1H), 7.71 (t, *J* = 7.9 Hz, 1H), 4.39, (s, 2H).
^{13}C NMR (150 MHz, MeOD): δ 167.4, 152.1, 141.7, 131.8, 131.2, 129.2, 127.3, 127.0, 126.1, 115.7, 42.3.
HRMS (+ESI): Calculated: 221.0476 ($C_{11}H_{10}N_2O$). Observed: 221.0473.

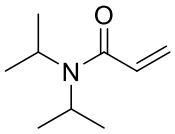

***N,N*-diisopropylacrylamide (TRH-1-167).**
To a solution of diisopropylamine (0.42 mL, 3.0 mmol) in dichloromethane (10 mL) was added acryloyl chloride (0.29 mL, 3.6 mmol) followed by triethylamine (0.50 mL, 3.6 mmol) at 0˚ C under N_2 atmosphere. After stirring for 20 minutes, the reaction mixture was allowed to warm to room temperature and was stirred for 19 hours. The solution was washed with a saturated solution of sodium bicarbonate followed by brine, dried with magnesium sulfate, and the resulting crude was purified by silica gel chromatography (0% to 30% ethyl acetate in hexanes) to yield 392 mg of a pale-yellow oil (84% yield).
^{1}H NMR (400 MHz, $CDCl_3$): δ 6.35 (dd, *J* = 10.6, 16.8 Hz, 1H), 5.98 (dd, *J* = 1.7, 16.8 Hz, 1H), 5.36 (dd, *J* = 1.7, 10.6 Hz, 1H), 3.85 (s, 1H), 3.56 (s, 1H), 1.18 (s, 6H), 1.06 (s, 6H).
^{13}C NMR (100 MHz, $CDCl_3$): δ 165.9, 130.5, 125.3, 47.9, 45.4, 21.1, 20.3.
HRMS (+ESI): Calculated: 178.1202 ($C_9H_{17}NONa$). Observed: 178.1201.

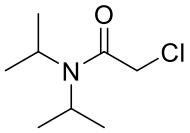

2-Chloro-*N,N*-diisopropylacetamide (TRH-1-168).
To a solution diisopropylamine (0.42 mL, 3.0 mmol) in dichloromethane (10 mL) was added chloroacetyl chloride (0.29 mL, 3.6 mmol) followed by triethylamine (0.50 mL, 3.6 mmol) at 0˚ C under N_2 atmosphere. After stirring for 20 minutes, the reaction mixture was allowed to warm to room temperature and was stirred overnight. The solution was washed with saturated sodium bicarbonate solution and brine, dried with magnesium sulfate, and the resulting crude was purified by silica gel chromatography (0 to 20% ethyl acetate in hexanes) to yield 376 mg of white solid (70% yield).

^{1}H NMR (400 MHz, $CDCl_3$): δ 3.93 (s, 2H), 3.88-3.82 (m, 1H), 3.38-3.31 (m, 1H), 1.29 (d, *J* = 6.5 Hz, 6H), 1.14 (d, *J* = 6.4 Hz, 6H).
^{13}C NMR (100 MHz, $CDCl_3$): δ 165.0, 49.7, 46.1, 43.2, 20.7, 20.0.
HRMS (+ESI): Calculated: 200.0813 ($C_8H_{16}NOClNa$). Observed: 200.0811.

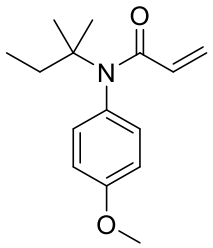

***N*-(4-methoxyphenyl)-*N*-(*tert*-pentyl)acrylamide (TRH-1-170).**
To a solution of 4-methoxy-*N*-(*tert*-pentyl)aniline (94 mg, 0.49 mmol) in dichloromethane (5 mL) was added acryloyl chloride (0.05 mL, 0.6 mmol) followed by triethylamine (0.09 mL, 0.6 mmol) at 0˚ C under N_2 atmosphere. After stirring for 15 minutes, the reaction mixture was allowed to warm to room temperature and was stirred for 18 hours. The solution was washed with a saturated solution of sodium bicarbonate followed by brine, dried with magnesium sulfate, and the resulting crude was purified by silica gel chromatography (0% to 20% ethyl acetate in hexanes) to yield 82 mg of a pale-yellow oil (68% yield).
^{1}H NMR (400 MHz, $CDCl_3$): δ 6.99 (d, *J* = 8.7 Hz, 2H), 6.85 (d, *J* = 8.7 Hz, 2H), 6.17 (dd, *J* = 1.9, 16.7 Hz, 1H), 5.76 (dd, *J* = 10.3, 16.7 Hz, 1H), 5.28 (dd, *J* = 1.9, 10.3 Hz, 1H), 3.81 (s, 3H), 2.11 (q, *J* = 7.5 Hz, 2H), 1.20 (s, 6H), 0.91 (t, *J* = 7.5 Hz, 3H).
^{13}C NMR (100 MHz, $CDCl_3$): δ 166.3, 159.0, 134.3, 131.49, 131.45, 125.6, 114.1, 61.7, 55.5, 32.0, 27.4, 9.4.
HRMS (+EI): Calculated: 247.1572 ($C_{15}H_{21}NO_2$). Observed: 247.1577.

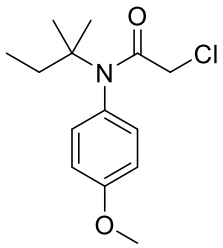

2-Chloro-*N*-(4-methoxyphenyl)-*N*-(*tert*-pentyl)acetamide (TRH-1-171).
To a solution 4-methoxy-*N*-(*tert*-pentyl)aniline (95 mg, 0.5 mmol) in dichloromethane (5 mL) was added chloroacetyl chloride (0.05 mL, 0.6 mmol) followed by triethylamine (0.085 mL, 0.6 mmol) at 0˚ C under N_2 atmosphere. After stirring for 15 minutes, the reaction mixture was allowed to warm to room temperature and was stirred overnight. The solution was washed with saturated sodium bicarbonate solution and brine, dried with magnesium sulfate, and the resulting crude was purified by silica gel chromatography (0 to 10% ethyl acetate in hexanes) to yield 99 mg of a yellow oil (74% yield).
^{1}H NMR (400 MHz, $CDCl_3$): δ 7.04 (d, *J* = 8.6 Hz, 2H), 6.87 (d, *J* = 8.6 Hz, 2H), 3.80 (s, 3H), 3.63 (s, 2H), 2.05 (q, *J* = 7.4 Hz, 2H), 1.16 (s, 6H), 0.90 (t, *J* = 7.4 Hz, 3H).

^{13}C NMR (100 MHz, $CDCl_3$): δ 166.0, 159.5, 133.2, 131.0, 114.5, 62.5, 55.5, 44.8, 31.8, 27.1, 9.3.
HRMS (+ESI): Calculated: 270.1255 ($C_{14}H_{21}NO_2Cl$). Observed: 270.1254.

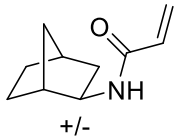

+/-

***N*-(*exo*-norborn-2-yl)acrylamide (TRH-1-176).**
To a solution of *exo*-2-aminonorbornane (0.24 mL, 2 mmol) in dichloromethane (10 mL) was added acryloyl chloride (0.20 mL, 2.4 mmol) followed by triethylamine (0.33 mL, 2.4 mmol) at 0˚ C under N_2 atmosphere. After stirring for 20 minutes, the reaction mixture was allowed to warm to room temperature and was stirred for 18 hours. The solution was washed with a saturated solution of sodium bicarbonate followed by brine, dried with magnesium sulfate, and the resulting crude was purified by silica gel chromatography (30% ethyl acetate in hexanes) to yield 271 mg of a white solid (82% yield).
^{1}H NMR (400 MHz, $CDCl_3$): δ 6.42 (s, 1H), 6.25 (dd, *J* = 2.3, 17.0 Hz, 1H), 6.18 (dd, *J* = 9.5, 17.0 Hz, 1H), 5.58 (dd, *J* = 2.3, 9.5 Hz, 1H), 3.8-3.77 (m, 1H), 2.27-2.24 (m, 2H), 1.78 (ddd, *J* = 2.1, 8.1, 13.0 Hz, 1H), 1.55-1.38 (m, 3H), 1.30-1.10 (m, 4H).
^{13}C NMR (100 MHz, $CDCl_3$): δ 165.0, 131.4, 125.8, 52.9, 42.4, 40.0, 35.7, 35.6, 28.2, 26.6.
HRMS (+EI): Calculated:165.1154 ($C_{10}H_{15}NO$). Observed: 165.1155.

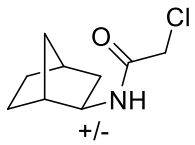

+/-

2-Chloro-*N*-(*exo*-norborn-2-yl)acetamide (TRH-1-177).
To a solution of *exo*-2-aminonorbornane (0.24 mL, 2 mmol) in dichloromethane (10 mL) was added chloroacetyl chloride (0.19 mL, 2.4 mmol) followed by triethylamine (0.33 mL, 2.4 mmol) at 0˚ C under N_2 atmosphere. After stirring for 20 minutes, the reaction mixture was allowed to warm to room temperature and was stirred overnight. The solution was washed with saturated sodium bicarbonate solution and brine, dried with magnesium sulfate, and the resulting crude was purified by silica gel chromatography (20 to 40% ethyl acetate in hexanes) to yield 345 mg of a white solid (91% yield).
^{1}H NMR (400 MHz, $CDCl_3$): δ 6.48 (s, 1H), 3.93 (s, 2H), 3.67-3.63 (m, 1H), 2.24-2.22 (m, 1H), 2.16-2.15 (m, 1H), 1.74 (ddd, *J* = 1.9, 8.1, 13.0 Hz, 1H), 1.50-1.36 (m, 2H), 1.30-1.26 (m, 1H), 1.21-1.14 (m, 3H), 1.09-1.03 (m, 1H).
^{13}C NMR (100 MHz, $CDCl_3$): δ 165.0, 53.1, 42.6, 42.2, 40.0, 35.6, 35.5, 28.0, 26.3.
HRMS (+ESI): Calculated: 187.0764 ($C_9H_{14}NOCl$). Observed: 187.0765.

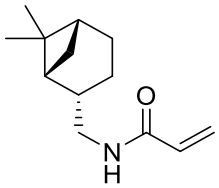

***N*-(((1*R*,2*S*,5*R*)-6,6-dimethylbicyclo[3.1.1]heptan-2-yl)methyl)acrylamide (TRH-1-178).**

To a solution of (-)-*cis*-myrtanylamine (0.34 mL, 2 mmol) in dichloromethane (10 mL) was added acryloyl chloride (0.20 mL, 2.4 mmol) followed by triethylamine (0.33 mL, 2.4 mmol) at 0˚ C under N_2 atmosphere. After stirring for 20 minutes, the reaction mixture was allowed to warm to room temperature and was stirred for 21 hours. The solution was washed with a saturated solution of sodium bicarbonate followed by brine, dried with magnesium sulfate, and the resulting crude was purified by silica gel chromatography (20 to 30% ethyl acetate in hexanes) to yield 369 mg of a white solid (89% yield).

^{1}H NMR (600 MHz, $CDCl_3$): δ 6.26 (dd, *J* = 1.5, 17.0 Hz, 1H), 6.11 (dd, *J* = 10.3, 17.0 Hz, 1H) 5.85 (s, 1H), 5.61 (dd, *J* = 1.5, 10.3 Hz, 1H), 3.39-3.29 (m, 2H), 2.38-2.34 (m, 1H), 2.26-2.21 (m, 1H), 1.98-1.90 (m, 4H), 1.88-1.83 (m, 1H), 1.53-1.47 (m, 1H), 1.19 (s, 3H), 1.04 (s, 3H), 0.89 (d, *J* = 9.6 Hz, 1H).

^{13}C NMR (150 MHz, $CDCl_3$): δ 165.7, 131.2, 126.2, 45.3, 43.9, 41.5, 38.8, 33.3, 28.1, 26.1, 23.3, 19.9.

HRMS (-ESI): Calculated: 206.1550 ($C_{13}H_{20}NO$). Observed: 206.1551.

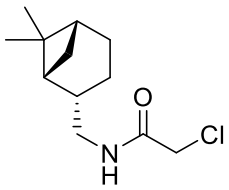

2-Chloro-*N*-(((1*R*,2*S*,5*R*)-6,6-dimethylbicyclo[3.1.1]heptan-2-yl)methyl)acetamide (TRH-1-179).

To a solution of (-)-*cis*-myrtanylamine (0.34 mL, 2 mmol) in dichloromethane (10 mL) was added chloroacetyl chloride (0.19 mL, 2.4 mmol) followed by triethylamine (0.33 mL, 2.4 mmol) at 0˚ C under N_2 atmosphere. After stirring for 20 minutes, the reaction mixture was allowed to warm to room temperature and was stirred overnight. The solution was washed with saturated sodium bicarbonate solution and brine, dried with magnesium sulfate, and the resulting crude was purified by silica gel chromatography (0 to 20% ethyl acetate in hexanes) to yield 405 mg of an off-white solid (88% yield).

^{1}H NMR (600 MHz, $CDCl_3$): δ 6.61 (s, 1H), 4.05 (s, 2H), 3.33-3.30 (m, 2H), 2.40-2.36 (m, 1H), 2.27-2.21 (m, 1H), 1.99-1.83 (m, 5H), 1.53-1.46 (m, 1H), 1.20 (s, 3H), 1.05 (s, 3H), 0.90 (d, *J* = 9.7 Hz, 1H).

^{13}C NMR (150 MHz, $CDCl_3$): δ 165.8, 45.5, 43.8, 42.9, 41.4, 41.2, 38.8, 33.3, 28.0, 26.0, 23.3, 19.8.

HRMS (-ESI): Calculated: 228.1161 ($C_{12}H_{19}NOCl$). Observed: 228.1162.

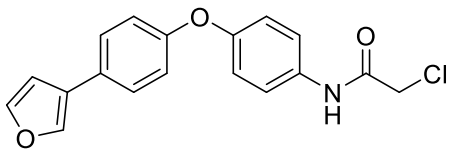

2-Chloro-*N*-(4-(4-(furan-3-yl)phenoxy)phenyl)acetamide (TRH-1-189).
A reaction vial equipped with a stirbar was charged with 2-chloro-*N*-(4-(4-chlorophenoxy)phenyl)acetamide (**TRH-1-140**, 74 mg, 0.25 mmol), 3-furanylboronic acid (44 mg, 0.38 mmol), and XPhos-G3-palladacycle (4 mg, 2 mol%) and placed under a nitrogen atmosphere. THF (1 mL) and an aqueous solution of tribasic potassium phosphate (0.5M, 2 mL) that was freshly degassed by sparging with N_2 were sequentially added, and the reaction was stirred for 1 hour. The reaction mixture was diluted with water and extracted three times with diethyl ether. The combined organics were dried over magnesium sulfate, and the resulting crude was purified by silica gel chromatography (10% to 30% ethyl acetate in hexanes) to give 19 mg of a white solid (23% yield).
^{1}H NMR (400 MHz, $CDCl_3$): δ 7.50-7.47 (m, 2H), 7.43 (dt, *J* = 2.6, 9.8 Hz, 2H), 7.30-7.24 (m, 3H), 6.95 (dt, *J* = 2.6, 9.7 Hz, 2H), 6.90 (dt, *J* = 2.7, 9.7 Hz, 2H), 6.43 (s, 1H), 3.58 (s, 2H).
^{13}C NMR (100 MHz, $CDCl_3$): δ 168.5, 156.2, 153.3, 144.2, 141.2, 133.4, 129.7, 128.1, 121.8, 119.7, 119.6, 117.9, 111.2, 33.9.
HRMS (-ESI): Calculated: 326.0589 ($C_{18}H_{13}NO_3Cl$). Observed: 326.0594.

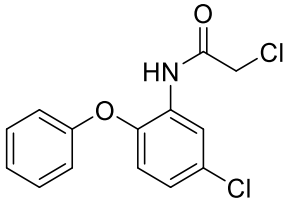

2-Chloro-*N*-(5-chloro-2-phenoxyphenyl)acetamide (TRH-1-191).
To a solution of 2-amino-4-chlorophenyl phenyl ether (2.20 g, 10.0 mmol) in dichloromethane (30 mL) was added chloroacetyl chloride (0.96 mL, 12.0 mmol) followed by triethylamine (1.67 mL, 12 mmol) at 0˚ C under N_2 atmosphere. After stirring for 20 minutes, the reaction mixture was allowed to warm to room temperature and was stirred for 16 hours. The solution was diluted with DCM, washed with a saturated sodium bicarbonate solution and brine, dried with magnesium sulfate, and the resulting crude was recrystallized from hexanes to yield 1.84 g of light-brown solid (62% yield).
^{1}H NMR (400 MHz, $CDCl_3$): δ 8.93 (s, 1H), 8.50 (d, *J* = 2.5 Hz, 1H), 7.40-7.35 (m, 2H), 7.19-7.15 (m, 1H), 7.04-7.01 (m, 3H), 6.81 (d, *J* = 8.7 Hz, 1H), 4.16 (s, 2H).
^{13}C NMR (100 MHz, $CDCl_3$): δ 164.0, 156.0, 144.7, 130.2, 129.6, 129.2, 124.7, 124.5, 120.6, 118.71, 118.68, 43.1.
HRMS (-ESI): Calculated: 294.0094 ($C_{14}H_{10}NO_2Cl_2$). Observed: 294.0101.

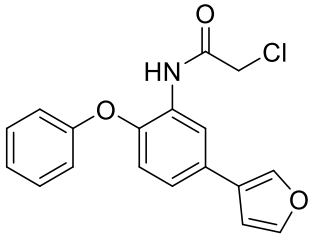

2-Chloro-*N*-(5-(furan-3-yl)-2-phenoxyphenyl)acetamide (TRH-1-194).
A reaction vial equipped with a stirbar was charged with 2-chloro-*N*-(5-chloro-2-phenoxyphenyl)acetamide (**TRH-1-191**, 297 mg, 1.0 mmol), 3-furanylboronic acid (171 mg, 1.5 mmol), and XPhos-G3-palladacycle (17 mg, 2 mol%) and placed under a nitrogen atmosphere. THF (2 mL) and a freshly degassed aqueous solution of tribasic potassium phosphate (0.5M, 4 mL) were sequentially added, and the reaction was stirred for 6 hours. The reaction mixture was diluted with water and extracted three times with diethyl ether. The combined organics were dried over magnesium sulfate, and the resulting crude was purified by silica gel chromatography (10% to 15% ethyl acetate in hexanes) to give 120 mg of a yellow solid (37% yield).
^{1}H NMR (400 MHz, $CDCl_3$): δ 8.53 (d, *J* = 2.4 Hz, 1H), 7.93 (s, 1H), 7.33-7.25 (m, 4H), 7.12 (t, *J* = 7.4 Hz, 1H), 6.97 (dd, *J* = 2.5, 8.7 Hz, 1H), 6.84 (d, *J* = 7.8 Hz, 2H), 6.79 (d, *J* = 8.7 Hz, 1H), 6.23 (s, 6.23), 3.52 (s, 2H).
^{13}C NMR (100 MHz, $CDCl_3$): δ 168.6, 156.3, 144.0, 143.4, 141.1, 130.9, 130.1, 129.7, 124.0, 123.9, 120.7, 119.6, 117.5, 117.4, 111.0, 34.2.
HRMS (-ESI): Calculated: 326.0589 ($C_{18}H_{13}NO_3Cl$). Observed: 326.0585.

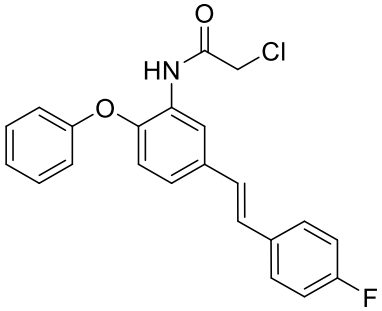

***trans*-2-Chloro-*N*-(5-(4-fluorostyryl)-2-phenoxyphenyl)acetamide (TRH-1-196).**
A reaction vial equipped with a stirbar was charged with 2-chloro-*N*-(5-chloro-2-phenoxyphenyl)acetamide (**TRH-1-191**, 296 mg, 1.0 mmol), *trans*-2-(4-fluorophenyl)vinylboronic acid (253 mg, 1.5 mmol), and XPhos-G3-palladacycle (17 mg, 2 mol%) and placed under a nitrogen atmosphere. THF (2 mL) and a freshly degassed aqueous solution of tribasic potassium phosphate (0.5M, 4 mL) were sequentially added, and the reaction was stirred for 21 hours. The reaction mixture was diluted with water and extracted three times with diethyl ether. The combined organics were dried over magnesium sulfate, and the resulting crude was purified by silica gel chromatography (5% to 15% ethyl acetate in hexanes) to give 256 mg of a yellow solid (67% yield).
^{1}H NMR (400 MHz, $CDCl_3$): δ 8.54 (d, *J* = 2.4 Hz, 1H), 8.00 (s, 1H), 7.27-7.20 (m, 4H), 7.10-7.06 (m, 1H), 6.99-6.93 (m, 3H), 6.84-6.79 (m, 3H), 6.47 (d, *J* = 15.9 Hz, 1H), 6.17-6.10 (m, 1H), 3.27 (dd, *J* = 1.1, 7.3 Hz, 2H).

^{13}C NMR (100 MHz, $CDCl_3$): δ 168.8, 163.8, 161.3, 156.2, 143.5, 134.6, 132.59, 132.56, 130.9, 130.1, 129.6, 128.1, 128.0, 123.98, 123.96, 121.20, 121.18, 120.7, 119.5, 117.6, 115.7, 115.4, 41.8.
HRMS (+ESI): Calculated: 404.0824 ($C_{22}H_{17}NO_2ClFNa$). Observed: 404.0828.

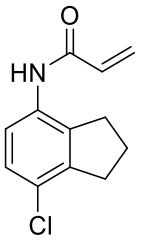

N-(7-chloro-2,3-dihydro-1H-inden-4-yl)acrylamide (YP-1-1)
A solution of N-(2,3-dihydro-1H-inden-4-yl)acrylamide (187 mg, 1.0 mmol) in PEG 400 (5.2 mL) was cooled to 0 ^{o}C. To the solution was added *N*-chlorosuccinimide (140 mg, 1.0 mmol). The solution was allowed to warm to room temperature after 30 min and stirred overnight. The solution was diluted with ethyl acetate and washed two times with brine and dried with magnesium sulfate. The crude product was purified via silica gel chromatography (30% ethyl acetate in hexanes). The obtained mixture of isomers was separated by recrystallization to afford the product in 22% yield as a white solid (47 mg).
^{1}H NMR (400MHz, $CDCl_3$): δ 7.78 (d, *J* = 8.8 Hz, 1H), 7.15-7.11 (m, 2H), 6.42 (dd, *J* = 1.4, 16.8 Hz, 1H), 6.26 (dd, *J* = 10.2, 16.8 Hz, 1H), 5.77 (dd, *J* = 1.4, 10.2 Hz, 1H), 2.98 (t, *J* = 7.6 Hz, 2H), 2.87 (t, *J* = 7.5 Hz, 2H), 2.12 (quint, *J* = 7.5 Hz, 2 H).
^{13}C NMR (100MHz, $CDCl_3$): δ 163.4, 143.1, 136.1, 132.2, 131.0, 128.0, 127.2, 126.7, 120.9, 32.7, 31.1, 24.0.
HRMS (+ESI): Calculated: 220.0535 ($C_{12}H_{11}ClNO$). Observed: 220.0533.

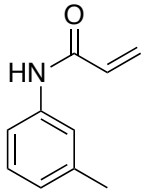

N-(m-tolyl)acrylamide (YP-1-16)
A solution of o-toluidine (107 mg, 1.0 mmol) in DCM (10 mL) was cooled to 0 ^{o}C. To the solution was added acryloyl chloride (109 mg, 1.2 mmol) followed by triethylamine (121 mg, 1.2 mmol). The solution was allowed to warm to room temperature after 40 min and stirred overnight. The solution was washed two times with brine and dried with magnesium sulfate. The crude product was purified via silica gel chromatography (20% to 40% ethyl acetate in hexanes) to afford the product in 86% yield as a white solid (139 mg).
^{1}H NMR (400MHz, $CDCl_3$): δ 7.82 (d, *J* = 7.9 Hz, 1H), 7.32 (s, 1H), 7.21-7.17 (m, 2H), 7.10-7.06 (m, 1H), 6.43-6.38 (m, 1H), 6.29 (dd, *J* = 10.2, 17.1 Hz, 1H), 5.75-5.72 (m, 1H), 2.25 (s, 1H).
^{13}C NMR (100MHz, $CDCl_3$): δ 135.5, 131.2, 130.5, 127.5, 126.8, 125.5, 123.4, 17.8.
HRMS (+ESI): Calculated: 162.0913 ($C_{10}H_{12}NO$). Observed: 162.0912.

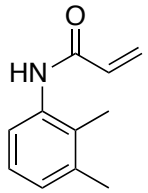

N-(2,3-dimethylphenyl)acrylamide (YP-1-18)

A solution of 2,3-dimethylaniline (121 mg, 1.0 mmol) in DCM (10 mL) was cooled to 0 ^{o}C. To the solution was added acryloyl chloride (109 mg, 1.2 mmol) followed by triethylamine (121 mg, 1.2 mmol). The solution was allowed to warm to room temperature after 29 min and stirred overnight. The solution was washed two times with brine and dried with magnesium sulfate. The crude product was purified via silica gel chromatography (30% to 40% ethyl acetate in hexanes) to afford the product in 88% yield as a white solid (154 mg).

^{1}H NMR (400MHz, $CDCl_3$): δ 7.49 (d, *J* = 7.9 Hz, 1H), 7.29 (s, 1H), 7.11-7.07 (m, 1H), 7.01 (d, *J* = 7.7, 1H) 6.40 (d, *J* = 17.1, 1H), 6.30 (dd, *J* = 7.3, 17.1 Hz, 1H), 5.74 (d, *J* = 10.1 Hz, 1H), 2.29 (s, 1H), 2.13 (s, 1H).

^{13}C NMR (100MHz, $CDCl_3$): δ 135.1, 131.2, 127.6, 127.3, 125.9, 122.3, 20.6, 13.9.

HRMS (+ESI): Calculated: 176.1070 ($C_{11}H_{14}NO$). Observed: 176.1068.

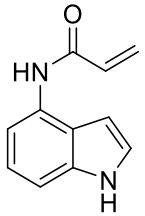

N-(1H-indol-4-yl)acrylamide (YP-1-19)

A solution of 4-aminoindole (132 mg, 1 mmol) in DCM (5 mL) and DMF (5 mL) was cooled to 0 ^{o}C. To the solution was added acryloyl chloride (109 mg, 1.2 mmol) followed by triethylamine (121 mg, 1.2 mmol). The solution was allowed to warm to room temperature after 26 min and stirred overnight. The solution was washed two times with brine and dried with magnesium sulfate. The crude product was purified via basic alumina chromatography (60% to 75% ethyl acetate in hexanes) to afford the product in 30% yield as a white-grey solid (56 mg).

^{1}H NMR (600MHz, MeOD): δ 7.51 (d, *J* = 7.6 Hz, 1H), 7.24-7.22 (m, 2H), 7.08 (t, *J* = 7.6 Hz, 1H), 6.64 (dd, *J* = 10.1, 16.7 Hz, 2H), 6.38 (dd, *J* = 1.7, 16.9 Hz, 1H), 5.78 (dd, *J* = 1.7, 10.3 Hz, 1H), 4.6 (s, 1H).

^{13}C NMR (150MHz, MeOD): δ 165.0, 137.2, 131.1, 129.2, 126.0, 123.8, 121.5, 120.9, 112.2, 108.4, 98.5.

HRMS (+ESI): Calculated: 187.0866 ($C_{11}H_{11}N_2O$). Observed: 187.0865.

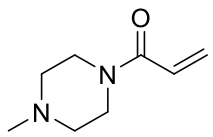

1-(4-Methylpiperazin-1-yl)prop-2-en-1-one (YP-1-22)

A solution of 1-methylpiperazine (100 mg, 1.0 mmol) in DCM (10 mL) was cooled to 0 ^{o}C. To the solution was added acryloyl chloride (109 mg, 1.2 mmol) followed by triethylamine (121 mg, 1.2 mmol). The solution was allowed to warm to room temperature after 30 min and stirred overnight. The solution was washed two times with brine and dried with magnesium sulfate. The crude product was purified via silica gel chromatography (85% to 100% ethyl acetate in hexanes) to afford the product in 29% yield as a yellow gel (44 mg).
^{1}H NMR (400MHz, $CDCl_3$): δ 6.56 (dd, *J* = 10.6, 16.9 Hz, 1H), 6.29 (dd, *J* = 2.0, 16.8 Hz, 1H), 5.69 (dd, *J* = 2.0, 10.6 Hz, 1H), 3.71 (s, 2H), 3.58 (s, 2H), 2.42 (t, *J* = 5.1 Hz, 4H), 2.32 (s, 3H).
^{13}C NMR (100MHz, $CDCl_3$): δ 165.4, 127.8, 127.5, 55.2, 54.6, 46.0, 45.7, 41.9.
HRMS (+ESI): Calculated: 155.1179 ($C_8H_{15}N_2O$). Observed: 155.1178.

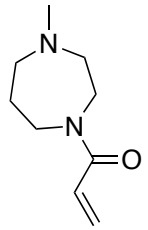

1-(4-methyl-1,4-diazepan-1-yl)prop-2-en-1-one (YP-1-23)
A solution of 1-methylhomopiperazine (114 mg, 1.0 mmol) in DCM (10 mL) was cooled to 0 ^{o}C. To the solution was added acryloyl chloride (109 mg, 1.2 mmol) followed by triethylamine (121 mg, 1.2 mmol). The solution was allowed to warm to room temperature after 32 minutes and stirred overnight. The solution was washed two times with brine and dried with magnesium sulfate. The crude product was purified via silica gel chromatography (1% to 10% methanol in DCM) to afford the product in 51% yield as a yellow oil (58 mg).
^{1}H NMR (400MHz, $CDCl_3$): δ 6.61-6.53 (m, 1H), 6.35-6.29 (m, 1H), 5.70-5.66 (m, 1H), 3.74-3.72 (m, 1 H), 3.69 (t, *J* = 6.4 Hz, 1H), 3.65-3.61 (m, 2H), 2.66-2.63 (m, 2H), 2.59-2.54 (m, 2H), 2.37 (s, 3H), 1.94 (quint, *J* = 6.2 Hz, 2H).
^{13}C NMR (100MHz, $CDCl_3$): δ 166.4, 166.3, 128.0, 127.9, 127.8, 127.6, 59.1, 58.0, 57.1, 56.8, 47.4, 47.1, 46.7, 46.6, 45.3, 44.8, 28.1, 26.9.
HRMS (+ESI): Calculated: 169.1335 ($C_9H_{17}N_2O$). Observed: 169.1333.

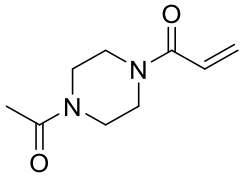

1-(4-acetylpiperazin-1-yl)prop-2-en-1-one (YP-1-24)
A solution of 1-acetylpiperazine (128 mg, 1.0 mmol) in DCM (10 mL) was cooled to 0 ^{o}C. To the solution was added acryloyl chloride (109 mg, 1.2 mmol) followed by triethylamine (121 mg, 1.2 mmol). The solution was allowed to warm to room temperature after 23 minutes and stirred for two hours. The solution was washed two times with brine and dried with magnesium sulfate. The crude product was purified via

silica gel chromatography (0% to 10% methanol in DCM) to afford the product in 18% yield as a yellow oil (40 mg).
^{1}H NMR (400MHz, $CDCl_3$): δ 6.57 (dd, *J* = 10.5, 16.8 Hz, 1H), 6.33 (dd, *J* = 1.8, 16.8 Hz, 1H), 5.75 (dd, *J* = 1.9, 10.5 Hz, 1H), 3.72 (s, 1H), 3.66-3.64 (m, 3H), 3.57 (s, 1H), 3.51-3.49 (m, 2H), 2.13 (s, 3H).
^{13}C NMR (100MHz, $CDCl_3$): δ 165.6, 128.7, 127.0, 41.9, 41.4, 21.4.
HRMS (+ESI): Calculated: 183.1128 ($C_9H_{15}N_2O_2$). Observed: 183.1126.

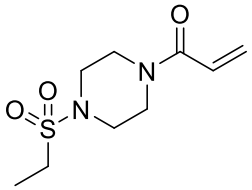

1-(4-(Ethylsulfonyl)piperazin-1-yl)prop-2-en-1-one (YP-1-25)
A solution of 1-(ethanesulfonyl)piperazine (178 mg, 1.0 mmol) in DCM (10 mL) was cooled to 0 ^{o}C. To the solution was added acryloyl chloride (109 mg, 1.2 mmol) followed by triethylamine (121 mg, 1.2 mmol). The solution was allowed to warm to room temperature after 27 min and stirred for two hours. The solution was washed two times with brine and dried with magnesium sulfate. The crude product was purified via silica gel chromatography (1% to 10% methanol in DCM) to afford the product in 70% yield as a white-yellow solid (163 mg).
^{1}H NMR (400MHz, $CDCl_3$): δ 6.57 (dd, *J* = 10.5, 16.8 Hz, 1H), 6.32 (dd, *J* = 1.9, 16.8 Hz, 1H), 5.76 (dd, *J* = 1.8, 10.5 Hz, 1H), 3.77 (s, 2H), 3.67 (s, 2H), 3.32 (t, *J* = 5.2 Hz, 4H), 2.98 (q, *J* = 7.5 Hz, 2H), 1.37 (t, *J* = 7.4, 3H).
^{13}C NMR (100MHz, $CDCl_3$): δ 165.5, 128.8, 127.0, 77.4, 45.9, 45.6, 44.2, 41.9, 7.8.
HRMS (+ESI): Calculated: 233.0954 ($C_9H_{17}N_2O_3S_1$). Observed: 233.0953.

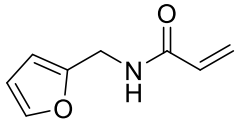

N-(Furan-2-ylmethyl)acrylamide (YP-1-26)
A solution of furfurylamine (97 mg, 1.0 mmol) in DCM (10 mL) was cooled to 0 ^{o}C. To the solution was added acryloyl chloride (109 mg, 1.2 mmol) followed by triethylamine (121 mg, 1.2 mmol). The solution was allowed to warm to room temperature after 17 min and stirred for two and a half hours. The solution was washed two times with brine and dried with magnesium sulfate. The crude product was purified via silica gel chromatography (35% to 70% ethyl acetate in hexanes) to afford the product in 86% yield as a white solid (132 mg).
^{1}H NMR (400MHz, $CDCl_3$): δ 7.33 (s, 1H), 6.60 (s, 1H), 6.31-6.22 (m, 3H), 6.15 (dd, *J* = 10.1, 16.9 Hz, 1H), 5.63 (dd, *J* = 1.6, 10.1 Hz, 1H), 4.48 (d, *J* = 5.6 Hz, 2H).
^{13}C NMR (100MHz, $CDCl_3$): δ 165.5, 151.2, 142.2, 130.6, 126.8, 110.5, 107.5, 36.5.
HRMS (+ESI): Calculated: 152.0706 ($C_8H_{10}O_2N_1$). Observed: 152.0706.

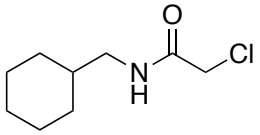

2-chloro-*N*-(cyclohexylmethyl)acetamide (YP-1-31)
Following **General Procedure B** starting from cyclohexanemethylamine (113 mg, 1.0 mmol), product was obtained after silica gel chromatography (100% dichloromethane to 3% methanol in dichloromethane) in 60% yield as a white solid (112 mg).
^{1}H NMR (400MHz, $CDCl_3$): δ 6.70 (s, 1H), 4.06 (s, 2H), 3.15 (t, *J* = 6.47 Hz, 2H), 1.77-1.65 (m, 5H), 1.56-1.46 (m, 1H), 1.30-1.10 (m, 3H), 1.00-0.90 (m, 2H).
^{13}C NMR (100MHz, $CDCl_3$): δ 165.8, 58.1, 46.0, 42.8, 37.7, 30.7, 26.3, 25.7, 18.2.
HRMS (+ESI): Calculated: 190.0993 ($C_9H_{17}ONCl$). Observed: 190.0992.

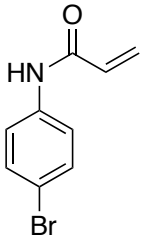

***N*-(4-bromophenyl)acrylamide (YP-1-36)**
Following **General Procedure A** starting from 4-bromoaniline (688 mg, 4.0 mmol), product was obtained after silica gel chromatography (30% to 60% ethyl acetate in hexanes) in 28% yield as a white solid (250 mg).
^{1}H NMR (400MHz, CD_3OD): δ 7.90 (s, 1H), 7.60-7.56 (m, 2H), 7.47-7.44 (m, 2H), 6.45-6.33 (m, 2H), 5.78 (dd, *J* = 2.8, 9.1 Hz, 1H).
^{13}C NMR (100MHz, CD_3OD): δ 164.7, 137.7, 131.4, 130.9, 126.7, 121.5, 116.3, 101.1, 78.1.
HRMS (+ESI): Calculated: 223.9716 (C_9H_7NOBr). Observed: 223.9719.

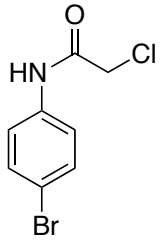

***N*-(4-bromophenyl)-2-chloroacetamide (YP-1-37)**
Following **General Procedure B** starting from 4-bromoaniline (688 mg, 4.0 mmol), product was obtained after silica gel chromatography (30% to 60% ethyl acetate in hexanes) in 49% yield as a white solid (491 mg).
^{1}H NMR (400MHz, CD_3OD): δ 7.9 (s, 1H), 7.57-7.53 (m, 2H), 7.50-7.47 (m, 2H), 4.17 (s, 2H).
^{13}C NMR (100MHz, CD_3OD): δ 166.0, 137.2, 131.5, 121.6, 116.7, 99.3, 78.1, 42.6.
HRMS (+ESI): Calculated: 245.9327 ($C_8H_6NOBrCl$). Observed: 245.9329.

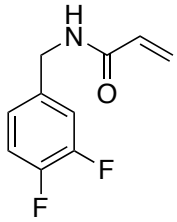

***N*-(3,4-difluorobenzyl)acrylamide (YP-1-38)**

Following **General Procedure A** starting from 3,4-difluorobenzylamine (286 mg, 2.0 mmol), product was obtained after silica gel chromatography (40% to 80% ethyl acetate in hexanes) in 61% yield as a white solid (239 mg).

^{1}H NMR (400MHz, $CDCl_3$): δ 7.56 (t, *J* = 6.2, 1H), 7.07-7.00 (m, 2H), 6.95-6.91 (m, 1H), 6.21-6.20 (m, 2H), 5.62-5.59 (m, 1H), 4.35 (d, *J* = 6.1, 2H).

^{13}C NMR (100MHz, $CDCl_3$): δ 166.1, 151.4 (d), 150.7 (d), 148.9 (d), 148.2 (d), 135.5-135.4 (m), 130.5, 126.8, 123.5-123.4 (m), 117.2 (d), 116.3 (d), 42.4.

HRMS (+ESI): Calculated: 196.0579 ($C_{10}H_8NOF_2$). Observed: 196.0582.

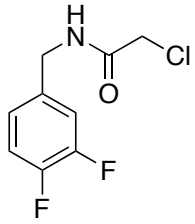

2-chloro-*N*-(3,4-difluorobenzyl)acetamide (YP-1-39)

Following **General Procedure B** starting from 3,4-difluorobenzylamine (286 mg, 2.0 mmol), product was obtained after silica gel chromatography (40% to 50% ethyl acetate in hexanes) in 82% yield as a white solid (359 mg).

^{1}H NMR (400MHz, $CDCl_3$): δ 7.23 (s, 1H), 7.15-7.08 (m, 2H), 7.03-7.6.99 (m, 1H), 4.42 (d, *J* = 6.1 Hz, 2H), 4.08 (s, 2H).

^{13}C NMR (100MHz, $CDCl_3$): δ 166.3, 151.5 (d), 151.0 (d), 149.1 (d), 148.5 (d), 134.7-134.6 (m), 123.7-123.6 (m), 117.5 (d), 116.6 (d), 42.6 (d).

HRMS (+ESI): Calculated: 218.0190 ($C_9H_7NOClF_2$). Observed: 218.0192

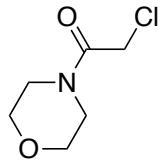

2-chloro-1-morpholinoethan-1-one (YP-1-40)

Following **General Procedure B** starting from morpholine (174 mg, 2.0 mmol), product was obtained after silica gel chromatography (85% ethyl acetate in hexanes) in 61% yield as a white solid (200 mg).

^{1}H NMR (400MHz, $CDCl_3$): δ 4.01 (s, 2H), 3.65-3.59 (m, 4H), 3.55-3.52 (m, 2H), 3.45 (t, *J* = 4.8 Hz, 2H).

^{13}C NMR (100MHz, $CDCl_3$): δ 165.1, 66.5 (d), 46.6, 42.4, 40.7.

HRMS (+ESI): Calculated: 186.0292 ($C_6H_{10}O_2NClNa$). Observed: 186.0292.

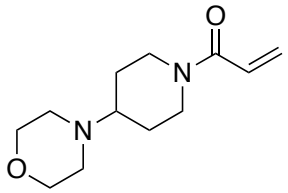

1-(4-morpholinopiperidin-1-yl)prop-2-en-1-one (YP-1-42)
Following **General Procedure A** starting from 4-morpholinopiperidine (336 mg, 2.0 mmol), product was obtained after silica gel chromatography (1% methanol and 80% ethyl acetate in hexanes) in 58% yield as a colorless oil (259 mg).
^{1}H NMR (400MHz, $CDCl_3$): δ 6.42 (dd, *J* = 10.6, 16.8 Hz, 1H), 6.06 (dd, *J* = 2.0, 16.8 Hz, 1H), 5.49 (dd, *J* = 2.0, 10.6 Hz, 1H), 4.45 (d, *J* = 12.8 Hz, 1H), 3.86 (d, *J* = 12.8 Hz, 1H), 3.52 (t, *J* = 4.7 Hz, 4H), 2.90 (t, *J* = 12.8 Hz, 1H), 2.55-2.48 (m, 1H), 2.37-2.35 (m, 4H), 2.26 (tt, *J* = 3.7, 11.0 Hz, 1H), 1.72 (d, *J* = 12.8 Hz, 2H), 1.30-1.20 (m, 2H).
^{13}C NMR (100MHz, $CDCl_3$): δ 165.0, 127.7, 127.3, 67.1, 61.6, 49.6, 44.9, 41.1, 28.9, 27.8.
HRMS (+ESI): Calculated: 225.1598 ($C_{12}H_{21}N_2O_2$). Observed: 225.1595.

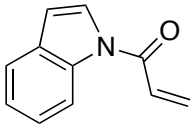

1-(1*H*-indol-1-yl)prop-2-en-1-one (YP-1-44)
A solution of indole (117 mg, 1.0 mmol) in 2-methyltetrahydrofuran (10 mL) was cooled to 0°C. To the solution was added sodium hydride (60 mg, 2.5 mmol). The resultant intermediate was subjected to **General Procedure A** and product was obtained after alumina gel chromatography (10% to 40% ethyl acetate in hexanes) in 8% yield as a white solid (14 mg).
^{1}H NMR (400MHz, CD_3OD): δ 8.48-8.46 (m, 1H), 7.82 (d, *J* = 3.9 Hz, 1H), 7.61-7.59 (m, 1H), 7.36-7.32 (m, 1H), 7.31-7.21 (m, 2H), 6.73 (dd, *J* = 0.8, 3.8 Hz, 1H), 6.64 (dd, *J* = 1.7, 16.7 Hz, 1H), 6.09 (dd, *J* = 1.7, 10.5 Hz, 1H).
^{13}C NMR (100MHz, CD_3OD): δ 164.3, 135.7, 131.0, 130.9, 128.0, 125.0, 124.4, 123.6, 120.5, 116.2, 108.9.
HRMS (+ESI): Calculated: 172.0757 ($C_{11}H_{10}NO$). Observed: 172.0756.

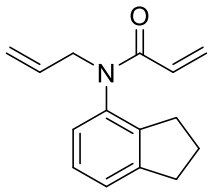

N-allyl-N-(2,3-dihydro-1H-inden-4-yl)acrylamide (IGA-1-12)
A solution of sodium hydride (96 mg, 4.0 mmol) in tetrahydrofuran (8 mL) was put under nitrogen atmosphere. To the solution was added N-(2,3-dihydro-1H-inden-4-yl)acrylamide (187 mg, 1.0 mmol) in tetrahydrofuran (2 mL). The solution was cooled to 0 °C and stirred. 3-bromoprop-1-ene (484 mg, 4.0 mmol) was added after 30 minutes, after which the solution was allowed to warm to room temperature and was stirred overnight. The solution was quenched with water and extracted with ethyl acetate. The

crude product was purified via silica gel chromatography (20% ethyl acetate in hexanes) to afford the product in 67% yield as a yellow crystalline solid (151 mg).
^{1}H NMR (400MHz, $CDCl_3$): δ 7.06-7.18 (m, 2H), 6.80-6.88 (m, 1H), 6.26-6.37 (dd, *J* = 16.8, 2.0 Hz, 1H), 5.76-5.96 (m, 2H), 5.38-5.48 (dd, *J* = 10.3, 2.1 Hz, 1H), 4.98-5.08 (m, 2H), 4.40-4.52 (ddt, *J* = 14.5, 6.3, 1.3 Hz, 1H), 4.00-4.11 (ddt, *J* = 14.5, 6.8, 1.2 Hz, 1H), 2.82-2.98 (m, 2H), 2.59-2.79 (m, 2H), 1.92-2.07 (m, 2H).
^{13}C NMR (100MHz, $CDCl_3$): δ 165.1, 146.5, 142.4, 137.9, 133.0, 128.4, 127.8, 127.48, 126.1, 124.3, 118.1, 51.6, 33.3, 30.9, 25.0.
HRMS (+ESI): Calculated: 228.13 ($C_{15}H_{17}NO$). Observed: 228.1381.

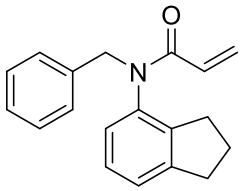

N-benzyl-N-(2,3-dihydro-1H-inden-4-yl)acrylamide (IGA-1-14)
A solution of sodium hydride (96 mg, 4.0 mmol) in tetrahydrofuran (8 mL) was put under nitrogen atmosphere. To the solution was added N-(2,3-dihydro-1H-inden-4-yl)acrylamide (187 mg, 1.0 mmol) in tetrahydrofuran (2 mL). The solution was cooled to 0 °C and stirred. Benzyl bromide (476 mg, 4.0 mmol) was added after 30 minutes, after which the solution was allowed to warm to room temperature and was stirred overnight. The solution was quenched with water and extracted with ethyl acetate. The crude product was purified via silica gel chromatography (20% ethyl acetate in hexanes) to afford the product in 63% yield as an orange oil (173 mg).
^{1}H NMR (400MHz, $CDCl_3$): δ 7.10-7.35 (m, 7H), 6.74-6.85 (dd, *J* = 7.8, 1.1 Hz, 1H), 6.40-6.55 (dd, *J* = 16.8, 2.1 Hz, 1H), 5.93-6.08 (dd, *J* = 16.8, 10.3 Hz, 1H), 5.49-5.62 (dd, *J* = 10.3, 2.1 Hz, 1H), 4.78-5.10 (m, 2H), 2.85-3.02 (m, 2H), 2.52-2.67 (m, 1H), 2.22-2.37 (m, 1H), 1.83-2.01 (m, 2H).
^{13}C NMR (100MHz, $CDCl_3$): δ 146.4, 142.9, 137.7, 137.3, 129.3, 128.4, 128.3, 128.0, 127.5, 127.5, 126.0, 124.3, 52.3, 33.2, 30.6, 25.1.
HRMS (+ESI): Calculated: 278.15 ($C_{19}H_{19}NO$). Observed: 278.1538.

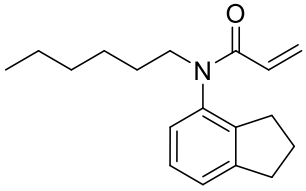

N-allyl-N-(2,3-dihydro-1H-inden-4-yl)acrylamide (IGA-1-15)
A solution of sodium hydride (96 mg, 4.0 mmol) in tetrahydrofuran (8 mL) was put under nitrogen atmosphere. To the solution was added N-(2,3-dihydro-1H-inden-4-yl)acrylamide (187 mg, 1.0 mmol) in tetrahydrofuran (2 mL). The solution was cooled to 0 °C and stirred. 1-bromohexane (660 mg, 4.0 mmol) was added after 30 minutes, after which the solution was allowed to warm to room temperature and was stirred overnight. The solution was quenched with water and extracted with ethyl acetate. The crude product was purified via silica gel chromatography (20% ethyl acetate in hexanes) to afford the product in 34% yield as a yellow oil (92 mg).

^{1}H NMR (400MHz, $CDCl_3$): δ 7.11-7.25 (m, 2H), 6.86-6.96 (dd, *J* = 7.5, 1.2 Hz, 1H), 6.30-6.40 (dd, *J* = 16.8, 2.1 Hz, 1H), 5.86-6.00 (m, 1H), 5.41-5.51 (dd, *J* = 10.3, 2.1 Hz, 1H), 3.82-3.96 (m, 1H), 3.42-3.56 (m, 1H), 2.90-3.04 (m, 2H), 2.65-2.85 (m, 2H), 1.98-2.16 (m, 2H), 1.47-1.63 (m, 2H), 1.20-1.36 (m, 6H), 0.80-0.90 (m, 3H).
^{13}C NMR (100MHz, $CDCl_3$): δ 165.16, 146.54, 142.38, 138.21, 128.59, 127.51, 127.35, 126.09, 124.13, 48.67, 33.26, 31.62, 30.85, 27.85, 26.72, 25.01, 22.59, 14.05.
HRMS (+ESI): Calculated: 272.19 ($C_{18}H_{25}NO$). Observed: 272.2007.

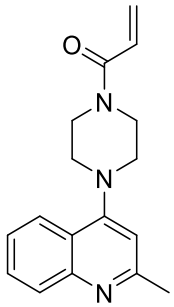

1-(4-(2-methylquinolin-4-yl)piperazin-1-yl)prop-2-en-1-one (IGA-1-26)
A solution of 2-methyl-4-(piperazin-1-yl)quinolone (455 mg, 2.0 mmol) in DCM (20 mL) was cooled to 0 °C. To the solution was added acryloyl chloride (217 mg, 2.4 mmol) followed by triethylamine (243 mg, 2.4 mmol). The solution was allowed to warm to room temperature and stirred overnight. The solution was washed with brine and the crude product was purified via basic alumina chromatography (100% ethyl acetate) to afford the product in 26% yield as a yellow oil (145 mg).
^{1}H NMR (400MHz, $CDCl_3$): δ 7.90-8.05 (m, 2H), 7.58-7.70 (ddd, *J* = 8.4, 6.8, 1.5 Hz, 1H), 7.40-7.50 (ddd, *J* = 8.2, 6.8, 1.3 Hz, 1H), 6.68-6.76 (s, 1H), 6.56-6.67 (dd, *J* = 16.8, 10.5 Hz, 1H), 6.30-6.40 (dd, *J* = 16.8, 2.0 Hz, 1H), 5.70-5.80 (dd, *J* = 10.5, 2.0 Hz, 1H), 3.70-4.06 (d, *J* = 54.7 Hz, 4H), 3.10-3.30 (t, *J* = 5.0 Hz, 4H), 2.62-2.72 (s, 3H).
^{13}C NMR (100MHz, $CDCl_3$): δ 165.5, 159.4, 156.2, 149.2, 129.26, 129.24, 128.3, 127.3, 124.9, 123.0, 121.6, 109.8, 52.3, 51.9, 45.8, 42.0, 25.6.
HRMS (+ESI): Calculated: 282.17 ($C_{17}H_{19}N_3O$). Observed: 282.1597.